Aus dem Institut für Medizinische Psychologie der Ludwig-Maximilians-Universität München

Vorstand: Prof. Dr. Martha Merrow Ph.D.

Novel strategies for the identification of clock genes in *Neurospora crassa* with insertional mutagenesis

Dissertation
zum Erwerb des Doktorgrades der Medizin
an der Medizinischen Fakultät
der Ludwig-Maximilians-Universität zu München

Vorgelegt von
Krunoslav Michael Sveric
Geboren in München
2014

Mit Genehmigung der Medizinischen Fakultät

der Ludwig-Maximilians-Universität München

Berichterstatter: Prof. Dr. Till Roenneberg

Mitberichterstatter: Prof. Dr. Gunnar Schotta

Priv. Doz. Dr. Dejana Mokranjac

Prof. Dr. Dr. Jürgen Heesemann

Mitbetreuung durch den

promovierten Mitarbeiter: Prof. Dr. Till Roenneberg

Dekan: Prof. Dr. med. Dr. h.c. M. Reiser, FACR, FRCR

Tag der mündlichen Prüfung: 27.03.2014

Table of contents

1 Introduction

1.1 Circadian Rhythms

Since the beginning, life has been subject to periodical changes of light and temperature caused by terrestrial rotation, and nearly all organisms have evolved a biological system in order to adapt to these determining factors.

This adaptive system is known as the circadian clock.

To live in surroundings that are influenced by periodical changes like the undulation of nutrition, fluctuations of temperature and the presence of predators, organisms require a mechanism that assists them in environmental accommodation and promises greater chances of survival. As an evolutionary consequence, circadian clocks grant species a benefit in the long term (DeCoursey and Krula 1998; Walker et al. 2000).

The beneficiary circadian system is present in a variety of organisms from plants, where photosynthesis, leaf movement and growth are controlled, to vertebrates, in which the locomotory activity is rhythmical (McClung 1992; Pittendrigh and Daan 1976).

Even unicellular organisms, such as cyanobacteria and algae, show mechanisms of internal timekeeping. In *Gonyaulax polyedra* flashing, glowing, cell aggregation and a special type of swimming behaviour are steered by circadian clocks (Roenneberg and Morse 1993).

Chronobiology does not epitomise an "ivory tower" in science. The research in this field explores important issues that concern the biology and sociology of nearly all beings on earth.

In recent years, new investigations have revealed the effects of the internal circadian clock on human life. Thus, variations in hormone levels, mental and physical performance, pharmacokinetics and aspects of diseases are strongly influenced by the circadian clock (Duffy et al. 2001, McFadden 1988, Lotze et al. 2000).

The importance of these findings has been increased by the fact that our human society is rapidly transforming into a culture in which traditional definitions of time and space are being reinterpreted. Voyages that used to take several months are

now viewed as short trips, and jet lags have become more common as a consequence. Although the term "jet lag" derives from transatlantic flights it is today applied in a broader sense, describing a mismatch between biological and social time.

Developed countries have been abandoning the traditional concept of working hours by expanding night shifts in the industrial and service sectors, and are mutating into an "all access 24/7" society. As a consequence, some individuals accumulate a substantial sleep deficit during the working week that they have to make up on days off. These and other implications for human health, behaviour and life quality will become sources of further investigations in chronobiology (Roenneberg, Wirz-Justice and Merrow 2003; Merrow, Spoelstra and Roenneberg 2005; Wittman, Dinich, Merrow and Roenneberg 2006).

1.2 Properties of a Circadian Clock

In general a biological clock is defined as a system that encloses an internal timekeeping mechanism capable of valuing time in the absence of any external cues. It drives and co-ordinates biological events within the organism. A specific characteristic of clocks is that they are susceptible to other external time cues and can interact in order to entrain with them in certain limits.

When the specific time cues are removed, the organism exhibits a "free running period", approximately the length of a day, and therefore the corresponding clock is called "circadian".

A circadian clock is characterised by a wide range of properties, which will be presented in the following sections.

1.2.1 Free Running Period and Sustainability

The endogenous rhythm is self-sustained and is generated within an organism, therefore it is not derived from earth's gravity, which has been demonstrated for the ascomycete *Neurospora crassa* in general (Ferraro et al. 1995).

The underlying genetics determine endogenous rhythms and display a period close to 24 h, although significantly shorter or longer periods exist, which are then called *ultradian* or *infradian* respectively.

An organism´s clock partially reveals its endogenous rhythm as a free running period (FRP or τ) in the absence of specific environmental cues under constant conditions. These rhythms are persistent and are therefore called self-sustained (Pittendrigh and Daan 1976).

The sort of constant condition that partially reveals the free running period is different for day active and night active organisms. On the one hand locomotor activity in rodents and asexual sporformation, known as banding, in *Neurospora* is free running in constant darkness (DD), on the other hand the bioluminescence of photosynthetic algae shows a free run under constant light (LL) (figure 1.1 A).

1.2.2 Homeostasis

Another important property of circadian clocks is the ability to preserve a precise timing of important functions despite changes in metabolic rates, even under sub-optimal conditions, e.g. low temperature fluctuations or starvation with changing levels of carbon or nitrogen sources. The clock system compensates for these within a defined range, hence the biological clock displays a stable free running period. The ability of compensation relies either on the instability of external conditions or on the genetically determined functionality of the clock system (Pittendrigh and Caldarola 1973).

In *Neurospora crassa* several strains with defective temperature compensation were described, while only one central clock gene was affected (Aronson et al. 1994).

1.2.3 Entrainment and Similar Occurrences

The term entrainment may be described as the synchronisation of an organism's clock to environmental cues (Zeitgeber), e.g. daily light pulses or daily temperature alternations. These two oscillating systems would swing in resonance with defined phase angles (Φ, Phi) (see figure 1.1 (B)).

However, biological entrainment needs a resetting of an organism's clock in order to synchronise functions with the environment on a daily basis. The underlying process is that the endogenous clock approximates to the period length (T) of the Zeitgeber and couples to those cycles with a specific phase angle. The phase

angle differences ($\Delta\Phi$) would represent the "compensated" variance between the endogenous period and Zeitgeber, while the clock would daily anticipate the Zeitgeber period (see figure 1.1 C). Hence, $\Delta\Phi$ would be dependent on τ and T and therefore be predictable from the τ/T relationship, known as "Aschoff´s rule (Pittendrigh, 1976; Roenneberg and Merrow, 2005).

As a consequence, the organism's clock establishes a stable phase relationship (Ψ) with its Zeitgeber, in which the phase angles change systematically in dependence on the period length of the Zeitgeber (T), but not necessarily in a linear fashion as depicted in figure 1.1 (D) (Pittendrigh 1981).

No systematic changes in Φ would be found in a "driven" clock. The system behaves like an hourglass where the clock is "slaved" and the environmental information is not processed actively by the organism's clock (see figure 1.2).

But there are also limits to entrainment. The "range" is defined by the extent of Zeitgeber and Zeitnehmer qualities, in which reliable synchronisation occurs, and the "range" is dependent upon following properties (Aschoff et al. 1978):

(i) It is influenced by Zeitgeber strengths, in particular the amplitude in light-dark cycle intensity differences, the length of Zeitgeber period (T) and the corresponding proportions of phase (i.e. photo- and thermoperiods).

(ii) The clock's capability to entrain with a Zeitgeber (see above) is affected by the organism's ability to receive and transduce time cues and by the organism's endogenous period, which can be altered genetically or by adaptive mechanisms and is influenced by the modified coupling of outputs to the circadian clock.

Outside the "range" organisms are less easily entrained and tend to free run or even show "relative co-ordination", i.e. a sort of free run with regular interactions with the Zeitgeber. In another case, if the Zeitgeber cycle is half of the organism's τ a "demultiplication of frequency" will typically occur. The clock is "inclined" to show activity once every two ore more external cycles in order to restore its endogenous period. In addition, "frequency multiplication" denotes the occurrence of at least two activity phases in one Zeitgeber cycle (Roenneberg, Daan and Merrow 2003; Roenneberg and Merrow 2005).
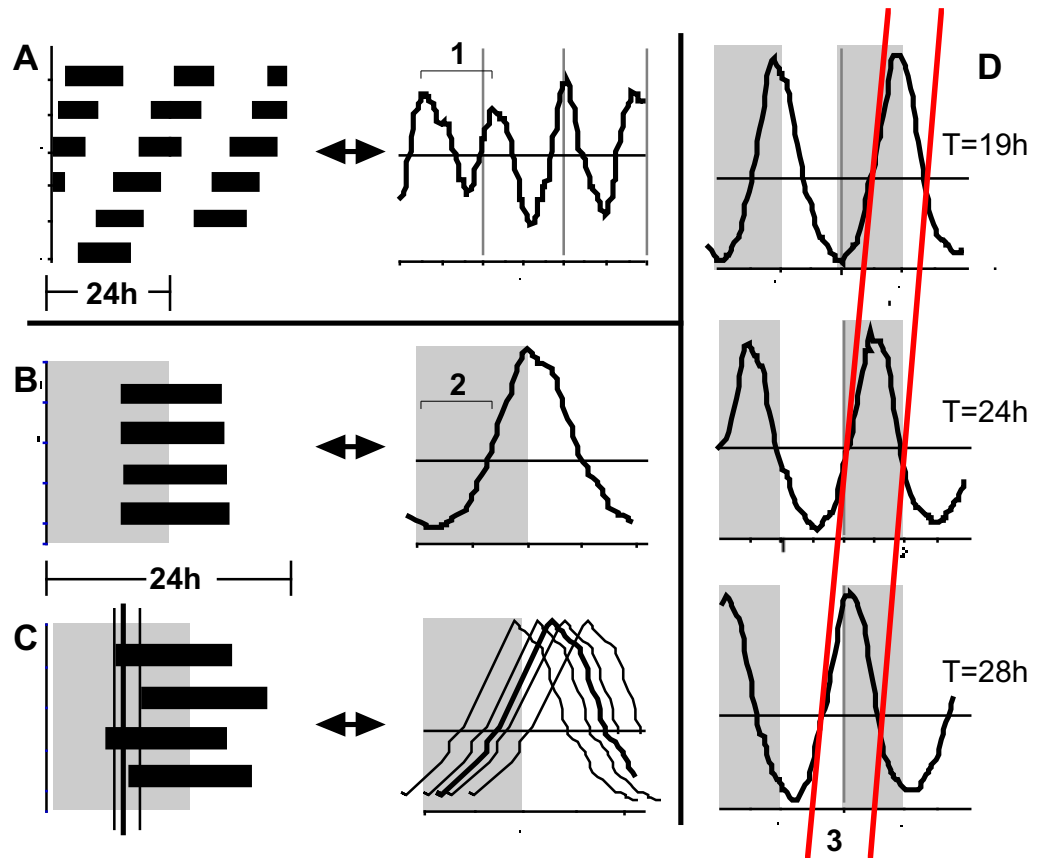
Fig.: 1.1 Cartoon of Clock Properties

Black bars represent a bout of rhythmic activity, e.g. spore formation or locomotor activity (alpha, α). In general the activity period α is described and calculated best as the following mathematical function: $\Phi_{off} - \Phi_{on} = \alpha$

A depicts the free running rhythm under its specific constant conditions, while the activities of sequential days are composed vertically and double plotted (left panel) or linearly plotted (right panel) in the context of 24 h. **1** describes the length of a period. **B** shows a strongly entrained rhythm to a period of exactly 24 h in a Zeitgeber cycle of light and darkness (grey area, left panel), while the right panel shows the averaged activity trace of four days. **2** describes the phase angle Φ in relation to the beginning of the dark portion (phase) of the Zeitgeber. **C** entrainment of lower strength, e.g. relative co-ordination, (left) the average of activity is represented as a dark line and the daily deviations as thin ones. **D** depicts entrainment to Zeitgeber cycles of different length (T). **3** denotes the phase relationship Ψ and its systematic changes (red lines) for the activity onset and offset in relation to the cycle length (the plots are scaled to the same size).

1.3 The Clock Model

The following section describes a clock model that is mainly based on studies in *Drosophila* and *Neurospora* and will make references to the clock system of vertebrates.

Initially, Pittendrigh, Bruce (1959, 1957 respectively) and Eskin (1979) proposed a clock model with three components: the "black box" contains the clock machinery and the corresponding unidirectional input (I) and output (O) pathways (see figure 1.2 (1)).

Since then, physiological and molecular studies have extended the knowledge about clocks and revealed that the input and output pathways are not "unidirectional" as had been supposed. These pathways are controlled by components (e.g. proteins) that are either expressed in a circadian or non-circadian fashion. The function of these proteins is described best with the term "gating". On the one hand these gating components perform a selective filtering of incoming information, and on the other hand they have direct influence on the response rate of the clock system (Heintzen et al. 2001; McWatters et al. 2000). There are feedback traits within the input and output pathways as well traits from the central oscillators to the input pathways (see figure 1.2 (2)).

Pittendrigh et al. (1958) presupposed that *Drosophila*`s clock might be composed of two oscillators. Morse and Roenneberg (1993) demonstrated that even a unicellular alga like *Gonyaulax polyedra* has two circadian osillators with two distinctive light input pathways.

The existence of mutiple oscillators as well as gating mechanisms may explaine why circadian clocks are so flexible in processing information, and why they respond differently to the same stimuli at different times of the day. The "non-linear" function of a Phase Response Curve or the occurrence of so called "phase-jumps" in the phase relationship of complex entrainment experiments might have their origin in these phenomena (Pittendrigh 1960; Merrow et al 2005).
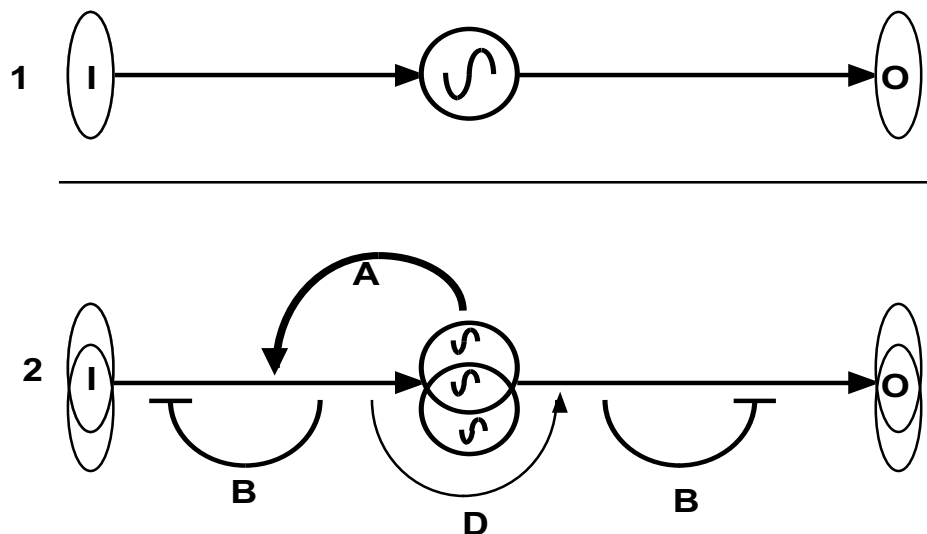
Fig.: 1.2 Models of Circadian Clocks. 1 Basic model; the input pathway (**I**) transduces Zeitgeber signals, e.g. light, to the rhythm generator (circle with a central wiggle). The oscillator generates a self-sustained rhythmicity and regulates various output pathways (**O**) (Pittendrigh and Bruce 1957). **2** Model of a circadian system consisting of two input pathways (**I**) and multiple oscillators with two outputs (**O**). **A** describes the Zeitnehmer feedback on the input, while the **B**s represent the information pathways that show a sort of self-feedback. **D** only symbolises the occurrence "driveness" (see section 1.2.3 for details).

1.3.1 A Molecular Clock Model is Changing

Hardin et al. (1990) proposed a theoretical model for the molecular basis of an oscillator in circadian clocks in *Drosophila*. This model included three components, a gene expressing RNA and the corresponding protein. The protein would have a negative influence on the transcription of its own gene and therefore represent a negative element (P-) in this clockwork (see figure 1.3 (1)). The gene expression would at least pause until the protein was degraded and the transcription could restart. This molecular model represents the broadly acknowledged basis of circadian oscillators, in which a translation-transcription feedback loop (TTFL) with its corresponding elements rhythmically induces other cellular elements, hence forming the cellular clock phenotype (Crosthwaite et al. 1997).

Yoshuira et al. (2002) demonstrated that a model with only one TTFL would exhibit a rhythmicity within a range of 2 to 4 h in an organism, solely based on molecular kinetics, and it was thus not possible to establish a full circadian rhythm of 24 h.

Recent clock modelling and molecular studies therefore support the existence of multiple TTFLs. These feedback loops form a molecular network and act through interdependent elements (e.g. proteins of a feedback loop) in order to form a 24 h cycle (Shearman et al. 2000; Roenneberg and Merrow 2002).

An interdependent element could act as a positive activator of transcription (P+) and would stabilise the TTFL (Talora et al. 1999). In general, protein phosphorylation or dephosphorylation keep time for the turn-over-rate of feedback elements and define the clock's period length (Liu et. al 2000, Yang et al. 2004) (see figure 1.3 (2,D)). Moreover, some elements function as filtering stations by "gating" information into the oscillatory system. These elements can be part of the oscillator or can be just part of an "attached" or interconnected feedback loop (McWatters et al. 2000, Heintzen et al. 2001, Lee et al. 2000) (see figure 1.3 (2,I)). Furthermore, modifications of elements on the level of translation by alternative initiation have been demonstrated in *Neurospora* (see figure 1.3 (2,C)). Hereby two isoforms of the negative element (here short and long FRQ) have an impact on the rhythmicity of the clock and display adaptive mechanisms in temperature changes (Liu, Garceau et al. 1997).

There are also modulations of feedback loops on the level of RNA. A recent study showed that cellular processes of the clock might be influenced by an unfamiliar transcription of a circadian core gene (i.e. *frq*) into antisense-RNA (Kramer et al. 2003). As a consequence, Diernfellner et al. (2005) found evidence of an alternative splicing in *frq*-RNA. The alternative splicing of *frq* is associated with different temperature levels and influences the clock's period length as well (see figure 1.3 (2,A and B)).

These diverse mechanisms of modulation expand the traditional TTFL and may explain on one hand the robust 24 h rhythmicity of a clock but on the other hand the clock's ability to adapt rapidly to changing conditions (see section on Entrainment and Homeostasis).
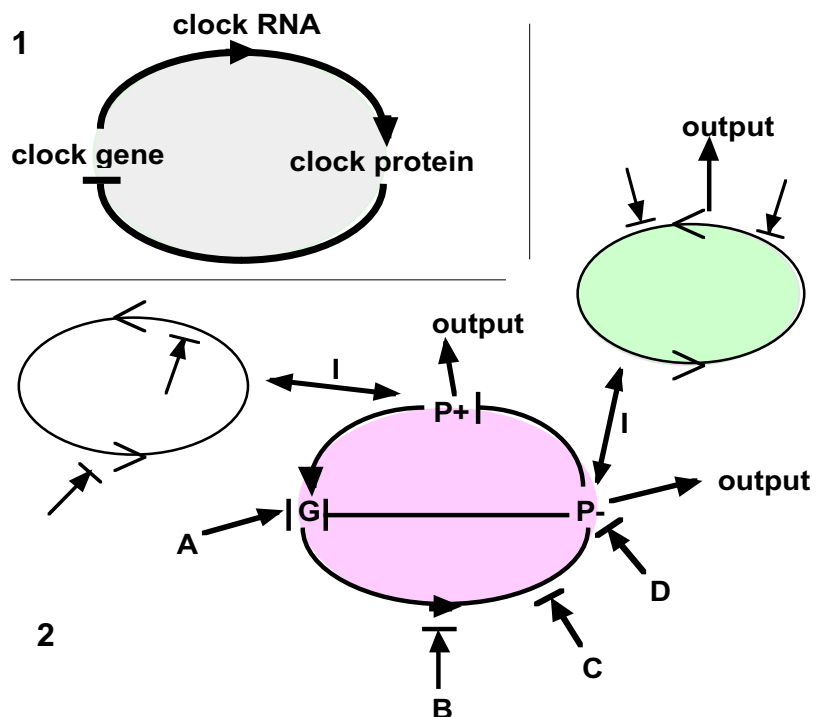
Fig.: 1.3 Models of Molecular Oscillators.

1 describes the simplified translation-transcription feedback loop that resembles the oscillatory system of a cellular clock.

2 depicts an expanded model with several interacting TTFLs (see text for details). **G** represents the clock genes, while **P** denotes the corresponding proteins with their negative (-) or positive (+) influence on the oscillators. Arrows and corresponding lines stand for a positive or negative modulation of the TTFL. **A** to **D** and **G** represent the modulation sites in an oscillator and are explained in the text. **I** and the double arrow-heads represent connections to other feedback loops or oscillators within a cell. These connections could be established directly by an element of the oscillator itself or by an independent element. An oscillator might have more than one output pathway.
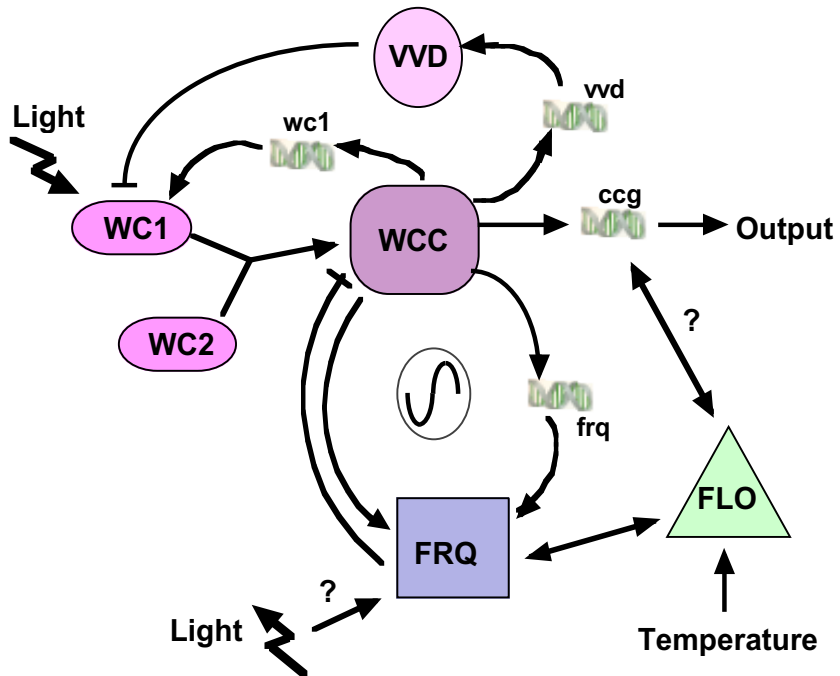
Fig.: 1.4 A Model of *Neurospora*`s Clock System

The lines represent enforcement (arrows) or suppression of genes and proteins. For a detailed description see text in section 1.3.2.
(Redrawn from Bell-Pedersen et al. (2005) and Dragovic et al. (2001))

1.3.2   The Model Clock *Neurospora*

This section will refer directly to figure 1.4 in order to explain the interactions of genes and proteins of *Neurospora's* clockwork.

The central clock gene *frequency* (*frq*) and its protein product FRQ represent the negative element in the TTFL. Mutations in the *frq* gene result in either short or long free running periods of the clock (Merrow et al. 1994). *frq* null mutants are arrhythmic when exposed to common conditions but recover their rhythmicity under nutritional supplementation (Aronson et al. 1994, Granshaw et al. 2003).

However, the *frq* RNA expression is activated directly by a White Collar Complex (WCC) containing the proteins White Collar 1 (WC1) and White Collar 2 (WC2). The FRQ proteins (short and long forms) guide their own transcription rate indirectly by inhibition of the WCC-heterodimer. This sort of inhibition lasts until the amount of FRQ reaches a certain threshold and stops its inhibitory influence on the WCC. The *frq* transcription is activated again, thus initiating a new bout.

WC1 and WC2 represent the more positive elements of the feedback loop in *Neurospora*. The formation of the WCC heterodimer is enforced by exposure to blue light (Talora et al. 1999). WCC hereby activates the *frq* transcription (see above) as well as the transcription of other genes, e.g. vivid (*vvd), white collar 1 (wc1)* and the *clock controlled genes compound* (*ccg*). Moreover, WC1 protein negatively regulates the transcription of *wc2* when the heterodimer (WCC) is dissociated.

Furthermore, the Vivid protein (VVD) is likely to gate light input to the system by the inhibition of the suggested blue light photoreceptor WC1. VVD is involved in the light adaptation of gene expression and represents a negative element in light induction (Heintzen et al. 2001, Lee et al. 2000). Hence, *vvd* mutants display an increased sensitivity of *frq* transcription and show altered phases in light entrainment than the wild type.

FRQ and WCC are supposed to represent the Frequency-White-Collar oscillator (FWC). The degradation of FRQ protein is modulated by phosphorylation via Casein Kinases (CK) showing altered turn-over rates. These turn-over rates are supposed to determine the period length of the clock (Goerl et al. 2001) (see section 1.3.1).

FRQ and WCC are directly involved in the induction *ccgs*. Some *cc*gs are involved in the formation of hyphae and conidia (i.e. important for banding) and are supposed to be only under direct control of the core clock elements FRQ and WCC.

Recent studies have shown that several *ccgs* exhibit circadian rhythmicity in spite of the absence of FRQ and WCC (Correa et al. 2003). Moreover, mutant strains without FRQ or WC1 and WC2 showed entrainment in light or temperature cycles (Merrow, Brunner and Roenneberg 1999; Dragovic et al. 2001 and 2002).

These findings suggest the existence of a FRQ-less oscillator (FLO), a second circadian oscillator in *Neurospora crassa*, although no further molecular components could be described.

1.3.3 The Clock Model in Vertebrates

The circadian systems in vertebrates, i.e. in mice and in man, are organised in differentiated hierarchies.

On cellular levels oscillations are generated by clock components that include transcription-translation feedback loops (TTFL) as in *Neurospora crassa*. These single cells then coordinate for their cell compound (i.e. tissue) a specific circadian rhythm via a not fully explored mechanism. These tissue oscillators (e.g. liver) are then synchronised in relation to the pacemaker in the brain, the suprachiasmatic nucleus (SCN) (see figure 1.5 A).
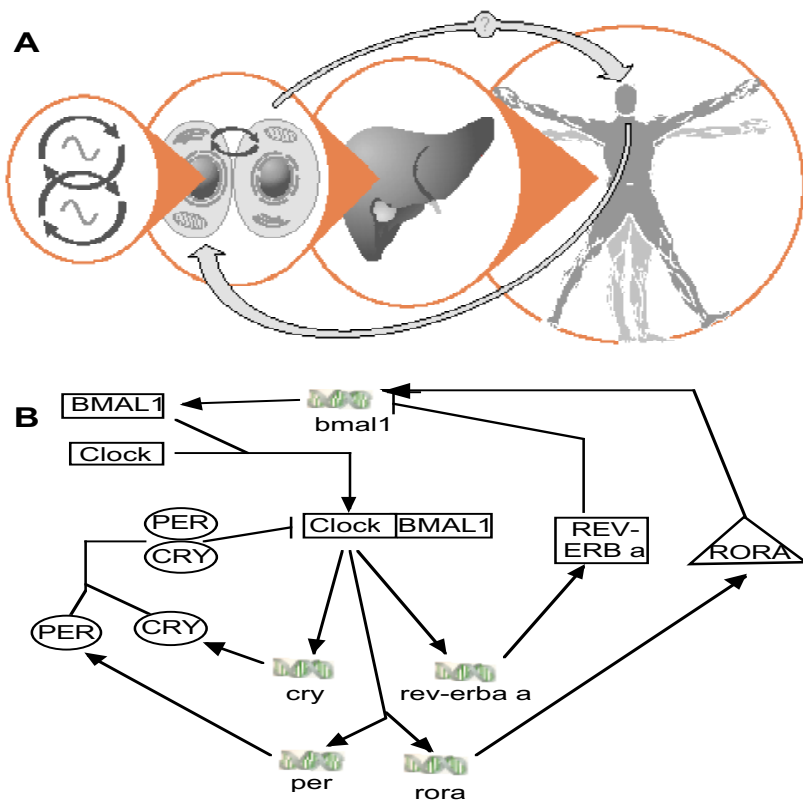
Fig.: 1.5 Clock Model in Vertebrates

A Hierarchical organisation of clocks in vertebrates (copied from Merrow et al. 2005). **B** Cartoon of the molecular transcription-translation feedback loop in vertebrates (see text for details) (redrawn from Bell-Pedersen 2005).

These circadian rhythms manifest as a sleep-wake cycle and show a circadian alternation in body temperature. The majority of parameters in endocrinology are secreted rhythmically, e.g. cortisone and glandotropines.

Most studies on the molecular mechanisms of the circadian clock of vertebrates are done in mice. A brief overview of the clock components in mice will be given in figure 1.5 B. The negative elements of the intracellular circadian oscillator are the period homologues 1, 2 and 3 (PER1-3) as well as cryptochrome 1 and 2 (CRY1 and CRY2) and the retinoic acid receptor-related orphan receptor RORA. In contrast, Clock, BMAL1 and the orphan nuclear receptor REV-ERBα act as positive elements of the TTFL. PER and the CRY proteins slowly accumulate as heterodimers and feed back in order to inhibit Clock-BMAL1 dependent transcriptions. Unlike these, REV-ERBα accumulates quickly and inhibits *bmal1* transcription, and RORA, which accumulates more slowly, activates *bmal1* transcription. This interlocked oscillator is supposed to control expression of genes in the output pathway, resulting in behavioural and physiological rhythms (Bell-Pedersen et al. 2005, Clayton et al. 2001, Reppert and Weaver 2001).

1.4 The Biology of *Neurospora crassa*

The filamentous fungus *Neurospora crassa* is an ascomycete. Depending on external conditions it propagates asexually or reproduces sexually. *Neurospora crassa* exists mainly as a haploid, and the diploid zygote immediately undergoes meiosis and generates haploid spores.

The genus *Neurospora* has traditionally been found in moist, tropical and subtropical areas. It can be also found growing indoors on food or food waste and is known to bakeries as a contaminant. However, *Neurospora* lives in an illuminated natural habitat and has developed a variety of light responses. These responses include mycelial carotenoid production (Harding and Turner 1981), sexual structure formation and phototropism (Degli-Innocenti and Russo 1984), and gene expression as described previously in section 1.3.2.

1.4.1 Asexual Propagation

In its asexual stage, *Neurospora crassa* forms a mycelium that is made of syncytial hyphae, which are tubular filaments with multiple haploid nuclei. The asexual cycle also includes formation of macroconidia (or simply called conidia) from aerial hyphae, and the conidia then have one to several haploid nuclei. Genetically different haploid nuclei can coexist in a single spore or in mycelia and such strains are called heterokaryonic. A conidium germinates to form hyphae, which grow by tip extension and branching to form a mycelium. In poor nutritional conditions, *Neurospora* produces uninucleate microconidia (see Methods).

However, *Neurospora* rhythmically displays these aerial hyphae forming conidial bands under special conditions in race tubes (see Methods). This conidial pattern is highly correlated to the molecular clock, reflecting directly the period length and phase of circadian oscillation, and represents one of the most important output pathways in *Neurospora* (Merrow et al. 1999). Analysis of the conidiation patterns therefore allows a deduction on the state of the circadian clock can be made.

1.4.2 Sexual Cycle, Genetics and Epigenetics

The sexual cycle of *Neurospora crassa* requires two mating types. Either strain may act as a "female" parent by forming a specialised multicellular knot of hyphae (protoperithecium) which contains the female gamete (ascogonium). Fertilisation occurs via specialised hyphae (trichogyne), which collect a conidium of the opposite mating type, and two gamete-nuclei (male and female) undergo simultaneous meiosis. At the same time the protoperithecium enlarges and forms a thick-walled, mature perithecium around the ascogonium. The ascogenous hyphae form asci with eight sexual ascospores and shoot ascospores away from the perithecium when mature. Dormant ascospores can survive in the soil for a long period until they are activated by heat or chemicals (see the Methods section).

Its haploid nature of nuclei and the existence of seven chromosomes makes *Neurospora crassa* an ideal subject for genetic studies. The analysis of gene segregation, formal genetics and linkage studies can be performed easily and had

been used for the "one gene, one enzyme" hypothesis by Beadle and Tatum in 1942.

However, Selker et al. (1987) described an occurrence of chromosomal rearrangements in *Neurospora* known as repeat induced point mutation (RIP). This process involves multiple point mutations, i.e. GC to AT transitions, as well as cytosine methylation in duplicated DNA regions. The length of the duplicate DNA region (>1 kb) as well as the distance between the homologous sequences is correlated highly with the severity of point mutation (i.e. transitions) and RIP might occur during the period of division of the haploid parental nuclei into ascogenous hyphae during a sexual cross. The process requires the homologous pairing of DNA sequences in the prefusion nucleus.

The RIP process seems to be important in the evolution of *Neurospora crassa,* inactivating transposable elements in order to prevent an accumulation of "foreign" DNA and thus stabilising the genome (Singer, Marcotte and Selker 1995).

Interestingly, Perkins et al. (1997) described a phenomenon in which plasmid DNA suffered serious alterations, although the strains have not undergone a sexual cycle in *Neurospora crassa*. Deletions, rearrangements and reiterations of sequences were found whilst these regions became heavily methylated. Whether these occurrences are a unique defence mechanisms in Neurospora crassa represent artefacts during the transformation, i.e. breakage or selective incorporation of plasmid in transient breaks, is not known and are subject of further molecular research.

1.5 Aim of This Study

In reviewing the results of previous experiments and the clock models it has become clear that the mechanism of the circadian clock is more complex than a simple "one-gene, one protein" feedback loop. Most experiments in detecting new clock mutants were performed either in constant conditions or in traditional entrainment cycles in *Neurospora crassa*. Moreover, most investigations focused on light as a main time cue in entraining a circadian clock, abolishing other classes of Zeitgebers such as temperature. Furthermore, these investigations tend to recapitulate a "constant state" rather than describing the "dynamic" functions of such an interdependent clock system. They thereby neglect the complexity as well as the plasticity of a system that shows an incredible ability to adapt and react to environmental changes. It is unlikely that new clock components will be discovered while the clock of *Neurospora crassa* is not "challenged". By challenging the circadian clock with temperature entrainment at the lower end of the range, i.e. in cycles of short length, several questions can be asked.

+ What is the shortest T length for reliable temperature entrainment?

+ Is it possible to reveal new clock mutants with short temperature cycles?

+ What are the options to rescue mutations in establishing a new method of plasmid rescue?

+ What are the characteristics of these new mutants?

+ Are there any associations with known clock mutants despite their screening background?

+ Is it possible to reveal new clock components or only components that show dependency on known clock genes?

2 Methods

2.1 Strains

All strains of Neurospora crassa used in this study carry the *bd* mutation, which prevents inhibition of conidiation by high CO_2 concentrations in closed culture vessels - especially in race tubes (Sargent and Kaltenborn 1972). Thus there is no need to exchange the air and risk contamination.

For this study the following strains were used or genetically modified:

bd a 30-7 (frq+), the standard laboratory strain with only the bd mutation, showing a free running period (FRP) of approximately 21 hours.

bd frq1, a short period mutant (FRP=16 hours), based on a single point mutation (transition G to A) in the *frequency* gene (Merrow and Dunlap 1994). Moreover this strain shows sensitivity to the pesticide BASTA.

- *bd frq9,* in which a base pair deletion in the *frq* ORF results in production of a truncated protein and loss of FRQ protein function (Loros and Feldman, 1986).

- *bd frq10,* generated by deletion of the promoter and almost the entire *frq* ORF (two central Bgl II fragments, 5.3 kb) (Aronson et al., 1994a).

- *bd wc–1 RIP#21,* (*wc1* for short), is a mutant with a non-functional *wc1* allele, generated by introducing stop codons in the entire ORF by the RIP process (Dragovic Z. personal communication, see He et al. (2002)).

bd komo 1 to *721*, mutants based on the *bd* a 30-7 strain produced only for this study by random plasmid insertion (pKSbar2) (see section 2.3.10) and therefore resistant against the pesticide BASTA.

Escherichia coli XMN (Stratagene Inc.)

2.2 Physiological Methods

2.2.1 Maintenance of Strains

To create a stock all strains were inoculated into reagent tubes with slanted Vogel´s minimal agar media (slants), then allowed to grow on the laboratory bench at room temperature for 7 days. After that period the tubes were sealed

individually with Parafilm and frozen at -20°C for long term storage. All working cultures were made out of the stockpile and stored in medium-sized slants at 4°C. The strains were dismissed two months after inoculation. All conidia used for further experiments were derived from working cultures. They were raised on medium sized slants for 7 days and maintained at room temperature.

The *komo* mutants were kept in existence at the same level as the standard laboratory strains with an addition of 3% BASTA.

2.2.2 Growth Conditions

Neurospora crassa is capable of growing both on solid and on liquid media.

A solid medium stimulates *Neurospora* to build both mycelia and conidia. Raised in slants, petri dishes or Erlenmeyer flasks (250 ml or 500 ml) it yields a high amount of conidia important for further procedures such as electroporation and race tube experiments.

On the other hand, when permanently shaken, liquid cultures of *Neurospora crassa* lack conidia. They show a healthy growth of mycelia instead. Hence liquid cultures are mainly used for DNA and RNA experiments.

All experiments in these studies were carried out at 25°C, except for temperature cycles (see section 2.2.4).

2.2.3 Race Tubes

2.2.3.1 Race Tube Assay

For continuous observations of physiological responses in *Neurospora crassa*, race tubes were used. These are stretched glass vessels about 30 cm long and with a diameter of 1.3 cm (produced by Höhn and Schmitz, Munich). Each end of the tube is bent (approximately 35°) to allow filling and prevent effusion. Six single race tubes were tied together for more practical usage. The single tubes were filled with 6 ml of molten race tube media (see appendix for recipe) (Vogel 1956). After autoclaving, the ends were sealed with sterile plugs to prevent contamination. The cooled race tubes were inoculated with a loop of conidia from the working slants at one end. They were allowed to germinate in constant light at

room temperature for 24 hours. The growth front of the mycelia was then marked on the bottom side of the glass vessels with a waterproof pen. Afterwards they were transferred into their experimental conditions. During the experiment the growth front in each tube was marked daily. This marking procedure allows an exact reference of experimental time points to the present phenotype of the fungus.

2.2.3.2   Growth in Race Tubes

Neurospora crassa grows by hyphal extension into the media. In long-stretched vessels it grows particularly linear from the point of inoculation towards the other end following a decreasing pH gradient. At special time periods the fungus develops aerial hyphae. These hyphae show a pattern of alternating zones of sparse and dense mycelium with conidiation, called bands. These bands are stable and do not disappear nor do they change in intensity or form.

When the mycelial front nearly reached the end of the tubes, the tubes were removed from the growth cabinet and densitometrically analysed.

2.2.3.3   Race Tube Analysis

To simplify the data analysis, race tubes were scanned and digitised (AGFA Snapscan 1236, settings greyscale, image resolution: 150 dpi), stored as PICT files and analysed with the CHRONO program (Roenneberg and Taylor, 2000). Conidiation was quantified by the number of white pixels in each vertical line of the image and set in correlation to the marked time points. All the data sets were plotted as functions of time.

For more convenience the line graphs of each day were plotted in rows beneath each other and two single plots were fused to a double plot.

To analyse the average onset, offset and peak of conidiation a composite curve was used. To ensure higher accuracy, the arithmetic mean for the composite curves of all race tubes was calculated. Onsets of conidiation were defined as the upward transitions through the non-rhythmic trend (50% mark of the average).

The calculations of periods were performed with "Periodogram Analysis", which is an integrated analysis tool of CHRONO (see section 2.5).

2.2.4 Experimental conditions

2.2.4.1 Temperature Cycles (TC)

All temperature cycles were performed in custom-made incubators filled with water. Two water bath machines alternately (according to the protocol) circulated warm or cool water through metal tubes at the bottom of the boxes. To achieve the proper temperature for experiments all temperature cycles were held in rooms at 25-26°C. Each increase in temperature from 22°C to 27°C was attained in 45 minutes, whereas each decrease from 27°C to 22°C took about 90 minutes.

2.2.4.2 Light-Dark Cycles (LD)

All light-dark cycle experiments were performed in custom-made light-proof boxes with individual extractor fans. The temperature inside the boxes was kept at
25°C at every stage of the cycle and continually monitored with a thermometer (Wilhelm Lambrecht, Göttingen). The light source within the boxes was a white fluorescent strip lamp (OSRAM Dulux L, 10 W) wrapped in a layer of diffuser (Cinegel #3026 Rosco) to homogenise light distribution. All light experiments were carried out at an equal light intensity of 3.5 $\mu E/m^2/sec$ (fluence was measured with an IL1400A Photometer, International Inc.).
A computer program controlled the light-cycles (Till Roenneberg, Munich).

2.2.5 Screening Assay for Mutants

In this study the standard laboratory strain *bd a* 30-7 was mutated by random plasmid (linearised) insertion (see section 2.3.4). A system was developed to screen all mutants made with electroporation. A high sensitivity and specificity were desirable for the test, but it also had to cope with the practicability of a high throughput screening. Therefore, the screening approach was organised into three steps.
At the first level, mutants were screened in 16 h temperature cycles in darkness, which consisted of a 8 hour cold phase (22°C) and a 8 hour warm phase (27°C). All experiments started with the cold phase. Each mutant was inoculated into one

race tube. The parental strain *bd a* 30-7 was included as a control group (3 race tubes for each temperature box). The analysis of the race tubes followed as described in section 2.2.3.3.

Mutants were screened for an altered phase angle (ϕ) showing more than 25° difference in comparison with the control strain. Furthermore, mutants with no entrainment or arhythmicity were selected, too.

The second step consisted of the verification of the previous 16 h temperature cycles. In addition to that, the phenotype of these mutants was checked in DD (constant temperature at 25°C) and in a symmetrical 24 h light-dark cycle (constant temperature, 3 μE/m^2/sec light intensity). At this level of screening all mutants and control strains were set up threefold for higher reliability of data (each strain was inoculated into three race tubes for each experiment).

The third step consisted of the molecular characterisation of these mutants and the novel plasmid rescue (see section 2.3.8).

2.2.6 Induction of Microconidia on Plates

Minimal media and standard growth conditions in Neurospora crassa as for example those in Erlenmeyer flasks, slants and race tubes, favour above all the development of macroconidia. These sorts of conidia consist of at least two nuclei. Thus, bares the bias towards heterogeneity in an organism. We therefore applied a method to induce uninuclear microconidia on plates (Pandit and Maheshwari 1993). 10 ml of a microconidia-inducing media (iodo acetate media, see appendix) were poured into a normal sized petri dish. The cellophane sheets were cut into circles matching the diameter of the plates. Before sterilisation the sheets were boiled in 1% KOH and thoroughly washed. The cellophane was placed tightly over the surface of solidified media and pierced in the centre where macroconidia were inoculated. The vessels were kept at 22°C-25°C under humid conditions under a bell jar. After 10 days mycelial growth and several macroconidia developed both under and over the plastic sheet. At this point the cellophane was removed and the plate and lid were washed with sterile distilled water and kept again under humid condition for 2 days. After examination under the microscope the microconidia were harvested with a minimal amount of water (1-2 ml), counted and plated on a sorbose medium (see Appendix). Incubation at 30°C allowed colonial

forming. Single colonies were individually picked up and transferred into minimal media containing slants with an addition of 0.8% BASTA. The derivatives were numbered and acquired their unique identification from the "parental" strain, followed by the isolate number. Derivatives were checked for their typical phenotype and genetics (see section 2.4).

2.2.7 Sexual Crosses

Neurospora crassa uses both sexual and asexual reproduction for propagation. The sexual cycle is favoured, especially on nitrogen and carbon deficient media (Westergaard and Hirsch, 1954). The mating type loci are called A and a, and either can represent a female parent by forming a multicellular protoperithecium. The fertilising agent is a nucleus of the opposite mating type supplied as a conidium. Two weeks after fertilisation the protoperithecium enlarges and darkens into perithecium, which shoots ascospores to the lid of the covering petri dish.

To isolate single (uninuclear) ascospores, they were collected by pipetting 100 μl of sterile water onto the lid. The spores were suspended and plated on a 4% agar petri dish. Every ascospore was individually picked by a sterile needle and separately inoculated into a minimal slant. The reagent tubes were heat shocked at 60° C for 30 minutes. The efficiency of activation was between 60% and 80%. Afterwards, the offspring grew at room temperature for 3 to 5 days. The isolates were numbered and acquired their unique identification from the cross number, followed by the isolate number. Afterwards the isolates were transferred to BASTA containing slants for selection. The resistant offspring were tested physiologically and formal genetics could begin (see section 2.4.2).

2.3 Molecular Methods

2.3.1 DNA Preparation

2.3.1.1 Genomic DNA Preparation from Mycelia

Tissue was grown in a 100 ml Erlenmeyer flask with 40 ml of Vogel´s minimal media for two days. The cultures were shaken all the time to prevent conidiation and allow a high yield of mycelia. The tissue was harvested by blotting and frozen in liquid nitrogen. It was homogenised in a mortar and pestle and about 150 µl of sand. Prior to grinding, the tools were cooled at the temperature of liquid nitrogen (-196°C). The ground tissue was immediately filled into 1.5 ml safe-lock cups with 500 µl of 2x CTAB buffer (Zolan and Pukkila, 1986; Taylor and Natvig, 1987; see Appendix for recipes).

The tube was vortexed vigorously until the suspension homogenised and was then incubated at 60°C for 30 minutes. Afterwards 500 µl of CIAA (see Appendix) were added into the tube and mixed in a shaker for 15 minutes at room temperature. The sample was centrifuged at 10,000 rpm for 10 minutes. The aqueous phase was transferred to another tube and the CIAA extraction was repeated. 1µl of RNase (10 mg/ml) was added into the aqueous solution and incubated at 37°C for 10 minutes. An equal volume of isopropanol was added and mixed gently until DNA precipitated at room temperature. The solution was frozen at -76°C for 2 hours and afterwards spun at 14,000 rpm for 5 minutes at 0°C to pellet the DNA. However, this time the aqueous phase was discarded and the DNA clump was washed several times with ice cold ethanol in decreasing concentrations. Excess ethanol was removed by brief drying in an electric vacuum desiccator. As a last step, the DNA pellet was suspended in 50µl of sterile double-deionised water. The DNA samples were quantified and kept at -20°C for long-term storage.

2.3.1.2   Preparation of Plasmid DNA from *E. Coli*

2.3.1.2.1 Mini-Preparation of Plasmid DNA

Small amounts of plasmid DNA were obtained by a method called mini-prep. 1 μl of a glycerol stock solution of E. coli was diluted with water (1:100) and plated on an ampicillin-containing agar. After 24 hours individual colonies were picked and inoculated into a reagent tube with 2 ml LB-AMPr-media (Luria Bertani media, see Appendix). Cultures were incubated and shaken overnight (at 37°C, 160 rpm). The next day 1 ml of each sample was centrifuged at 14,000 rpm for 2 minutes. The aqueous supernatant was discarded and the cell debris was suspended in 100 μl of GET and 150 μl of alkaline lysis buffer. Incubation on ice followed for 5 minutes. For DNA precipitation 120 μl of 3M NaAcO were added to each sample; all the samples were then chilled once more. For protein discharge 370 μl of IAA (25:24:1) were added and samples were mixed to extract the proteins. Centrifugation at 14.000 rpm followed for 3 minutes. Afterwards the supernatant was transferred to a new tube, and 1 μl of RNase A was added. This time the incubation was performed at 37°C for 10 minutes. 1 ml of ice-cold ethanol (100% v/v) was added into each sample and incubated again on ice for 5 minutes. After a last centrifugation at 4°C (14,000 rpm) for 5 minutes the pellets of DNA were cleaned according to the protocol for genomic DNA extraction (see section 2.3.1.1). Plasmid DNA was stored at -20°C.

2.3.1.2.2 Midi-Preparation of Plasmid DNA

To yield large amounts of plasmid DNA, a "Jetstar Plasmid Purification Kit" was used. Colony selection and starter cultures were prepared as described in the section above. 1.5 ml of the LB-AMP media containing the cultures were inoculated into a 1,000 ml Erlenmeyer flask with 250 ml of LB-AMP media. The culture of considerable size was incubated at 37°C by vigorous shaking (~300 rpm) for at least 13 hours. All steps for plasmid purification were done according to the company's protocol.

2.3.2 Quantification of DNA

2.3.2.1   Quantification through Spectrophotometer

DNA has a maximum absorption at 260 nm; hence, it is possible to quantify the concentration of DNA dissolved in an aqueous solution. The measuring was performed by a Beckman spectrophotometer (UV-DU-64). To obtain exact read outs, several DNA dilutions (1:10 to 1:1000) were examined. Only readings between an optical density (OD) of 0.1 and 1 were considered for further calculations (1 $OD_{260\,nm}$ = 50 μg/ml of DNA).

Moreover, the quality of genomic DNA extraction was controlled using the Warburg program at 260 nm and 280 nm (peak of absorbency of proteins). Ratios between 1.8 and 2.0 were considered acceptable.

2.3.2.2   Quantification by Gel Electrophoresis

1 μl of an exactly defined DNA ladder dilution (standard molecular weight markers of New England BioLabs) was loaded on an agarose gel on either side of a sample. The brightness of the bands was compared to the brightness of the sample and the DNA concentration of the probe was calculated. Due to its inaccuracy, this method was used only for estimation, but it proved to be a good indicator of the DNA's quality. Stretched and diffuse bands suggested a degradation of genomic DNA. Therefore, all samples of genomic and plasmid DNA used in our study were controlled regularly.

2.3.3 Restriction, Digestion and Ligation of DNA

All restriction digestions were applied with New England BioLabs (NEB) restriction enzymes and corresponding buffers.

To achieve an efficient digestion, not more than 1-3 μg of DNA were used with 1-2 U of restriction enzyme (see unit definition at NEB) for simple digestions (see exceptions in section 2.3.8.2). Reactions were carried out in 1x NEB buffer (individual buffers for enzymes among NEB specification) and an optional addition

of BSA (New England BioLabs). These reactions were performed in a total volume of 50 μl. Before incubation at 37°C overnight the samples were mixed thoroughly. For inactivation of enzymes the samples were heat inactivated at 65°C for 20 minutes. To proceed to further steps, for instance multiple digestions and PCR, the solutions were purified by precipitation with sodium acetate and ethanol. No–enzyme and no-DNA samples were included in all restrictions experiments.

T4 DNA ligase (NEB) was used for ligations mainly at the stage of plasmid rescue (see section 2.3.7). These ligations were performed in buffers provided with the enzyme at 16°C for 2 hours or overnight. 20 μl ligation mixtures were set up with an addition of 800 U of T4 ligase per 1 μg of DNA and 1x T4 ligase buffer (NEB). Care was taken that the concentration of total DNA in the reaction mixture was not higher than 0.5 μg/μl. To avoid interactions in subsequent PCR reactions or electroporation, the electrolytes were removed from ligation reactions by ethanol precipitation.

2.3.4 Separation and Purification of DNA on Agarose Gel

Agarose gel electrophoresis was performed according to standard methods (Sambrook et al., 1989). DNA fragments used for cloning, PCR or sequencing were separated by low agarose electrophoresis. After separation the gel was observed with a transilluminator and the band or region of interest was excised with a sterile razor blade. DNA extraction from agarose gel was done by centrifugation. LSKG ELO 50 filters (Millipore) were used for gel slices under 150 μg of weight. 1500 μg Ultrafree-CL filters (Millipore) had to be used for slices up to 1,500 μg. The gel slices were placed in filter columns and spun for 30 minutes at 5,000 g. DNA from the filtrate was precipitated with ethanol and sodium acetate to remove agarose and TAE buffer.

2.3.5 Amplification of DNA with Polymerase Chain Reaction (PCR)

In this study the technique of PCR was used extensively. Therefore, I have included this section containing a general overview over the method.

PCR can be used to directly amplify specific DNA parts when the sequences of both ends are known. This makes it a powerful tool for detecting known mutations,

constructing new plasmids, creating markers for Southern Blots easily and even discovering new mutations (see section 2.3.8).

In general, genomic or plasmid DNA has to be heated at 94°C to be denatured into single strands. Thus, two synthetic oligonucleotides are allowed to anneal at the complementary parts of the DNA fragment of interest. The annealing temperature corresponds to the melting point of the primers. It is lower than the template's due to its smaller size. The primers were added in large excess to guarantee a strong binding. During extension time at 72°C the bound primers were enlarged with a supply of deoxynucleotides and with a temperature-resistant, DNA-dependant DNA polymerase. The extension times varied according to the size of the fragment.

After these steps the entire mixture was heated again to denature the newly formed DNA duplexes. That allowed further amplification. 30 to 35 cycles were repeated for one PCR. At the end the samples were cooled at 4°C.

The reactions were carried out in 100 μl Eppendorf tubes. One vessel contained 0.1 ng genomic DNA (plasmid DNA around 100 times less), 50 pmol each of forward and reverse primer, 5 μl of 10x PCR-buffer (Finnzymes), 1 μl of dNTPs (10mM, Finnzymes), 0.5 μl Taq polymerase (2 U/μl, Finnzymes) and sterile double-distilled water. The final volume was 50 μl. (see Table 2.1 and Table 2.2)

Table 2.1 PCR set-up		
Intial	first denaturation	5 min. 94°C
30-35 cyles	denaturation of DNA	1 min. 94°
	annealing primers	1 min.. x°C
	extension step	y min. 72°C
Final	final extension	4 min. 72°C
	cooling	at 4°C

x: annealing temperature depends on primer sequence (see Tab 2.2)
y: extension time depends on fragment size: <1.5 kb = <1min.
                                              >1.5 kb = 1-2 min.
                                              >4.0 kb = >2 min.

Table 2.2	PCR Primers used in this study		
name	**sequence**	**Tm°C**	**purpose**
T3	5´-AAT TAA CCC TCA CTA AAG GG-3´	53.2	DIG -
T7	5´-TAA TAC GAC TCA CTA TAG GG-3´	53.2	labeling
pBsk(-) T3	5´-GAA TTA ACC CTC ACT AAA GGG AAC A-3´	59.7	
pBsk(-) T7	5´-TTG TAA TAC GAC TCA CTA TAG GGC G-3´	61.3	
nT3-SK	5´-AAG CTG GAGG CTC CAC CG-3´	57.6	plasmid
bar2.1	5´-TCA AGC ACG GGA ACT GG-3´	55.2	rescue
bar2.2	5´-CAG CCT GCC GGT ACC GC-3´	62.4	
bar2.3	5´-TGC CCG TCA CCG AGA TC-3´	57.6	
bar2.4	5´-GCC CGT CAC CGA GAT CT-3´	57.6	
cpc1-Rev	5´-AAC ATTA TGG ATG CGC GC-3´	52.8	
frq1 5´	5´-GGT GCT CCG GAT GCG GAA A-3´	61.0	frq1
flbd 3´	5´-TTT CGG AGA CAG CTT GGC G-3´	58.8	mutant
frqwt 5´	5´-GTT GCT CCG GAT GCG GAA G-3´	61.0	screen

2.3.6 Plasmids

Two different plasmids were applied in this study. Vector pKSbar2 was used primarily for mutant production in *Neurospora crassa* (see section 2.3.10), while the plasmid pBsk-II was used for plasmid rescue in mutants (see section 2.3.7).

2.3.6.1 Plasmid pKSbar2

The circular plasmid pKSbar2 is 4014 bp large and consists of two open reading frames (ORFs). One is coding for a BASTA resistance protein (a phosphinothricin acetyltransferase) and the other for an ampicillin resistance protein (beta-lactamase). Moreover, the vector sequences for the T3 and T7 promoters. U. Schulte donated the plasmid (see figure 2.1):
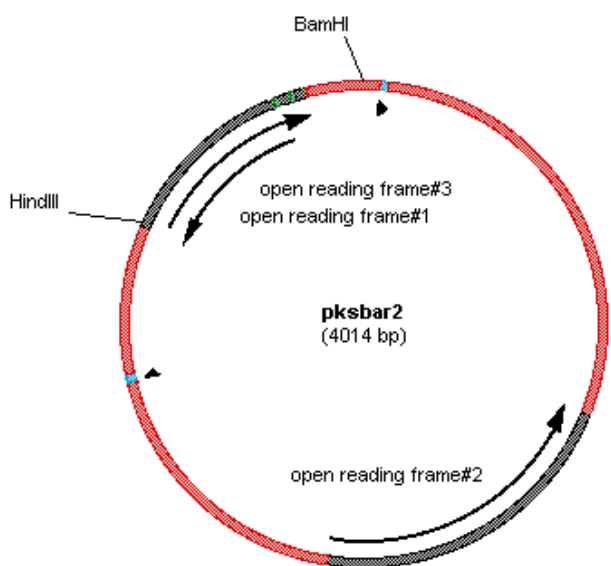
Fig.: 2.1 pKSbar2
Arrows depict the ORF of BASTA resistance gene (baR) and Ampicillin resistance gene (ampR) respectively. The plasmid was linearised by restriction with BamHI prior to electroporation.

2.3.6.2 Plasmid pBSk-II

pBSk-II is a commercial plasmid, delivered in an aqueous solution (Stratagene Inc.). It has 2961 bp and possesses two ORFs. One gene encodes for an ampicillin resistance protein (beta-lactamase) and the other gene for a beta-galactosidase, applicable for a blue/white screening in E. coli. This vector is ideal for gene cloning and rescue, especially when it contains the T3 and T7 promoters. To avoid degradation of plasmid DNA at -20°C, we constructed a plasmid library in E. coli as background stock.

2.3.7 Southern Blot Assay

A Southern blot is a method of enhancing the result of an agarose gel electrophoresis by marking specific DNA sequences. The probe shows which of the fragments of the electrophoresis separation contains a certain DNA sequence. In this study we performed the Southern blot with DIG-labelled markers rather than radioactive-labelled ones (DIG Application, Roche). This system provides a safe,

non-radioactive method for working with stable probes and short exposure times on x-ray films.

2.3.7.1   Construction of Marker-DNA

The preparation of DIG-labelled markers was applied with the PCR-DIG-Probe Synthesis Kit (Roche). The template used for the marking step was the BASTA resistance gene bar in the circular plasmid pksbar2. The PCR reactions were carried out according to the company's protocols:

5 µl of PCR buffer (Roche)

5 µl of PCR-DIG mix (Roche; DIG-dUTP: dTTP ratio 1:6)

 or 5 µl of 10 x dNTPs stock solution (no-DIG control)

10-50 pg of plasmid pksbar2

 or no DNA (no-DNA control)

0.5 µM each of upstream and downstream primer: T3 and T7

0.75 µl of Enzyme mix (Roche; Expand high fidelity)

up to a final volume of 50 µl

The samples were put on ice for the whole pipetting step.

The PCR regime was set to:

Initial denaturation at 95° C for 2 minutes

30 cycles of: denaturation at 95°C for 30 seconds

annealing at 57°C for 30 seconds

elongation at 72°C for 40 seconds

Final elongation at 72°C for 7 minutes

Stored at 4°C.

The PCR results were checked on an 0.8% agarose gel (stained with EtBr) containing the DIG-marked samples, a standard molecular weight ladder, the linearised plasmid pkSbar2 (BamHI), the no-DNA control and the no-DIG control.

Both the labelled experimental probe and the unlabelled control sample were clearly visible on the agarose gel. The unlabelled control probe showed the predicted size of 1.2 kb. The DIG labelled experimental probe migrated more slowly and therefore appeared to be larger than expected by about 200 bp.

After the gel purification of the DIG-labelled band (Millipore: gel purification columns) the concentration of marker was estimated by direct colour detection

with the chemicals NBT/BCIP (Roche). First, two series of a standardised and defined dilution-set of DIG-labelled control DNA (Roche) and a sample of gel purified DIG-labelled marker of undefined concentration were pipetted onto a nitro-cellulose membrane. After UV-crosslinking the membrane was incubated in blocking solution, then exposed to an antibody solution (Anti-DIG), thoroughly washed in washing buffer and covered with a colour substrate solution (freshly prepared NBT/BCIP + detection buffer).

The moistened membrane was allowed to develop in the dark for half an hour.

The two series were compared to each other and the concentration of the DIG-labelled marker was estimated.

2.3.7.2 Preparation of DNA Samples

After the extraction of genomic DNA and the measurement of concentration and quality (see section 2.3.1.1 and 2.3.2.1) the samples were digested by restriction enzymes at 37°C over night.

The digested DNA samples ran in an 0.8% agarose gel at 20 V for 16 hours for a better separation of large DNA fragments (>4 kb, pKSbar2).

After electrophoresis the gel was photographed beside a ruler to facilitate measurements in the photograph.

2.3.7.3 Blot

After gel separation the fragments were transferred to a nitro-cellulose membrane (Hybond-N, Amersham Biosciennce) through capillary transfer. The gel was first soaked in 0.2 M HCl for 20 minutes at room temperature with gentle shaking, then in two changes of denaturation solution (see appendix) for 20 minutes each. Subsequently it was immersed in neutralisation solution (see appendix) twice for 20 minutes each time.

Afterwards, the gel was placed upside-down on a sheet of Whatman-paper, which was previously soaked in 20 x SSC (solution of sodium citrate, see appendix). The nylon membrane was put tightly onto the gel and covered by two sheets of Whatman paper. Both paper towels and weights were put on top of each other, too. The blotting took place over night.

After an UV-crosslink (UV Stratalinker at 120 mJ) to immobilise the DNA, the sample was ready for hybridisation.

2.3.7.4   Prehybridisation and Hybridisation

The membrane was placed in a hybridisation tube containing 15 ml of Prehybridisation solution at 50°C for 2 hours. Afterwards it was incubated in hybridisation solution at 50° C overnight, containing the heat denatured DIG-DNA probe in a final concentration of 15 ng/μl.

2.3.7.5   Detection

On the following day, the membrane was first washed twice in a 2x wash solution for 15 minutes each at room temperature and subsequently equilibrated two more times in a 0.2x wash solution at 68°C to remove impurities on the membrane.

At this point the loaded nitro-cellulose was ready for detection steps with CSPD (Roche). This substance is a chemiluminescent substrate for alkaline phosphatase; its enzymatic dephosphorylation generates a phenolate anion, which decomposes and emits light. The luminescent light was recorded on X-ray films.

These crucial steps of detection were performed in the following way:

The membrane was blocked in blocking solution with gentle shaking for 60 minutes. After this step it was incubated in antibody solution (see appendix) for 30 minutes. After the binding procedure the membrane was rinsed and washed in washing buffer (see Appendix) at least 2 times for 15 minutes each. After the removal of surplus antibodies the membrane was equilibrated in a detection buffer (see Appendix) for 2 minutes. At this stage of the procedure, care was taken to prevent the membrane from drying out. The nitro-cellulose was placed carefully in a clean plastic bag. 0.5 ml of chemiluminiscent substrate was spread evenly over the membrane and after 1 minute excess liquid was removed. The plastic bag was sealed and incubated at 37°C for 15 minutes. As a last step the sealed membrane was exposed to X-ray film. Each membrane was subjected to multiple exposures of different length.

Based on the markings on the membrane and photographs of the gel, each fragment was calculated according to the localisation of the positive probe

(pksbar2 $\cong$ 4kb) that contained the bar gene. The linearised plasmid could be seen both on the agarose gel and on film as a clear band.

2.3.8   Plasmid Rescue of *Neurospora crassa* Mutants (SSFPR)

Mutants selected by the screening test (see section 2.2.4) had to be characterised genetically. Because of the unknown position of plasmid in the mutant's genome, a new method of rescue had to be developed. Therefore the method of inverse-PCR (I-PCR) (Ochman and Gerber, 1988) and the technique of subgenomic DNA libraries (Seed and Parker, 1982) were modified and applied. The new method of plasmid rescue was called *Single Size Fragmentation Plasmid Rescue* (*SSFPR*). Several procedures had to be executed step by step to obtain the exact localisation of the integrant and adjacent DNA. Due to its complexity the method will be presented here in three parts:

- Restriction mapping
- Cloning and PCR
- Verification of sequencing

2.3.8.1   Restriction Mapping of the Mutant's Genomic DNA of Interest

This method begins with the digestion of genomic DNA from the target tissue by a variety of restriction enzymes individually and in combination, which had cutting sides in and outside the integrant. Endonucleases with six base-pair recognition sequences were used first (e.g. SpeI, AvaI, StuI, ScaI, XbaI, HindIII, ClaI and XhoI). Thus it was possible to create a restriction mapping using the Southern Blot technique with a hybridisation marker that probed against the BASTA resistance gene of pKSbar2 (see section 2.3.6). This made it possible to determine the integrity of the vector, and to roughly estimate its putative chromosomal localisation (Bloch, 1987; Danna, 1980). Moreover, the number of insertions in clock mutants (*komo*) could be determined exactly. Blotting results were compared with predicted fragment sizes of the plasmid (Gene Construction Kit). Especially the digestions of HindIII or XbaI were of tremendous interest because they allowed

usage of the multiple cloning site regions in pBsk-II flanked by high efficient promoter sites (see figure 2.2 A and B).

2.3.8.2   Size Fractionation of Genomic DNA and Cloning into pBsk-II

For a plasmid rescue at least 20 μg of genomic DNA had to be digested with several restriction enzymes (see section 2.3.3). Therefore, a multiple digestion was performed with HindIII or XbaI and additional endonucleases (see above), which cut outside the pure HindIII or XbaI sites. This restriction procedure should guarantee r a less complex genomic DNA.

Digested genomic DNA ran on an 0.8% agarose gel at 55 V for 60 minutes.

A piece of gel was cut out at the place of interest (the predicted HindIII or XbaI fragment) within a distance of 0.5 kb. This protection zone had to be included for circumspect excision considering the absence of any bands.

After gel purification (see section 2.3.4) the DNA was suspended in 10 μl of water.

The aqueous DNA solution was quantified (see section 2.3.2.1) and adjusted according to the formula for insertion-vector ratio in ligation experiments, considering the unknown amount of DNA of interest in the fractionated sample.

Therefore, an experiential multiplier of 10 was added to this equation (Cranenburgh, 2004):

$$10 \times \text{weight of insertion (ng)} = \frac{\text{weight of vector (ng)} \times \text{lenght of insertion (bp)}}{\text{lenght of vector (bp)}}$$

After overnight ligation with 20 ng of HindIII or XbaI linearised pBsk-II at 16°C, the samples were heat inactivated and precipitated with ethanol to remove salts and impurities, which could inhibit PCR reactions. A non-genomic DNA sample with only linearised pBsk-II was always added to the ligation experiments as a control (see figure 2.2 B to D).

2.3.8.3   Inverse PCR and Nested PCR

The amplification of the DNA with a polymerase chain reaction was the core and crucial step of plasmid rescue. To this end, 0.5 μl of each purified ligation

experiment (vector + insert and vector – insert) were used as a template for the first PCR (see section 2.3.5 for PCR regime). The pBSK-T3 and pBSK-T7 primers were designed to bind exclusively at the T3 and T7 promoter binding sites in the MCS region of the clonal vector pBsk-II.

The bar primers (bar2.1 to bar2.4) were constructed as a correspondent primer set, which binds at the BASTA resistance gene in the plasmid pKsbar2.

Due to the unknown orientation of the inserted plasmid in the HindIII or XbaI digested MCS region of pBsk-II, both primer combinations (T3 - bar2.1 and T7 – bar2.1) had to be supplied in PCR samples.

5 μl of a 1:10 dilution of the results of the first PCR were used as template in the second amplification step. In opposition to the previous PCR, the primer bar2.2 was used instead.

No-DNA samples were always included in the PCR reactions as controls.

Afterwards, the second amplification all PCR samples was checked on an agarose gel electrophoresis. When the band of interest appeared, calculated with the results of restriction mapping, it was picked out, purified and sent for sequencing (Medigenomix, Munich) (see figure 2.2 E).

2.3.8.4   Verification of Sequencing

Results obtained by sequencing procedure had to be checked. Therefore, new primer sets for the PCR reactions were constructed that bound outside the plasmid pKsbar2, upstream and downstream in the region of flanking genomic DNA. If the insertion was determined correctly, a continuos PCR fragment of distinct length with defined cutting sites would result. Otherwise a longer fragment or multiple fragments would indicate to chromosomal rearrangement (see section 1.4.2).
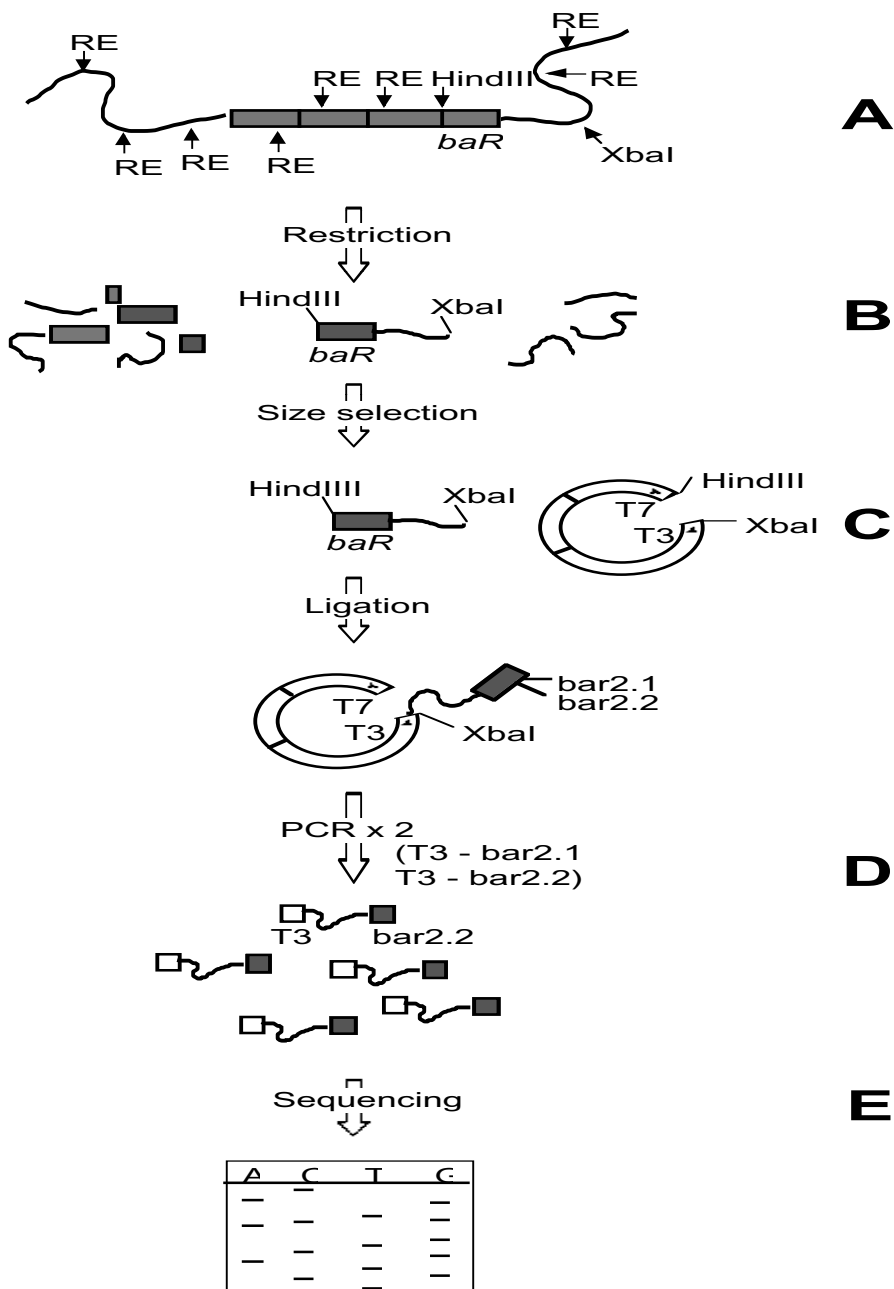
Figure 2.2. Depiction of the new rescuing method *(SSFPR)*

A restriction map of the DNA region of interest was performed (**A**). Hence the appropriate size of the insertion site was calculated and purified (**B-C**) in order to clone into an expression vector (**D**). Hence subsequent PCR reaction could be done. (**E**) Sequencing

2.3.9 Construction of a Plasmid Library

2.3.9.1 Plasmid Assay

The circular plasmids were checked for integrity, quantity and pureness.

The following enzymes performed multiple digestions: HindIII, XmnI, XholI, BamHI and the combination XholI/HindIII (supplied by New England BioLabs Inc.). Digestion was performed among the company's protocols and individual buffers (see section 2.3.3). After overnight digestion at 37° C the DNA samples and a standard ladder (New England BioLabs: 1 kb) were loaded on an 0.8% agarose gel in a TAE buffer (TrisAcetat-EDTA) and ran at constant voltage (100 V) for 45 minutes. The bands on gel were photographed and their size calculated according to the reference ladder. In addition, the concentration of plasmid DNA was measured by a spectrophotometer and on agarose gel (see section 2.3.2)

2.3.9.2 Production of Electrocompetent *E. coli* Cells

For electroporation the XMN cells had to be electrocompetent viz. susceptible to plasmid DNA. Therefore, E. coli cells were streaked to an LB plate without ampicillin. After overnight incubation at 37°C a single colony was picked and transferred to an overnight culture in 3 ml of LB-medium (Luria Broth, see Appendix). On the next day 2 ml of the overnight culture were added to 0.5 l of LB and the culture was shaken at 37°C until growth reached the mid-log phase (OD600 = 0.5 – 0.6).

From this point every step was performed in the cold room, and all instruments were chilled on ice before use. The culture was split into four sterile 125 ml centrifuge bottles and spun for 15 minutes at 4000 g at 4°C. After decanting the supernatant the pellets were suspended in a total of 0.5 l HEPES (see appendix) and spun again under the same conditions. The supernatant was removed again and the cell pellets were suspended in 10ml of ice-cold 10% glycerol. The next centrifugation step was done in two 15 ml falcon tubes. After centrifugation in glycerol the supernatant was removed by careful pipetting. At the end the pellets were suspended again in 2 ml of ice cold 10% glycerol and aliquoted to 50 μl. The samples were immediately frozen and stored at -70°C.

2.3.9.3   Transformation of *E. coli* by Electroporation

For each transformation an 0.2 cm long sterile electroporation cuvette was cooled on ice. Electrocompetent E. coli (see section 2.3.9.3.) was thawed on ice. The electroporation instrument (BioRad Gene Pulser, BioRad) was set at 2.5 kV, 200 ohms and 25 microfaradays. 1 μl of DNA from the supplied tubes or from negative control samples was added to 40 μl of *E. coli* suspension. The cells were immediately placed into the ice-cold cuvette. After deliverance of a 5 ms long electric pulse the cells were immediately transferred into a sterile test tube filled with 1ml of SOC (see appendix). The recovery at 37°C took 1 hour. Afterwards the cells were placed in a 1.5 ml Eppendorf tube and centrifuged briefly. The supernatant was removed and cells were resuspended with the remainder of the media. Cells were plated on a petri dish with LB-Amp-agar media.

2.3.10   Mutant Production in *Neurospora crassa*

pKSbar2 was first linearised with BamHI in an overnight digestion at 37°C.
The BamHI site in the vector was unique. The results were checked on an 0.8% agarose gel in a TAE buffer and ran at constant voltage (100V) for 2 hours. After gel purification (Millipore: gel purification columns) the vector was aliquoted in aqueous solution and restored as a working sample at -20°C.

2.3.10.1   Preparation of Conidia

A 500 ml Erlenmeyer flask with 100 ml of minimal media was inoculated with conidia from the working stocks. After 7 days of growth the conidia were harvested with about 50 ml of 1M sorbitol and filtered thorough a layer of several sterile cheesecloths to remove mycelial fragments. The suspension was centrifuged (Heraeus) at 2000 rpm at 4°C for 10 minutes and the supernatant was decanted. Again 50 ml of 1M sorbitol were added to the pellet and gently shaken. The washing and spinning steps were repeated four times. The concentration of conidia was measured by a spectrophotometer (Beckman UV-DU-64) with a maximum of absorption at 420 nm. The measured suspension was adjusted to the

final concentration of 2.5×10^9 conidia/ml (1 OD 420nm = 2.86×10^6 conidia/ml). The purified conidial solution was kept on ice to prevent germination until electroporation was performed.

2.3.10.2   Electroporation of Conidia

40 μl of washed conidia, 10 μl of linear plasmid (0.25 μg/μl) and no-DNA samples were put together in an Eppendorf tube and chilled on ice for 5 minutes.

After that period the mixture was set into a 0.2 cm sterile ice-cold cuvette and quickly set under electrical shock. Electroporation of Neurospora conidia was performed according to Margolin et al. (1997). The electroporation parameters (BioRad Gene Pulser) were set at a voltage of 1.5 kV/cm, the capacitance at 25 μF and the resistance up to 600 Ohms. Conidia were immediately recovered in 1 ml of 1M sorbitol and carefully mixed. Afterwards 10 μl of the solution was pipetted into 10 ml of molten TopAgar (see Appendix) and slightly turned around. The warm media was poured onto a plate containing 25 ml of BottomAgar (see appendix) with an addition of 3% BASTA. After the media had solidified, the plates were incubated at 30°C for at least 48 hours until colonies were observed. The colonies were picked up with a sterile needle and inoculated into small minimal media slants with 0.5% of BASTA, then incubated at 30°C for 1 day until mycelia was seen. Room temperature was appropriate for further growth. Mutants were screened in temperature cycles (see section 2.2.4). The slants were stored in the dark at 4°C.

2.3.11 RNA Methods

2.3.11.1   RNA Extraction

Frozen *Neurospora* tissue was ground with liquid nitrogen and sand using a mortar and pestle. The addition of sand was necessary to obtain good homogenisation. Powdered frozen mycelial tissue was added to 600 µl of RNA extraction buffer (see Appendix) and 500 µl "phenol for RNA extraction", pH 4.5-5.0 (see Appendix). The tube was vigorously vortexed (in 10 minutes intervals) and shaken

at maximal speed (300 rpm or more). After 30 min of extraction, the samples were spun at 28,000g at 4°C for 30 minutes. The supernatant was removed to 500 µl of chloroform:isoamylalchocol (24:1), vortexed, briefly extracted and spun. After this second extraction, the supernatant (300-400 µl) was precipitated with 40 µl of 3 M NaOAC and 1 ml of ice cold 100% ethanol for 1-2 hours at -20°C. The sample was centrifuged at 28,000g at 4°C for 30 minutes.

The supernatant was removed and the pellet was washed with 70 % ethanol. Once all ethanol had been removed, the pellet was air-dried for 20 minutes with a vacuum centrifuge. For Real Time PCR analysis samples the pellet was dissolved in 1X RNAsecure reagent (see Appendix) and treated according to the company's instruction manual.

2.3.11.2 RNA Quantification

The concentration of RNA was determined spectrometrically. Absorbances at 260, 280 and 320 nm were determined. A ratio of $OD_{260}:OD_{280}$ between 1.8 and 2.0 indicates an absence of phenol. OD_{320} was always lower than 0.01, indicating a low level of protein contaminants. Calculations assumed that at 260 nm, an absorbance of 1.0 in a cuvette with a 1 cm path length indicates 40 mg/ml RNA.

2.3.11.3 Real Time PCR Analysis

For all RT PCR assays, a two-step SYBR green assay was applied. In the first step samples were reverse transcribed with random hexamers and, in the second, they were quantified in a Real Time PCR reaction.

2.3.11.4 DNase Digestion and Reverse Transcription

For Real Time PCR analysis RNA samples were prepared as described. To remove residual DNA, RNA samples were treated with RNase-free Dnase 1 (Roche) at a final concentration 3 U/µl (Unit definition according to Roche) in 1X a Dnase1 buffer (see Appendix). In the DNase1 mixture, the final RNA concentration was 0.1 µg/µl. The incubation was 10 min at 25°C followed by 10 min at 65°C.

RNA was reverse transcribed to cDNA in a three-step incubation: 10 min at 25°C, 30 min at 42°C and 5 min at 95°C. For reverse transcription I used chemicals from an AB Kit for reverse transcription (Reverse transcription reagents N8080234). Final concentrations were as follows:

RNA (final concentration) 0.02 μg/μl

Reverse Transcriptase buffer 1X

MgCl2 5.5 mM

dNTPs 500 μM each

Random hexamers 2.5 μM

RNase inhibitor 1 U/μl

Reverse transcriptase 3.125 U/μl

Water Up to desired volume

Volume of reaction: min 25 max 100 μl

After reverse transcription samples were diluted 1:1 with RNase free water.

2.3.11.5 Primer Design

Primers for RT PCR reaction were designed with Primer Express software version 2.0 (Applied Biosystems). The desired DNA sequence was copied into a blank 'DNA PCR Document'. All primers were chosen based on following parameters:

Minimum melting temperature 58°C

Maximum melting temperature 60°C

Optimum melting temperature 59°C

Minimum GC % 20

Maximum GC % 80

3' GC clamp of 0 residues

Minimum primer length 9

Maximum primer length 40

Optimum primer length 20

Minimum amplicon melting temperature 0°C

Maximum amplicon melting temperature 85°C

Minimum amplicon length 50 bp

Maximum amplicon length 150 bp

Care was taken that primer pairs have a 'penalty score' lower than 10 points. All primers were ordered (from SigmaARK, http://www.sigma-ark.com/ or Metabion, http://www.metabion.com/) as HPLC purified. The final concentration of primers in the RealTime PCR reaction was 200 nM.

2.3.11.6 Real Time PCR Analysis

An ABI Prism 7000 Sequence Detection System was used.

The thermal cycler was set for three stages:

- Stage 1: 50°C for 2 minutes
- Stage 2: 95°C for 10 minutes
- Stage 3: 40 cycles of: 95°C for 15 seconds followed by 60°C for 1 minute.
- Volume of the samples: 25 µl
- "Emulation" of the 9600 ABI instrument was disabled.

All detectors were set for the fluorescent dye SYBR Green, which does not require a quencher. ROX was used as a passive reference.

Dissociation analysis was used to check the quality of PCR products by determining the dissociation temperature of the amplicon. This analysis is available when the SYBR Green based chemistry is used. It was used when a new set of primers was characterised. Once the run was finished, the raw data was saved and the instrument was disconnected. To analyse the data, seven sub-tabs in the "Results" tab of the ABI 7000 software were checked and set according to the instruction manual. Once all of the criteria were satisfied and the analysis finished, the plate document was saved. The results from the Report tab were printed or exported as a comma-separated .csv file.

List of primers for Real Time PCR analysis:

Name	Sequence
G8E07-FO	CGATGCCGTTGGCTTAATAGA
G8E07-RE	AAAAGGGAACTCGGCACCA
frq-FO sy1	CGC CTT GCG CGA GAT ACT AG
frq-RE sy1	TCC CAG TGC GGA AGA TGA AG

2.3.12 Protein Methods

2.3.12.1 Protein Extraction

Tissue was harvested with blotting or vacuum filtration and frozen in liquid nitrogen. Frozen tissue was homogenised with a mortar and pestle with liquid nitrogen and 200-300 µg of sand. The ground tissue was added to 1.5 ml tubes with 300-500 µl of protein extraction buffer (see Appendix). The volume of protein extraction buffer and pulverised mycelia should be approximately the same. The ground tissue was mixed vigorously by vortexing and incubated on ice for 20 minutes. Additional vortexing during the incubation increased the yield. Samples were centrifuged at 2°C for 20 to 40 minutes and the clear supernatant was removed and stored at -20°C or -75°C.

2.3.12.2 Protein Quantification by Bradford Assay

1 ml of 1x Bradford reagent (see Appendix) was pipetted into 1.5 ml disposable test tubes. 10 µl of protein solution was added and mixed by inverting the tube a few times (not vortexing). Development time for this reaction is 5 min. OD595 was measured within the next 15 minutes to prevent error due to protein precipitation and subsequent colour loss. Each assay was accompanied by the generation of a new standard curve. As a protein standard, we used bovine IgG or BSA (see Appendix). A standard curve was determined as a best linear fit for 4-5 dilutions of the standard protein solution.

This formula was applied to samples with unknown concentrations. For these calculations, the Kaleidagraph program was used (www.synergy.com). The Bradford assay remained linear only in the range of 0.1-0.7 (A595). Care was taken to ensure that the absorbance of unknown protein samples did not fall outside of this range. If the protein concentration of the sample was too high, dilutions were made. Disposable plastic cuvettes were used to prevent errors arising from dye carryover in the cuvette and on cuvette walls.

2.3.12.3 Protein Electrophoresis SDS-PAGE

For SDS polyacrylamide gel electrophoresis, two different gel apparati were used:

- BioRad Mini-Protean II cell
- Custom made gel apparatus (see Appendix for specifications)

The gel sandwich was assembled according to the manufacturer's instructions for the Biorad setup. For the custom-made gel apparatus, a gel-sandwich was assembled with heavy-duty paper-clips. Plates and spacers should always be perfectly flush before tightening the sandwich assembly. A mark 2.5 cm below the top of the front plate (with a section cut out) was made to indicate where the "separating" or "running" gel should stop. Liquid 1% agar or agarose was added to bottom of the base to prevent leakage and then the plate sandwich was inserted. A toothpick was stuck between the base and the glass plate to insure a tight seal. The agar solidified in 10-15 min, the running gel (see Appendix) was added and covered with isopropanol to prevent contact with air and allow polymerisation. After polymerisation (45 min to 1 h) isopropanol was entirely washed out with water and the gel was briefly dried. A stacking gel (see Appendix) was poured on the solidified running gel and a comb was inserted and fixed with a paper-clip for the next 30 min. Prior to running, the gel-sandwich was placed in an electrophoresis chamber. Protein extracts were denatured in 1x Laemmli buffer (see Appendix) at 95°C for 5 minutes, cooled at room temperature and briefly spun. Prior to loading, the wells were washed with running buffer (important). Electrophoresis was run at 80 V for 1.5 hours and then changed to 125 V. The electrophoresis was run until the dye reached the end of the gel.

2.3.12.4 Western blotting

Nitrocellulose was used for all applications because it has a high ability of protein-binding and is compatible with different kinds of stains. Blocking for unspecific antibody binding is simple, and it is relatively inexpensive.

2.3.12.4.1 Wet Blotting

For wet blotting I used two apparati: Biorad trans blot cell and Biorad mini protean II cell. For the transfer buffer, 2x transfer buffer (see Appendix) without SDS and with 20% (v/v) methanol was used. This buffer was kept at 4°C. The blotting chamber was filled with transfer buffer until it was 3/4 full. The opened transfer cassette was submerged in a shallow tray, half full with the transfer buffer. On each side of the transfer cassette a well-soaked fibre-pad was placed. The gel was wetted by pouring 10-20 ml of buffer onto it. A wetted sheet of nitrocellulose (see Appendix) was placed on the gel and in turn covered with wetted Whatman paper over. A small glass test tube was rolled over the sandwich to remove any air bubbles. This sandwich was carefully removed from the other glass plate, turned upside-down and placed on the same glass plate. Another Whatman paper was placed on the gel, bubbles were removed and the sandwich was placed in the opened transfer cassette. The sandwich was covered with the second fibre-pad, and then the cassette was closed and slid into the buffer tank (when the Biorad protean II cell was used, a frozen cooling unit was also inserted). The tank was topped off with transfer buffer. A stir bar was inserted into the chamber and the entire apparatus was placed on a magnetic stir plate. The electrode-lid was attached and the power supply was switched on. For the Biorad trans blot cell, 800 mA (constant current) was applied for 2 h. The electrode distance was always 8 cm. For the small BioRad cell, 100 V (constant voltage) was applied for 1 h.

2.3.12.4.2 Semi-Dry Blotting

For proteins smaller than 80-90 kD, it was also possible to use semi-dry blotting. Custom-made transfer cells with two graphite electrodes (see Appendix) were used. For semi dry transfers, constant current of 2 mA per 1 cm^2 of sandwich area was used. Transfer time was usually 1.5 h.

2.3.12.5   Staining of SDS-Polyacrylamide Gels with Coomassie Blue (CB)

After electrophoresis, the stacking gel was removed from the running gel. The running gel was submerged in CB staining solution (see Appendix). The CB solution and gel were briefly boiled (only for a few seconds) in the microwave oven and incubated for an additional 10 min at RT. After staining, the CB solution was poured off and the gel was rinsed with the destaining solution (see Appendix). To get sufficient destaining, 3 incubations of 15 min in new destaining solution were necessary. For permanent storage gels were dried on 3MM filter paper for 2 h with vacuum and heat (80° C).

2.3.12.6   Staining of Nitrocellulose Membranes with Ponceau-S

To verify the efficiency of Western blotting, proteins transferred to nitrocellulose were reversibly stained with Ponceau-S staining solution (see Appendix). The membrane was rinsed with distilled water and submerged in staining solution for 1-2 minutes. The membrane was destained with water and dried by air at room temperature. To remove Ponceau-S stain, the membrane was soaked in TBS (see Appendix) and placed on a shaker for 10 to 20 minutes.

2.3.12.7   Immunodetection of Proteins

The membrane was blocked in 5% low-fat milk in TBS. The membrane was shaken gently for 1 h at RT, taking care that the entire sheet was in contact with the blocking solution. Primary antibodies were added to the blocking solution and incubated for an additional hour. After incubation, the primary antibody was poured off, the membrane was rinsed three times and washed on a shaker 2 times for 15 minutes with TBS. Secondary, HRP labeled, antibody (see Appendix) was added at a 1:5,000 dilution (for primary monoclonal antibodies) or 1:10,000 (for primary polyclonal antibodies). Membranes were usually incubated with secondary antibodies on a shaker, overnight at +4°C. After this incubation, the membrane was vigorously rinsed a few times and washed in TBS with at least 3 changes. To develop the membrane, a commercial ECL substrate was used (see Appendix). In this part of the procedure, care was taken that the membrane did not dry out. The

nitrocellulose was carefully placed in a clear plastic bag and excess TBS was removed. 1ml of ECL solution was spread over the membrane. After 1 minute, excess liquid was removed, the membrane was placed in a cassette and exposed to X-ray film. Multiple exposures of different length were made for each membrane.

List of antibodies used in this study:

Antibody Antigen Origin

a FRQ (3G11) MPB-FRQ (65-989 aa) (Merrow et al., 2001) monoclonal, mouse

a WC-1 GST-WC-1 (354-838 aa) (Talora et al., 1999) polyclonal, rabbit

a WC-1 (4H4) GST-WC-1 (972-1168 aa) monoclonal, mouse (Goerl, thesis 2002) polyclonal, rabbit

2.4   Genetic Methods

Neurospora crassa shows a haploid genotype in its vegetative stage. As the hyphae are multinucleate and coenocytic at the asexual cycle, they form conidia (macroconidia) with at least 2 nuclei. This study used mainly macroconidia for mutant production (see section 2.3.11).

Mutagenesis with electroporation would insert plasmids randomly into the genome, making a separation into different general classes necessary. Mutants with a single insertion would have differing nuclei. Homokaryons would contain only nuclei with the same insert, while heterokaryons (with single insertions) would contain wild type nuclei besides the mutated ones.

Mutant strains with multiple insertions could also be either homo or heterokaryons. It is possible that one nucleus could contain all multiple insertions, or that the integrants could be distributed among all of the different nuclei that form a genetic mosaic.

A physiological and molecular analysis of heterokaryons would result in unreliable data, unless different purification strategies for homokaryosis were applied. These strategies are described in the following sections.

2.4.1 Homokaryon Test

After the first screening step (see section 2.2.4) the mutant strains were tested for homokaryosis. Therefore, the homogeneity of *Neurospora* nuclei was estimated. Equal dilutions of mutant conidia (50 ml) were pipetted into 20 ml of molten Top Agar containing the selective agent BASTA (0.5 g/l) and agar without the pesticide. The media were poured into plates to solidify. After two days of incubation at 30°C the number of colonies was counted. An equal or comparable number of colonies on selective and non-selective media indicated the homokaryotic nature of the mutant. In contrast to that a higher number of colonies on the non-selective medium de-masked the mutants as heterokaryons (Pittenger et al. 1955).

2.4.2 Purification for Homokaryons

After testing the mutants to be heterokaryonic two techniques were used for vegetative purification.

The first method was an alteration of the homokaryosis test called single colony isolation. One or two colonies were picked from the selective agar and inoculated into small slants containing the pesticide (0.5 g/l). After three days of incubation, the conidia was harvested. Again equal dilutions of conidia were made and plated on the two types of media (see section 2.4.1). The whole procedure of picking and plating took on average three repetitions for each mutant until a comparable ratio of colonies on selective and non-selective media was achieved.

All genetically impure transformants underwent this kind of proceeding as a matter of routine.

In addition to that, this study used a second method of vegetative purification by induction of microconidia on plates (see section 2.2.5). Thus, heterokaryonic insertions could be separated without a sexual cross, avoiding the possible mutational processes (RIP).

The derivatives were checked for their typical abundant phenotype, e.g. in temperature cycles or light-dark cycles. Moreover, the possible separation of plasmids was controlled by Southern hybridisation against the BASTA resistance

gene of pKSbar2. If there was no separation of inserts, these mutants had to be crossed with another strain.

2.4.3 Separation of Multiple Insertions and Linkage Test

After homokaryotic purification by single colony isolation, new clock mutants (*komo*) were crossed with other *Neurospora crassa* strains.

Back crosses with the parental strain *bd* a 30-7 were performed, both to separate uninuclear multiple insertions and to assure in general the association between insertion and mutant phenotype. In addition to that, possible background mutations of komo strains should be removed by mating with wild type genome. The progenies of these crosses were tested for their original abundant phenotype, for their BASTA resistance and for their baR markers, respectively. Therefore the filial generation of mutants with single insert should show segregation in a 2 : 2 ratio for each of these three characteristics. In contrast to that two insertions should assort in a ratio of 2 : 2 : 2 : 2 (A^{bar} B^{bar} : A^{bar} B : A B^{bar} : A B), allowing 3/4 of the progeny to resist the pesticide BASTA. Moreover, the offspring's actual clock phenotype was compared with its number and with the restriction mapping of the insert for loss or any alteration of the original phenotype.

Crosses between new clock mutants (mainly with single insertions) and *frq1* strain were performed to determine genetic linkage between the *frq* locus and the site of insertion.

Therefore, a genetic segregation ratio of 2 : 2 : 2 : 2 (A^{bar} frq^+ : A frq^+ : A^{bar} frq^1 : A frq^1) should be expected, 1/2 of the progeny should be sensitive to BASTA.

In general all genes should assort independently in accordance with the Mendelian rules of inheritance and random spore analysis. Each deviation in the segregation ratio with a lower frequency of recombinant meiotic products (A^{bar} B + A B^{bar} < A^{bar} B^{bar} + A B or A frq^1 < A^{bar} frq^1) would indicate a possible link between these markers (Perkins, 1954).

2.5 Mathematical Fits and Statistic analyses

All mathematical fits were carried out by an iterative, least square method.

- negative reciprocal function in figure 3.2 $y = -1/x*b+c$

- s-curve in figure 3.15 $y = a*(((x+b)/c)/(1+((m0+b)/c)^2)^.5)+d$

- negative exponential function in figure 3.24 $y = exp(-x*a)+b$

- two component cosine function used in table 3.8

    $y = a+b*cos(x/c*p+d)+f*cos(x/c*p+g)$ (p = corresponding cycle length T)

All statistical analyses were carried out with the Excel AddIn "XLStatistics" provided by Rodney Carr (rodneyc@deakin.au), freeware. Furthermore, the statistical tests were applied in accordance with general rules as described by Montgomery and Runger (1999). The descriptive statistics were performed according to Schulze (2000).

Additional data analysis and statistics used in this study:

Fluence titration experiments and the experiments in determining the optimal phenotype (see figure 3.1 and 3.15) were analysed by averaging the race tube data for each strain at each fluence rate or T cycles respectively (3-4 race tubes per strain; all race tubes were used). The degree of Zeitnehmer synchronisation was assessed by periodogram analysis (Sokolove and Bushell 1978, Refinetti 2004). Results were expressed as non-dimensional Qp/χ^2-values or as the percentage of the highest Qp value for a given strain (see figure 3.1 and 4.1). Fluence response curves were fitted as described previously in Dragovic et al. (2002). Qp/χ^2-values above 1 were considered as significant.

The mathematical regression function of table 3.8 was applied according to Roenneberg and Aschoff (1990) and Roenneberg et al. (2005).

In section 3.2.1, the term "differential mutant phenotype" was used in order to describe the mutants` deviation of phase angle reference points in phase onset (Φ_{on}), maximum (Φ_{max}) and offset (Φ_{off}), as well the activity time alpha (α).

3 Results

3.1 Establishing an Optimal Phenotype for Screening Mutants

In this study the *frq+* strain *bd a* 30-7 (*bd*) was used for insertional mutagenesis and would function as a control strain for the upcoming mutant screen in symmetric temperature cycles.

At first, the entrainment behaviour of *bd* a 30-7 on symmetric temperature cycles (22°C cold and 27°C warm) in constant darkness (DD) with different cycle lengths (T= 14 h, 15 h, 16 h, 18 h, 22 and 24 h) on two different media types was tested in order to determine the lowest range of sustainable entrainment. The phase angle onset of conidiation (Φ_{on}) and the Qp/χ^2-ratio of the periodogram analyses were chosen as read-outs (see Methods 2.5 and Roenneberg, 2005).

3.1.1 Different T-Cycles with Standard Race Tube Medium

bd entrained beyond the significance level of a Qp/χ^2-ratio of 1 in all these symmetric temperature cycles on standard medium, except for one sample at T=14 h with a ratio of 0.8. An increase of cycle length revealed higher Qp/χ^2-ratios with a maximum of 3.7 for T= 22 h and T= 24 h.

In order to compare the power of entrainment of *bd* for different T, a relative strength of entrainment was calculated as the percentage of the highest Qp value at T= 24 h, while a threshold value beyond 50% was considered as significant (Dragovic et al 2002). *bd* showed most sustained entrainment in temperature cycles with a T>15 h on standard medium. These results are depicted in figure 3.1.

3.1.2 Different T-Cycles with Minimum Medium

Sustainable entrainement studies for longer T (e.g. 24 h) on minimal media were shown earlier by Merrow et al. (2003). In order to retest the hypothesis of abundant entrainment in short temperature cycles (T= 14 h, 15 h and 16 h) these experiments were carried out on minimal media. The Qp/χ^2-ratios of all *bd*

samples were below the significance level of 1, and showed rather conidiation periods with lengths of 21 h to 23 h (see figure 3.2).

In summary, a sustainable synchronisation of the *bd* strain was found in T-cycles longer than 15 h on standard race tube medium. In shorter T-cycles *bd* tends to show a conidiation period between 20 and 23 hours, thus representing the specific free running period (τ) dependent on the nutritional surroundings, as described by Merrow et. al. (2003).

Therefore, a temperature cycle with T= 16 h on standard medium was chosen as a basis for the mutant screen with abundant phenotypes in order to bypass possible nutritional effects.
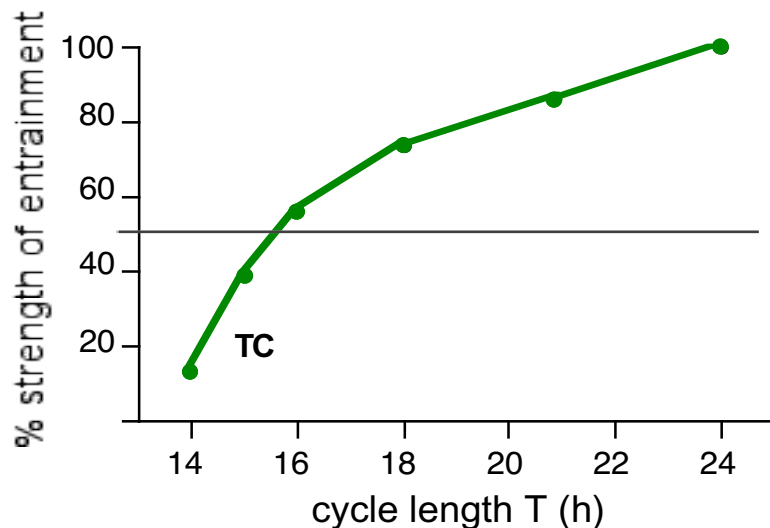

Fig. 3.1. Strength of entrainment in different T-cycles for standard race tube medium. Green dots represent the average of 3 race tubes of *bd* for each T-cycle (x-axis). The relative strength of entrainment (y-axis) was expressed as the percentage of the highest Qp-value (here for T= 24 h). Entrainment strength showed a stronger decrease between T=14 and T=16 h. At T=16 h, strain samples entrained more strongly than in T=15 h. The dashed horizontal indicates the 50% threshold.
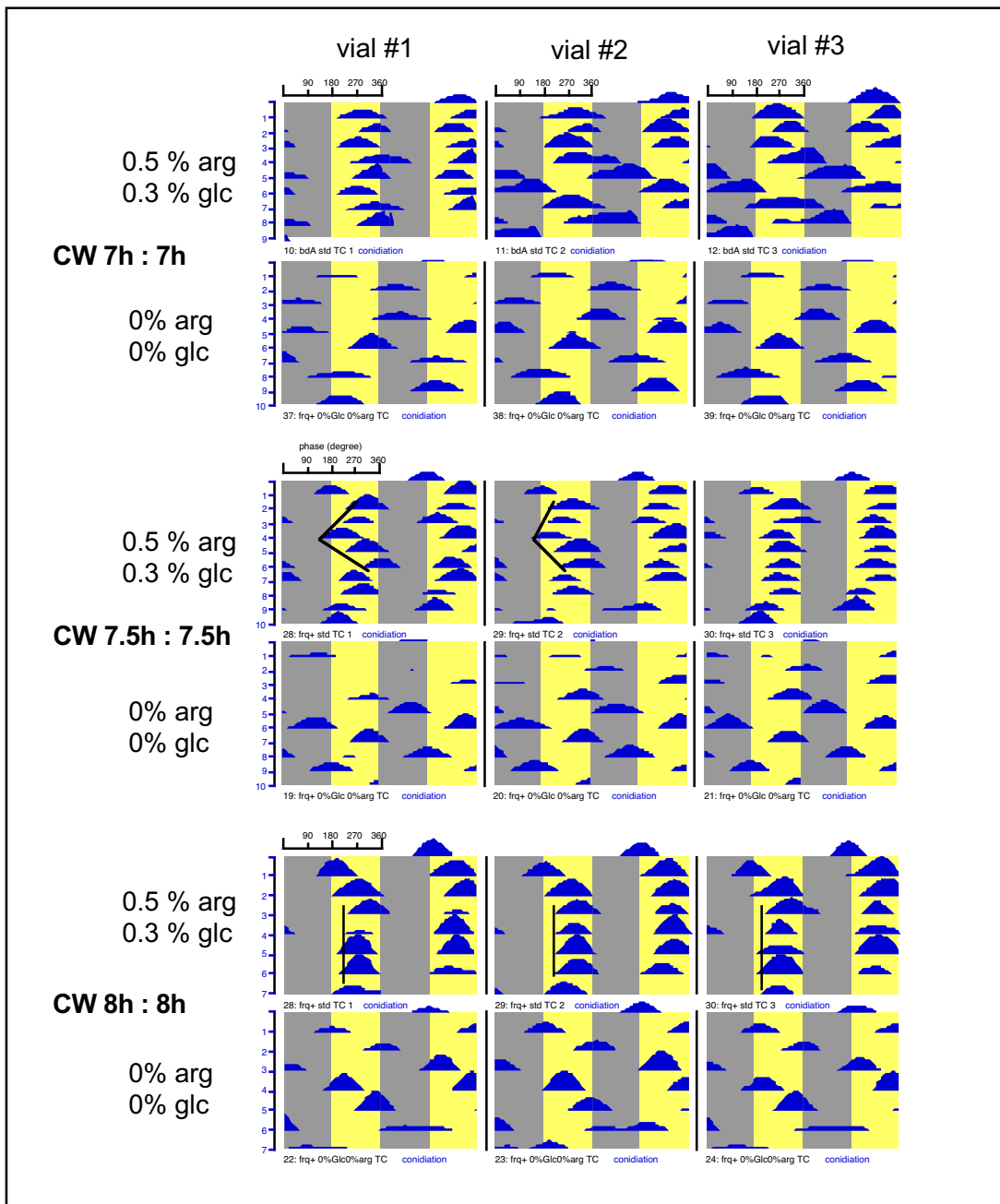
Fig.: 3.2. Comparison of entrainment behaviour on different race tube media. *Bd A* 30-7 (frq+) in low amplitude temperature cycles of different T. Conidiation (blue areas) of *bd* was double plotted over one week in order to visualise trends. Grey areas indicate cold phases (22° C) and light areas warm phases (27° C). The length (hours) of cold and warm in each thermoperiod (CW) as well the media type are indicated on the left side. At T= 16 h a straight ordering of conidiation onset is seen on standard medium, indicating a sustained entrainment of *bd* .

3.2 Mutant Screen

The screening assay for mutant chronotypes consisted of three major steps: after electroporation of macroconidia and selection for BASTA, these mutants were tested on 16 h temperature cycles in the first screen for an abundant chronotype. The second screen retested the phenotypes, while the third major step involved the characterisation of entrainment properties in different Zeitgebers (see Methods 2.25 and figure 3.3).
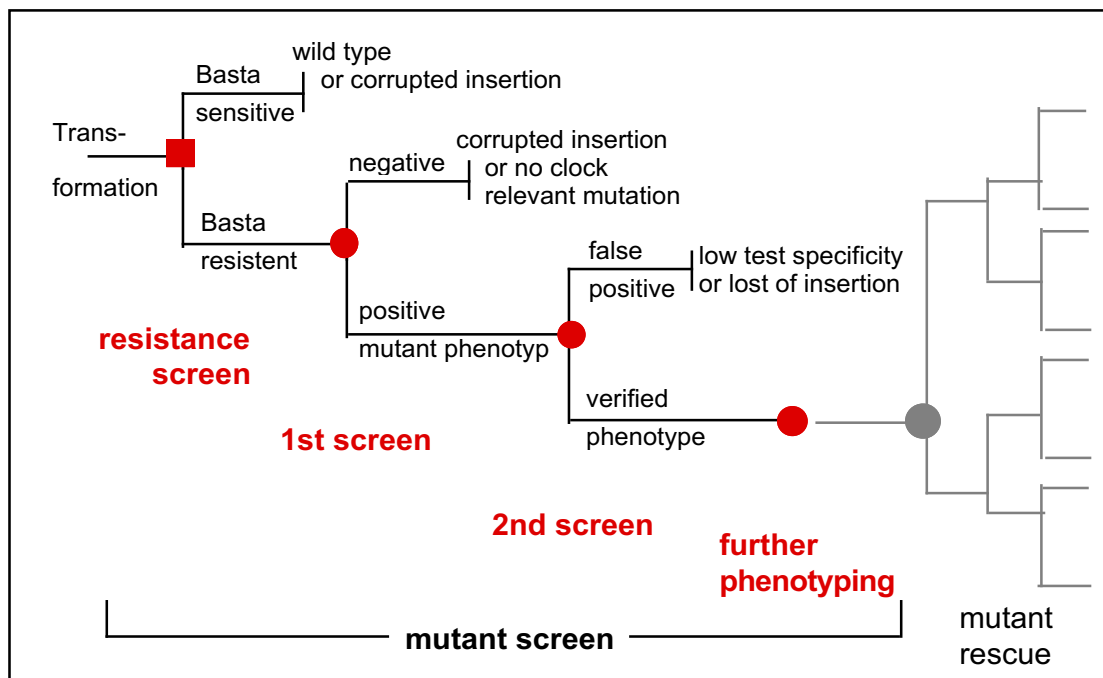

Fig.: 3.3 Mutant screen taxonomy based on possibilities that have to be considered. Dots represent major screening steps for the phenotypic identification. Tests for entrainment properties on different Zeitgebers were generalised as "further phenotyping" (see text for details).

3.2.1 First Step of Mutant Screen

After selection for BASTA resistance, the first screen included symmetrical 16h-temperature cycles (22° C cold, 27° warm) in DD. 748 mutants (*komo*) were screened consecutively in 9 experiments for an altered chronotype.

Results of the first screen of *komo* mutants showed the following:

The phase reference points of *komo* (i.e. onset, maximum and offset of conidiation) showed a higher variability (from +15° to +33°), while the mean conidiation period alpha were equal to the control strain *bd* (F-test and t-test respectively with p≤0.01).

In order to bypass inter-experimental variability of phase reference points a correction of the data ("raw") was performed, calculating the relative difference of phase points between *komo* and the actual control strain *bd* of each temperature box as the so called "differential" mutant phenotype (ΔΨ). Negative values (-) indicate the advancement in phase angle and positive values (+) stand for a delayed phase onset compared to the control strain. Table 3.1 gives an brief overview of the collected data and calculated values.

reference points	*bd* "raw"	*komo* "raw"	*komo* "differential"
	mean (°) ±sd	mean (°) ±sd	ΔΨ mean (°)
Φ_{on} (Phi onset)	210 ± 20	180 ± 40	-15
Φ_{max} (Phi maximum)	281 ± 55	249 ± 54	-33
Φ_{off} (Phi offset)	32 ± 20	362 ± 36	-15
α (alpha)	189 ± 15	190 ± 17	0

Table 3.1 Phase angle reference points of the first screening. The first column describes the mean phase angle points of onset, peak and offset of conidiation (Φ_{on}, Φ_{max}, Φ_{off}), and alpha (α) represents the bandwidth of conidiation: Φ_{off} - Φ_{on} = α. sd stands for standard deviation.

For better comprehension the corrected phase angle reference points (Δψ) of all screened *komo* mutants are presented as stack histograms in figure 3.4.

Statistical data analysis revealed a higher peakedness (kurtosis 6.3 to 10.6) as well as a slight asymmetry towards negative values (skewness from -0.6 to -2.5) for distribution of onset, maximum and offset of conidiation. The conidiation period alpha showed a normal distribution tested by inspection of the probability plot, by a least square fit to a representative normal curve (r=0.98, p≤0.001) and by calculation of the Shapiro-Wilks test (W<<Wα, p≤0.01).
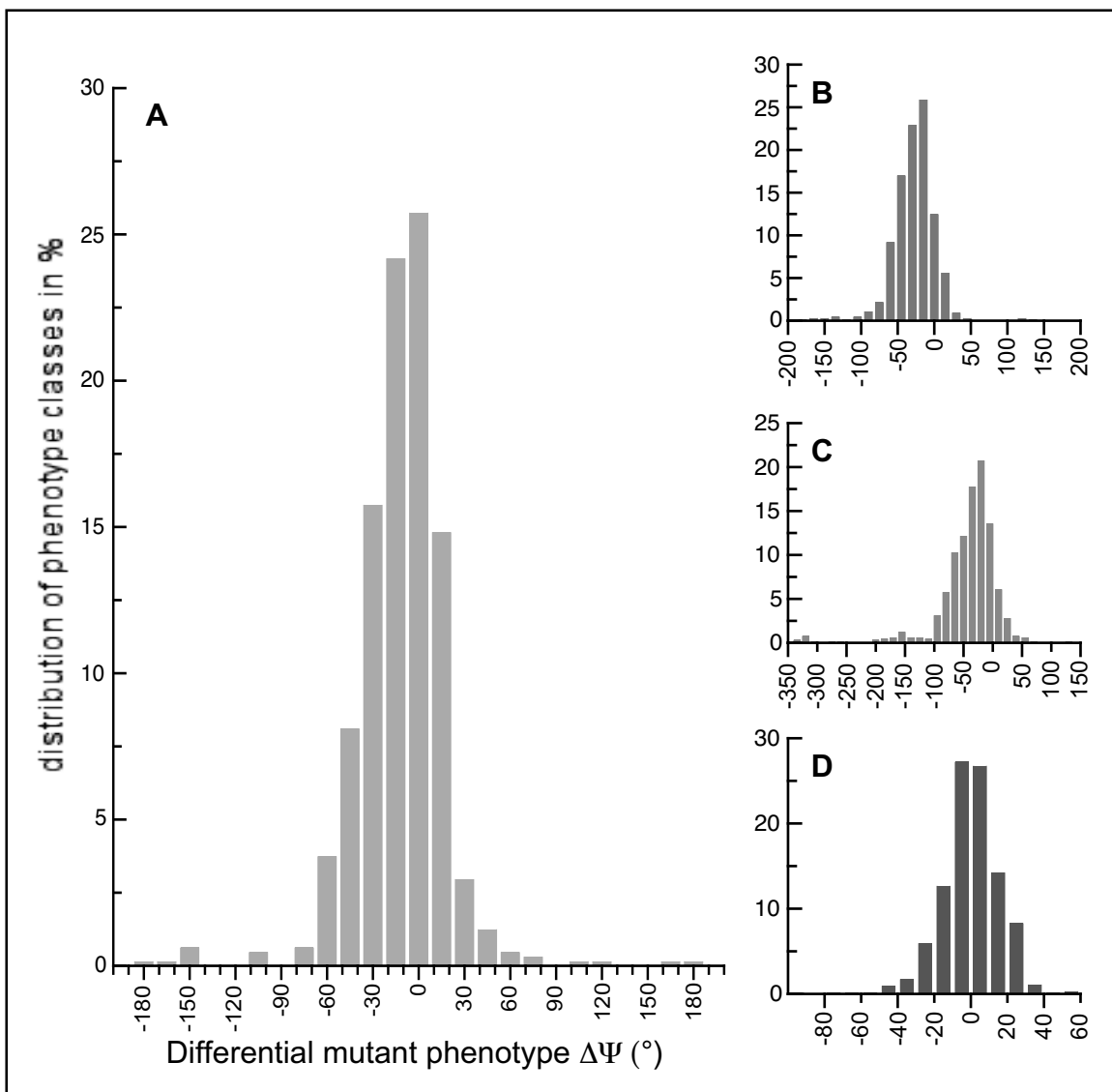
Figure 3.4 Stack histogram of phase reference points of all screened *komo* mutants in the first screening step. The x-axis shows the differential mutant phenotype ($\Delta\Psi$). The y-axis represents the relative distribution of phenotypes in percentage.

A. conidiation onset, **B.** conidiation maximum, **C.** conidiation offset and **D.** conidiation activity. Statistical analysis proved gaussian distribution for the differential phenotypes (see text for details).

Analysis and comparison of percentiles between the data sets of *komo* and controls proved a higher variability in phase angles for mutant strains (see table 3.2). These findings are consistent with the higher standard deviations of phase angles as previously shown in table 3.1.

In synopsis, considering the advanced onsets of mutants and the given threshold for phase angles, 31% of mutants entrained differently within the range of a symmetric 16 h temperature cycle. Herein, 5% showed a delayed (>30°) and 95% showed an advanced (beyond -30°) phenotype relative to *bd* (see figure 3.5). According to the screening protocol, these mutants had to be screened in the second step in order to verify the mutant phenotype.
Only six mutants grew slowly on race tubes (less than 2 cm/day) and had to be checked again (see figure 3.6).

	bd		*komo*	
	q75-q25	q95-q5	q75-q25	q95-q5
Φ on	32.00	59.50	39.50	96.00
Φ max	32.00	49.50	52.00	133.50
Φ off	30.50	77.25	39.50	106.00
α	22.00	50.50	24.00	55.50

Table 3.2 Inter-quantile ranges of phase reference points.
The raw data presented here reflects that the variance in *komo* mutants for conidiation onset and offset is higher than in the corresponding control strain *bd*. Thus variance analysis supports the hypothesis of extreme abundant mutant phenotypes to be screened in the next step of mutant screening (ANOVA $p < 0.01$).
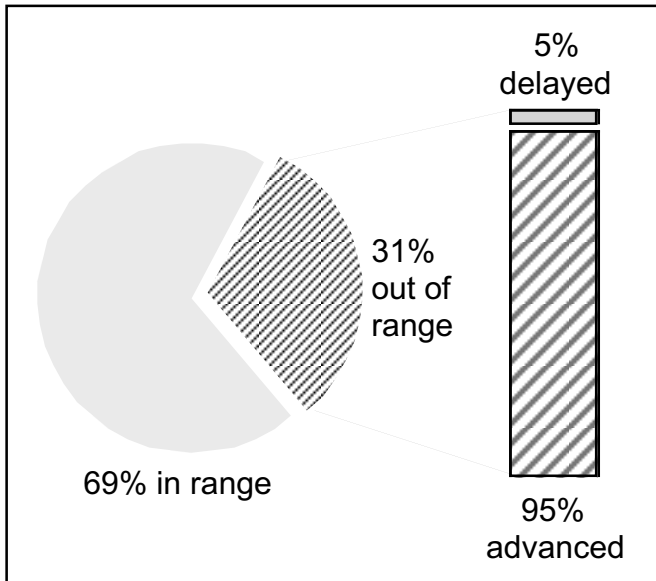
Fig.: 3.5 Taxonomy of *komo*. 200 of 742 screened strains from the first screen had to be checked for their altered phenotype in the second screening step. A majority of putative clock mutants showed an advanced phase rather than a delayed one.

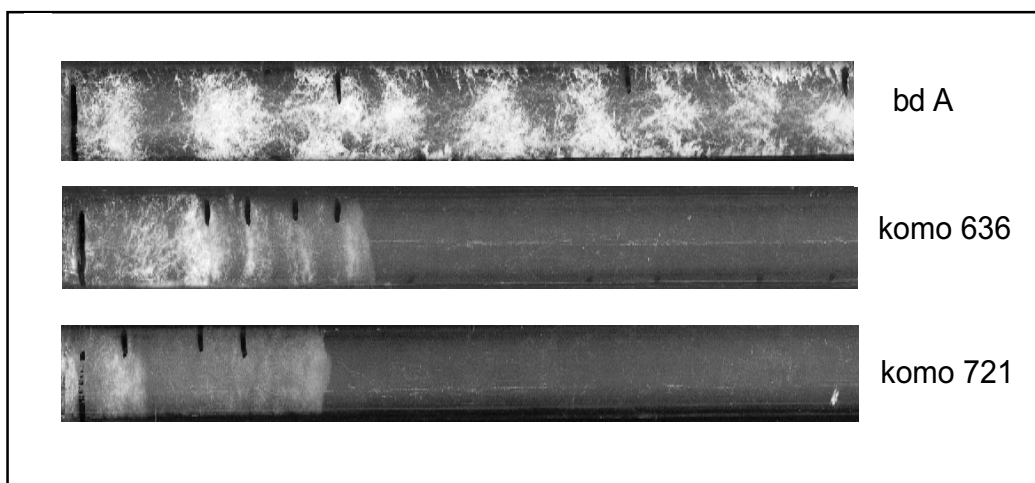
Fig.: 3.6 Inhibited growth in *komo* mutants.

Six mutants displayed extremely slow growth. Here only two mutants are shown (*komo636* and *komo721*) with the corresponding control strain (*bd A*). Pictures of race tubes are scaled 1 : 1 where bd A exhibits a mean growth rate of about 3.5 cm/day and these two mutants less than 1 cm/day. Moreover, no conidiation could be found in *komo721*.

3.2.2 Second Step of Mutant Screen

The second screen was performed to verify the altered circadian properties for these 200 *komo* mutants, but with 3 tubes per isolate instead. Therefore, 57 mutants with extremely abundant clock phenotypes (more than 45° in difference of phase onset compared to *bd*) and 6 mutants with deficient growth were chosen for this second screening procedure.

Results of the re-screen are depicted in figure 3.7.

The abundant clock phenotype (< -30° 30°<) was verified in 64% (n=37) of mutants. In contrast, 26% (n=20) of *komo* entrained in the given range similar to the control strain *bd*. Here, 80% (n=16) of *komo* ranged in the first standard deviation of the control group bd (±20°).

In accordance with the general terms of screening methods the group of mutants will be called "verified" or "false" from now on. The "verified" mutants were classified further into subgroups with delayed and advanced phases, in classes of 30° as a reference to the initial threshold value.
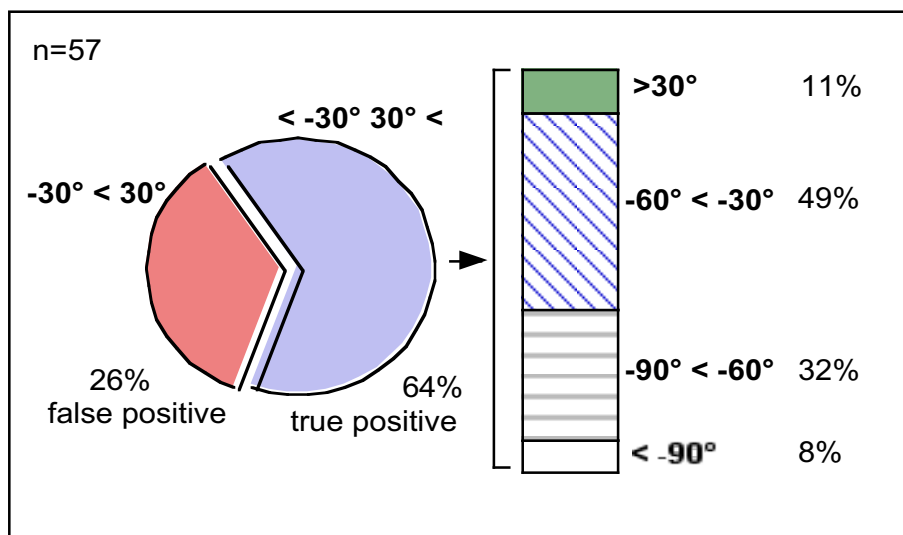

Fig.: 3.7 Results of second screen on 16 h temperature cycle. The group of "verified" mutants was subdivided into further categories, taking the onset of conidiation into account as the previously described differential mutant phenotype ($\Delta\Psi$). The corresponding control group was set at 0° for its onset.

3.3 Additional Physiological Characterisation of Putative Clock Mutants

The third major step of the *komo* mutant screen followed the verification step (see figure 3.3) and consisted of further entrainment experiments in order to characterise the chronotype for different Zeitgebers.

Therefore, chronobiological behaviour was tested in symmetric 24 h light-dark cycles (12 h light and 12 h dark, 3 μE, 25°C) and in constant darkness (DD, 25°C). Section 3.3.3 will give a summary and comparison of results.

3.3.1 Physiological Results of 24 h LD Cycles in Constant Temperature

All 37 "verified" clock mutants (see section 3.2.2), with an altered chronotype on temperature cycles showed a significant advance in $\Delta\Psi_{on}$, $\Delta\Psi_{max}$ and $\Delta\Psi_{off}$ of conidiation on symmetric 24 h LD cycles compared to the control strain *bd* and these "false" mutants (n = 16), as shown in table 3.3.

For example, the $\Delta\Psi_{on}$ appeared at -16° for "verified" mutants but isolates of the "false" group entrained in the same way as *bd* (- 6°), and the activity phases (α) of these strains showed no statistical differences (t-test and F-test for all p< 0.01).

reference points	"verified" mutants	"false" mutants
	mean (°) (± sd)	mean (°) (± sd)
$\Delta\Psi_{on}$	-16 (29)	-7 (11)
$\Delta\Psi_{max}$	-25 (25)	-10 (6)
$\Delta\Psi_{off}$	-21 (19)	-7 (8)

Table 3.3 Juxtaposition of $\Delta\Psi$ of "verified" and "false" *komo* mutants showing the mean values and the corresponding standard deviations sd in brackets. The intra-experimental variability of phase reference points made it necessary to transform the data sets ($\Delta\Psi$). The control strain *bd* was set as reference with 0°. Negative values indicate an advanced phase.

The wider ranges of standard deviations and higher variances in "verified" mutants were significantly different for all phase reference points compared to *bd* and "false" mutants (F-Test, Mann-Whitney-U-test, p≤ 0.01, confidence level 95%). The "false" mutants did not differ substantially in entrainment behaviour compared to the controls. Results are depicted in figure 3.8.
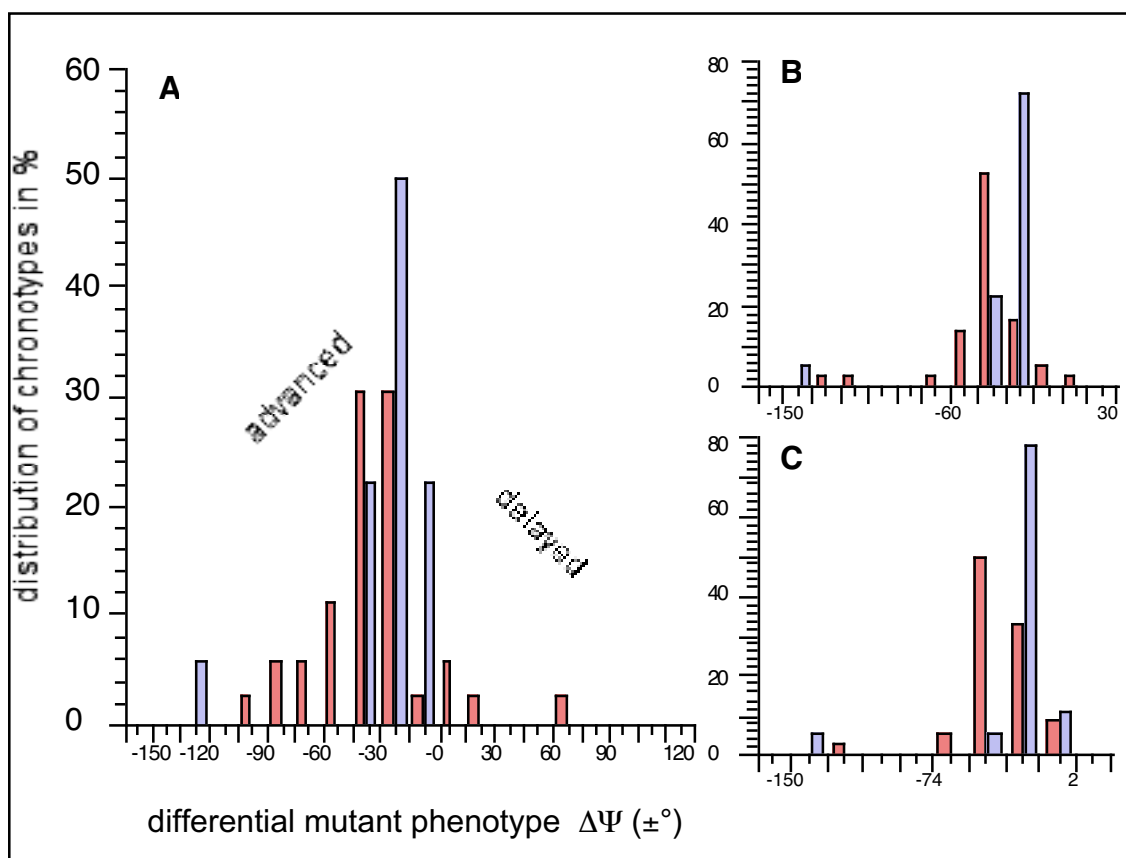

Fig.: 3.8 Distribution of differential chronotypes (ΔΨ)

The x-axis shows the differences to the corresponding *bd* strain in degrees (ΔΨ), whereas the y-axis represents the relative percentage. Column-widths do not reflect the actual range of degrees, where red columns represent the "verified" clock mutants and blue columns the "false" strains for the conidiation onset (A), maximum (B) and offset (C). The comparison of ranges and distributions shows a significantly different variability of phase angles for the "verified" mutants (see text for details). The control strain *bd* was set at 0°, while negative values indicate an advanced phase angle and positive a delayed one.

3.3.2 Physiological Results in Constant Darkness (DD)

The mean of free running periods (τ) in the "verified" mutants lay at 20 hours with a wide spread from 18 h to 23 h, thus displaying a higher variability. In addition, the wild type *bd* as well the group of "false" mutants showed similar ranges of period length (mean τ = 20.8 h). These findings were depicted in table 3.4 and figure 3.9.

	bd	"verified" mutants	"false" mutants
	mean (±sd)	mean (±sd)	mean (±sd)
τ in hours	20.9 (±0.5)	20.4 (±1.2)	20.7 (±0.4)

Table 3.4 Differences in free running periods (τ.). The group of "verified" mutants showed a twice-higher standard deviation (sd) than "false" mutants and *bd*.
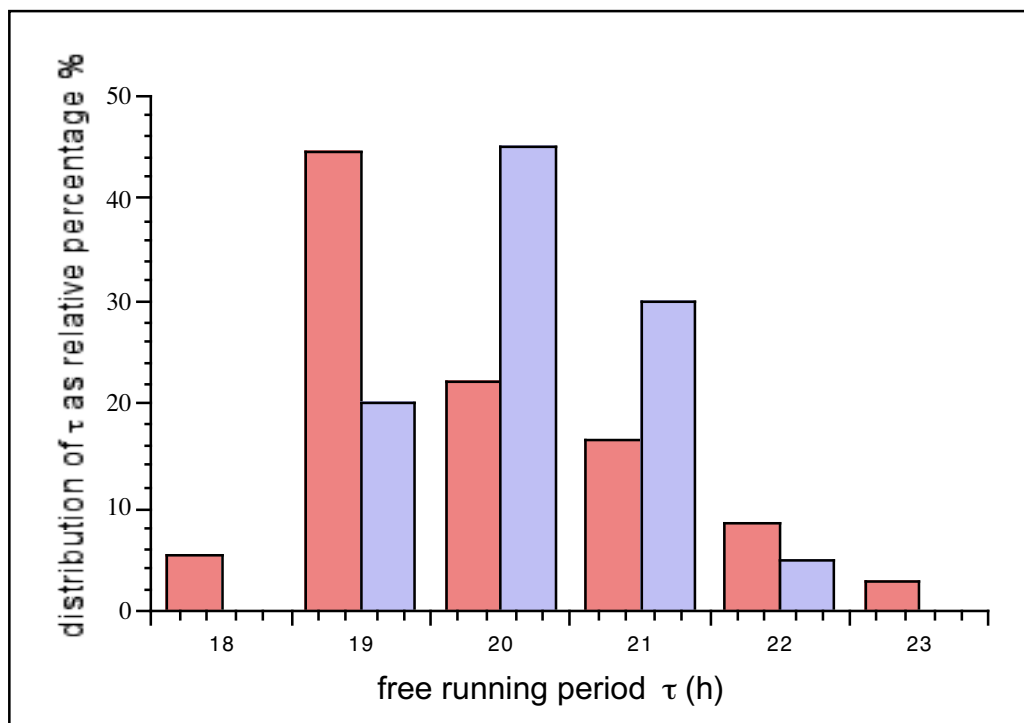

Fig.: 3.9 Distribution of free running periods (τ.) red columns represent the verified mutants and blue columns the "false" strains. τ is represented on the x-axis (in hours), while the y-axis is scaled to relative percentage.

Statistical data analysis proved a difference in the variances of free-running periods for mutants with a "verified" altered chronotype (Mann-Whitney-U-test confidence level 95%, p=0.04).

In addition, one isolate in the group of "verified" mutants showed unstable free running periods in constant darkness (*komo303*). Statistical data analysis (periodogram-test, p≤0.01) could not assert a stable free running period.

3.3.3 Entrainement Properties of Mutants in Different Zeitgeber

The results of the 24 h LD cycles and the 16 h temperature cycles of the sections 3.2.2 and 3.3.3 will now be compared and analysed:

In LD, less than a half of the "verified" mutants showed a higher phase-angle difference in conidiation onset ($\Delta\Phi$) of more than 1.3 hours compared to the control strain *bd*, while a vast majority of "false" mutants entrained within this given range (see table 3.5). The proportions in $\Delta\Phi$ for these two mutant groups were significantly different (Fisher´s exact test, confidence level 95%, two-tailed p=0.009).

In addition to these findings, 90% of mutants showed an advancement of phases in both temperature cycles as well as in the LD cycles, while 10% of mutants entrained in a divergent way, showing a delayed phase in temperature cycle, but an advancement of phases in light-dark regimes or viceversa. Figure 3.10 (A) shows a comparison of these phase angle differences ($\Delta\Phi$) for those two Zeitgebers on a standardised scatter plot.

n= 57	"verified" mutants	"false" mutants
$\Delta\Phi_{LD}$< 1.3h	20 (54%)	17 (85%)
$\Delta\Phi_{LD}$ > 1.3 h	17 (46%)	3 (15%)

Table 3.5 Phase angle differences in the 24 h LD cycle

$\Delta\Phi$ stands exclusively for the corrected phase angle reference point $\Delta\Psi$ of the conidiation onset, while LD denotes the symmetric 24 h light dark cycle.

Second, the results of free-running periods (in DD, 25° C) and the 16 h temperature cycles will be compared and analysed:

81% of the verified mutants showed a free running period (τ) that differed significantly from that of *bd*, which is less than 1.3 hours ($\Delta\tau$), and the majority of "false" mutants showed periods within this given range (Fisher´s exact test, confidence level 95%, two-tailed p=0.12). These statistical results are concordant with findings in section 3.3.2. Table 3.6 gives an overview of the results.

	"verified" mutants	"false" mutants
$\Delta\tau$ < 1.3 h	29 (80%)	19 (95%)
$\Delta\tau$ > 1.3 h	7 (20%)	1 (5%)

Table 3.6 Free running period differences ($\Delta\tau$) compared to the control strain *bd*. $\Delta\tau$ denotes the difference of free running periods of mutants to *bd* with a predetermined cut-off value of 1.3 hours.

In addition to the previous findings, several "verified" mutants showed an arbitrary association of period length and $\Delta\Phi$ in LD, which is divergent to known clock mutants (e.g *frq1*). Some isolates exhibited prolonged periods as well a phase-advancement in temperature cycles or viceversa (see figure 3.10 B).

In synopsis, only 48% of the "verified" mutants showed an altered phenotype in light-dark cycles or in DD and only 20% of "false" mutants did not entrain within the range or presented a longer free running period τ (see table 3.7).

Out of range only	"verified" mutants	"false" mutants
$\Delta\tau$ > 1.3 h	3	1
$\Delta\Phi_{LD}$ > 1.3 h	12	3
$\Delta\tau$ and $\Delta\Phi_{LD}$ >1.3 h	2	0

Table 3.7 Further phenotypic classification of mutants Abbreviations are the same as in tables 3.6 and 3.5
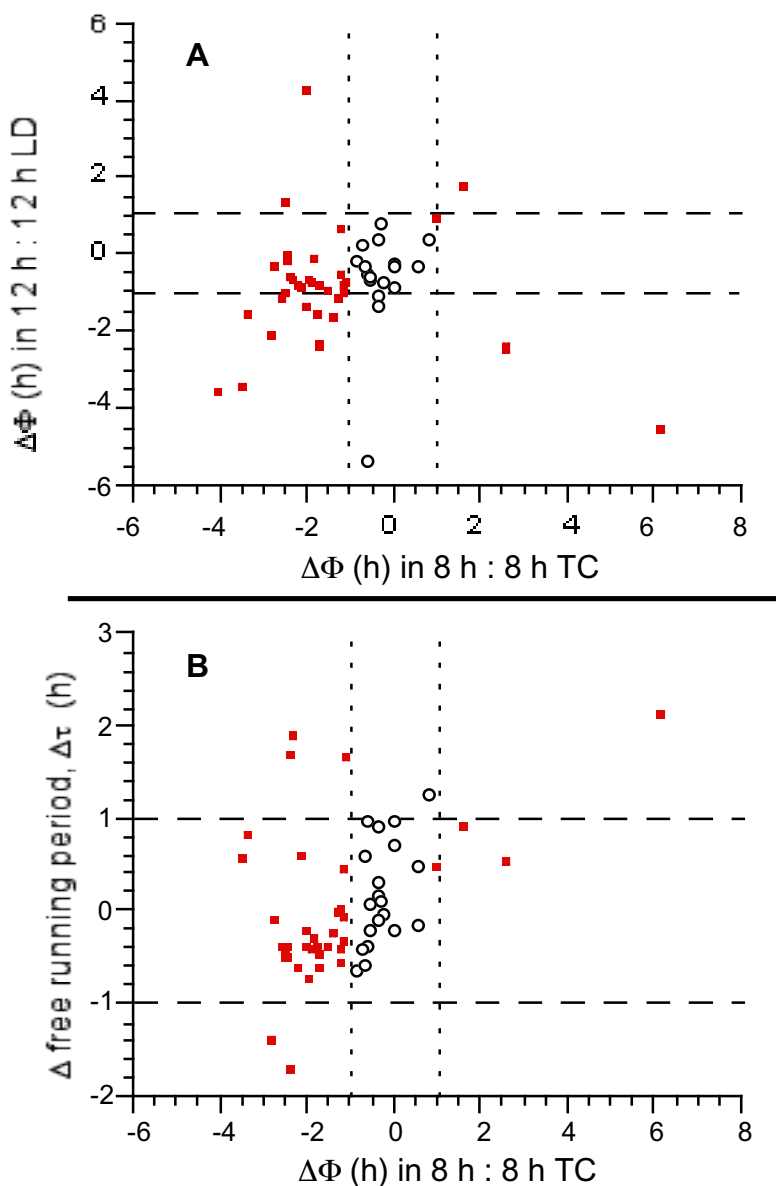
Fig.: 3.10 Comparison of mutant chronotypes in LD vs TC (A) and LD vs TC (B). Each dot represents the average of three race tubes per experiment and mutant strain, while filled squares stand for "false" and open circles for "verified" mutants. For better orientation the control strain *bd* was set at 0 h. Negative values indicate an advanced and positive values a delayed chronotype – respectively a shorter or longer τ. Dashed lines represent the threshold value of 1.3 h (real time, ≈ 30°) used as the cut-off value in the temperature screen (see Methods).

3.4 Mutants of Interest

This chapter will present the physiological, molecular and genetic characterisations of *komo58* and *komo303*. Figure 3.11 gives an overview of circadian characteristics of some interesting strains from the mutant screen.
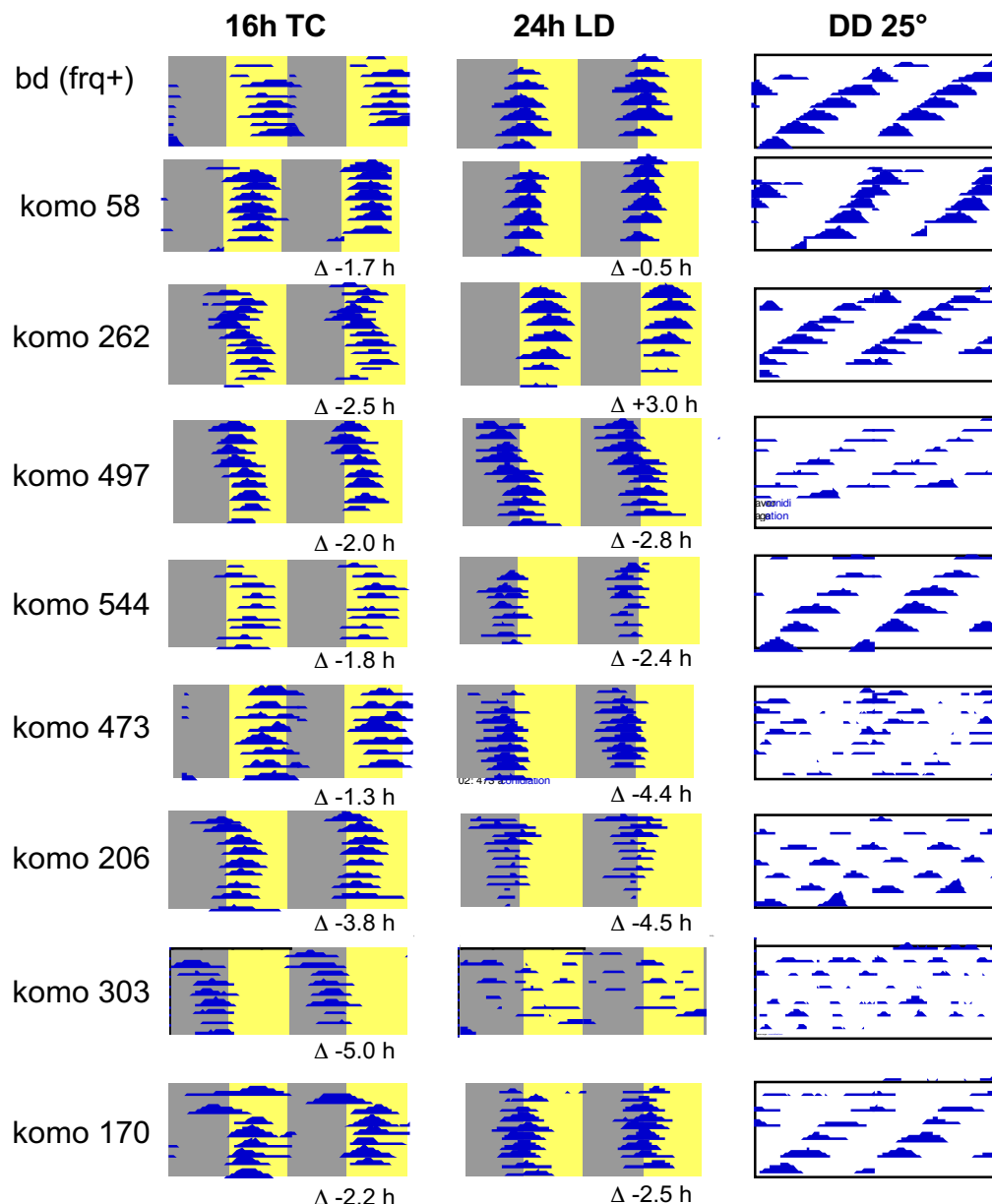

Fig.: 3.11 Overview of some mutants. Coloured double-plots are adjusted to the actual cycle length; right hand plots depict τ and are scaled on T= 24 h. Values beyond the plot stand for the differential phase onset of conidiation, while the control *bd* was set to zero.

3.4.1 Mutant *Komo58*

The mutant *komo58* showed a significantly advanced phase angle of conidiation onset in 16 hour temperature cycles ($\Delta\Phi$ = 50), while the free-running period was slightly longer (τ = 21.5 h) than that of *bd*. In contrast, no significant differences ($\Delta\Phi$< 15°) were found in symmetric 24 h LD cycles.

3.4.1.1 Genetic Results

Komo58 was purified to homokaryon by the plating assay with macroconidia (see Methods section 2.4.2). After the purification steps, one isolate was picked and prepared for a sexual cross with the known clock mutant *frq1* for genetic linkage and phenotype testing.

150 spores were picked randomly, while 128 isolates grew up and were tested further for their BASTA sensitivity. 51% (n=65) of the filial isolates (CR40#n, see section 2.2.7 for nomenclature) showed a resistance against the pesticide.

37 isolates were taken as a random sampling from the first generation to test for their circadian phenotype and linkage to the known resistance gene.

Three independent experiments were conducted, i.e. DD at 25°C, 8 h warm and 8 h cold cycles and 12 h light and 12 h dark cycles with three tubes per isolate. The parental strain *Komo58*, *bd* and the *frq1* mutant were included as controls.

The results of our phenotyping showed a clear separation into two distinguishable groups within the 37 isolates:

21 isolates (56%) showed no BASTA resistance (baR-) as well as a circadian property comparable to the *frq1* mutant, and 16 isolates (44%) revealed a BASTA resistance (baR+). All baR+ isolates entrained similarly to the parental strain *komo58* in temperature, in constant darkness (DD) and in LD cycle. Results are depicted in figure 3.12.

In synopsis, there was a clear phenotypic and genotype segregation into 2:0:0:2 for the free-running periods and entrainment in LD and TC (Mann-Whitney-U-test, Fisher's exact test, confidence level 95%, p≤0.001 for all). Hence, these findings imply a significant association and co-dependency between the mutant-specific chronotype of *komo58* isolates and the presence of the marker-insertion (baR).

D	baR -	*frq1*	baR +	*komo58*	*bd*
τ (FRP)	16.8h±0.5	16.4h±0.3	21.7h±0.4	20.5h±0.7	21.4h±0.6
ΔΦ 8W:8C	82°±18	76°±21	175°±14	180°±19	225°±15
ΔΦ 12L:12D	21°±23	19°±15	64°±15	59°±17	67°±14
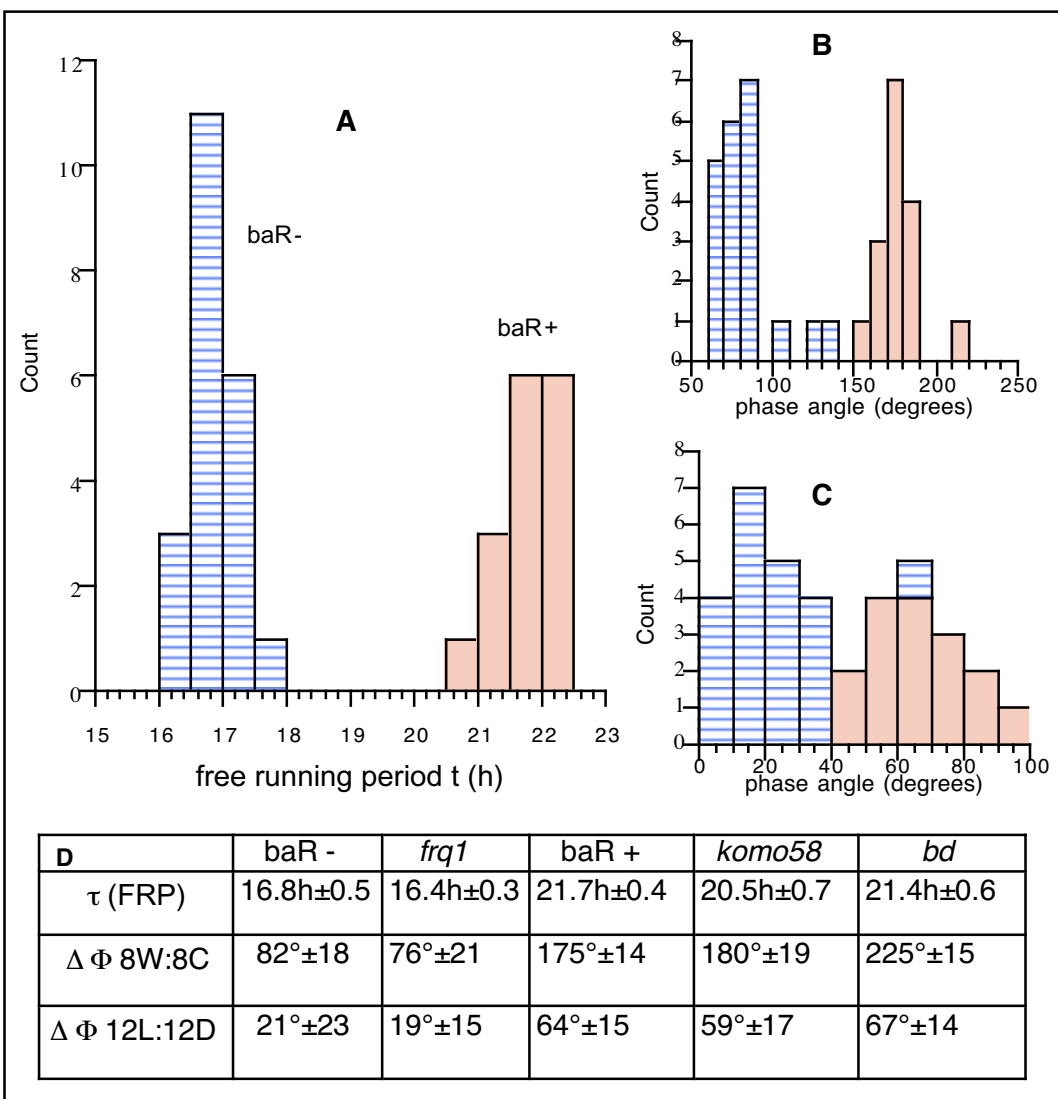
Fig.: 3.12 Chronotype-distribution in the offspring of CR40

A shows the distribution of free running periods (τ). **B** depicts the phase-angles of conidiation onset (Φ_{on}), an **C** gives an overview of Φ_{on} in 24 h light-dark cycles. Segregation and statistical analysis imply a strong connection between mutant-specific chronotype and the occurrence of BASTA resistance (see text for details). Blue columns stand for BASTA sensitive (baR-) and red columns for BASTA resistant (baR+) isolates. The y-axes depict the absolute counts. **D** shows the mean values of reference points with corresponding standard deviations.

3.4.1.2   Further Physiological Result

After a second macroconidial purification, *komo58* and its offspring were tested systematically in temperature cycles T=24 h with varying lengths of the cold phase in order to prove chronotype behaviour. Results are depicted in figure 3.13.

The baR+ *komo58* isolates as well as the parental *komo58* strain showed divergent entrainment characteristics. The phase angles of conidiation onset and offset showed a maximum advancement of 70 degrees (3 h real time) in non-symmetric cycles, while differences could not be found for the symmetric one. Its conidiation started at the nearer end of warm phases in cycles with short cold periods (33% of T). In addition, the control-strains *bd* and *frq1* entrained exclusively in warm periods. The BASTA sensitive isolates showed no differences to the corresponding controls.
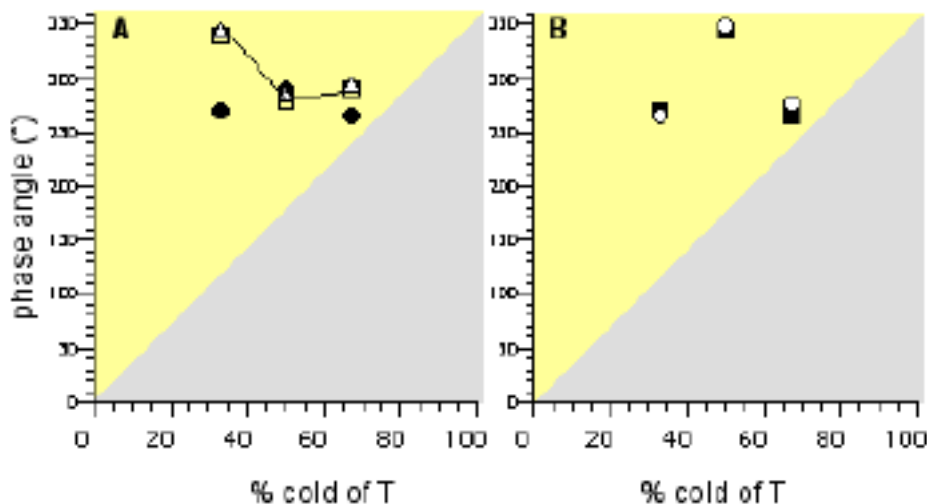
Fig.: 3.13 Plot of temperature cycles (TC) T=24 h with varying periods of cold. Dots represent the mean of conidiation onset for three race tubes per strain and isolates (standard deviations were not included because of a more comprehensible presentation). Grey areas represent the cold portion of the temperature cycle.

A. Filled circles represent *bd*, while empty signs represent the BASTA resistant isolates as well as the original *komo58* strain. **B**. Filled squares represent *frq1* and empty circles the BASTA sensitive isolates with a *frq1*-specific phenotype.

The second step in phenotyping the circadian properties of *komo58* and its isolates, i.e. *CR40#28* and *CR40#46*, was to explore systematically the entrainment behaviour in symmetric light-dark cycles (with 3 μE of "white" light) for different T.

The results of the experiments are depicted in figure 3.14 (A). No relevant differences in ΔΦ of conidiation could be found between *komo58* and the *bd*. As a matter of fact, the maximum of difference lay at 15°. Both start their conidiation around mid of the subjective day and show no dependence on the length of T.
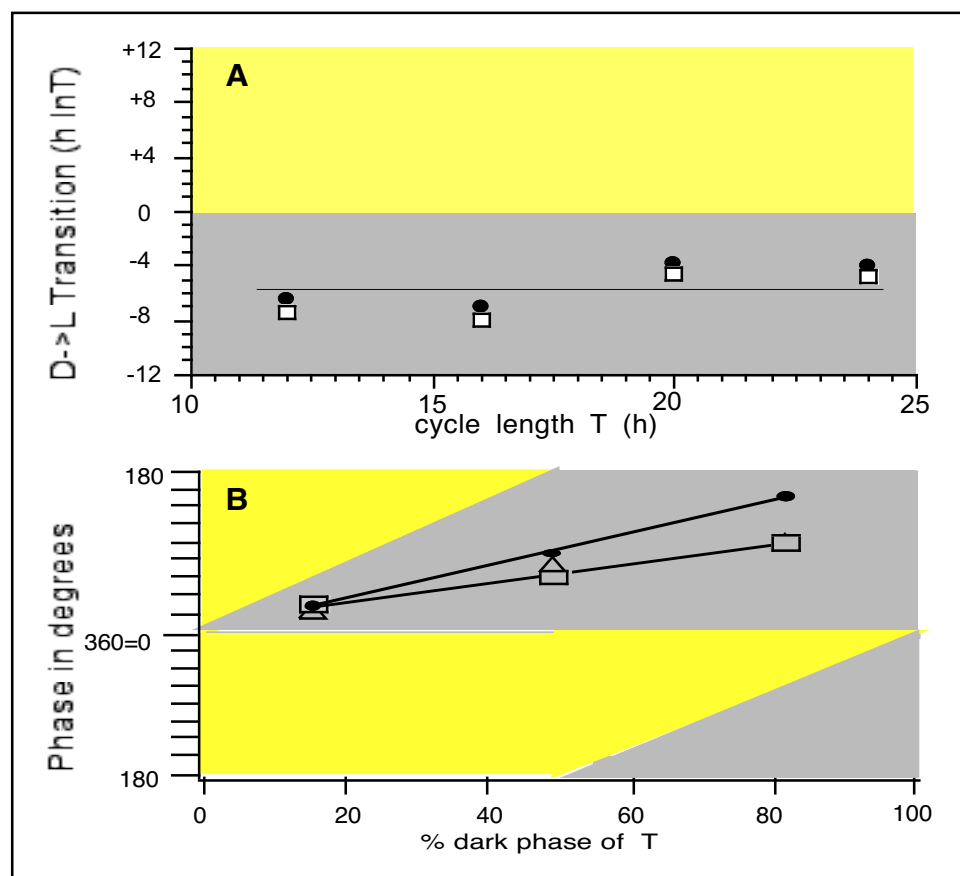
Fig.: 3.14 Entrainment plots of LD with different T. Grey areas represent the dark portions. Filled circles describe the *bd*, while the empty signs represent *komo58* and its isolates *CR40#28 and #46*.
A. Conidiation onsets are plotted here in hours of internal time (InT). The full line represents the subjective mid-day for all T. **B.** Z-plot with cycles (T=24 h) of different portions (duration) of light are shown. The onsets of conidiation are plotted in degrees. Here divergent phases are observed between *komo58*-isolates and *bd*.

In contrast to the previous results, *komo58* displayed divergent phases of entrainment in the non-symmetrical light-dark cycles instead. Here, the phase of conidiation onset advanced linearly with the decrease of the light portion of the Zeitgeber. A maximum phase difference to the wild type *bd* ($\Delta\Phi$ of -55°) was found in a T-cycle with a prevalent dark phase (figure 3.14 B).

As a consequence of the previous findings an impaired light sensitivity of *komo58* was assumed, therefore entrainment experiments in short light-dark cycles (T= 12 h) with different light intensities (between 0.5 nE and 3 μE) on constant temperature (25° C) were performed.

Komo58 showed different phase angles for the lower sort of light intensities. All relevant phase reference points, i.e. conidiation onset and conidiation offset, showed the highest advancement in a range from 5 nE to 80 nE of light intensity compared to *bd* (*frq+*). Differences of -50° (1.7 h real time) in conidiation onset were measured herein, while no distinctions could be made at 3 μE. Figure 3.15 depicts the results.

Due to these results, the impaired light sensitivity in entrainment of *komo58* and its baR+ isolates, both were tested for their properties of "freerun" in constant conditions. The strains grew in two sets of race tubes under continuos illumination (LL) of 5 nE or 2.9 μE of "white" light at 25°C. As a control, another sample of the collection of these strains was kept in constant darkness (DD, 25°C), where the genuine free running period was observed.

The DD samples showed a free running period for *komo58* and its isolates *CR40#26* and *#48* of 21.5 h, but no self-sustained rhythm could be found under theses two LL conditions. In periodogram analysis no reliable τ was calculated for these four strains (Qp/χ^2-values ≤ 0.5, p$\leq$0.05). The results of this experiment are depicted in figure 3.16 as a comparison of double plots.
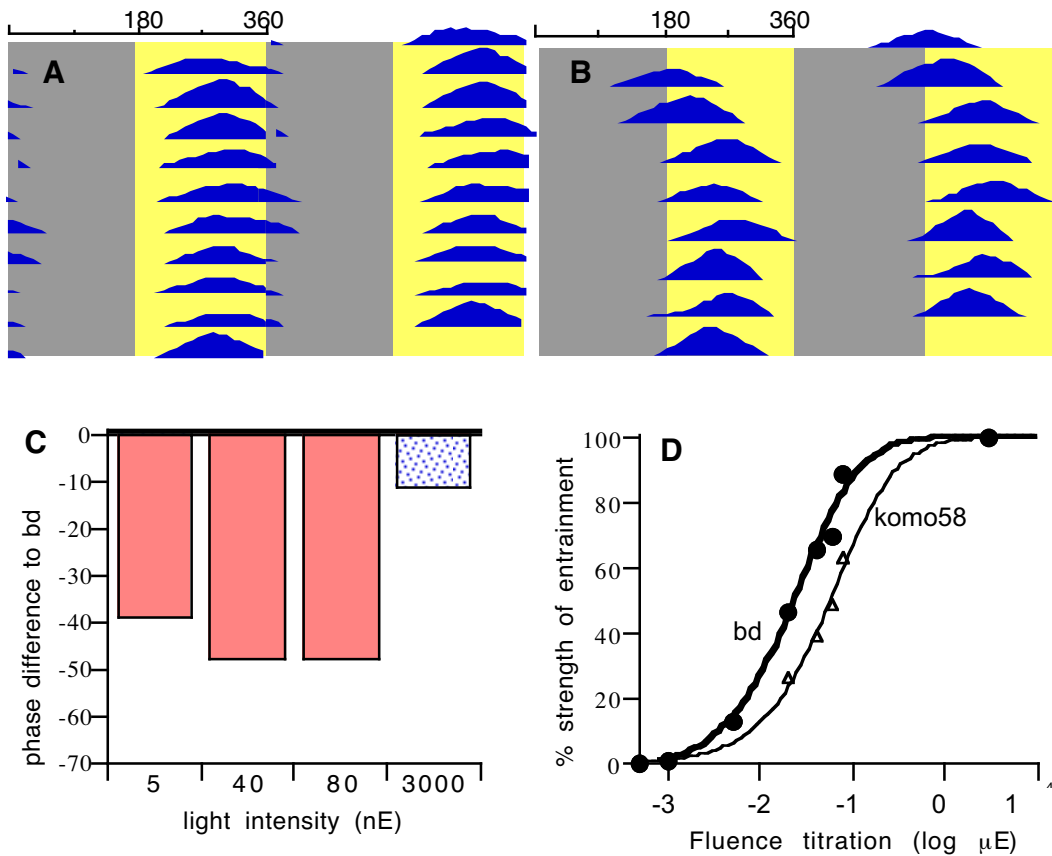
Fig.: 3.15 Fluence titration on light-dark cycles of T=12 h

The grey areas of the double plots (**A** *b d* and **B** *komo58*) represent the dark phase of the cycle. Here the conidiation onsets of the two strains differ greatly at 80nE of light intensity.

In addition to this, the property of entrainment in the mutant *komo58* is diminished for that level of light intensity.

C Phase angle differences of *komo58* to the corresponding control strain *bd* are shown in degrees. A fivefold higher difference is found at the levels of 5 nE, 40 nE and 80 nE as compared to the maximum light intensity. Moreover there was no reasonable entrainment at 0.1 nE and 1 nE light intensity.

D The results of the fluence titration with "white" light on 12h LD cycles show a reduced sensitivity to light in *komo58*. The relative strength of entrainments (y-axis) is calculated in accordance with Dragovic et al. (2001) (see Methods). Curves represent the least square fit for S-functions (r=0.99, p≤0.001).
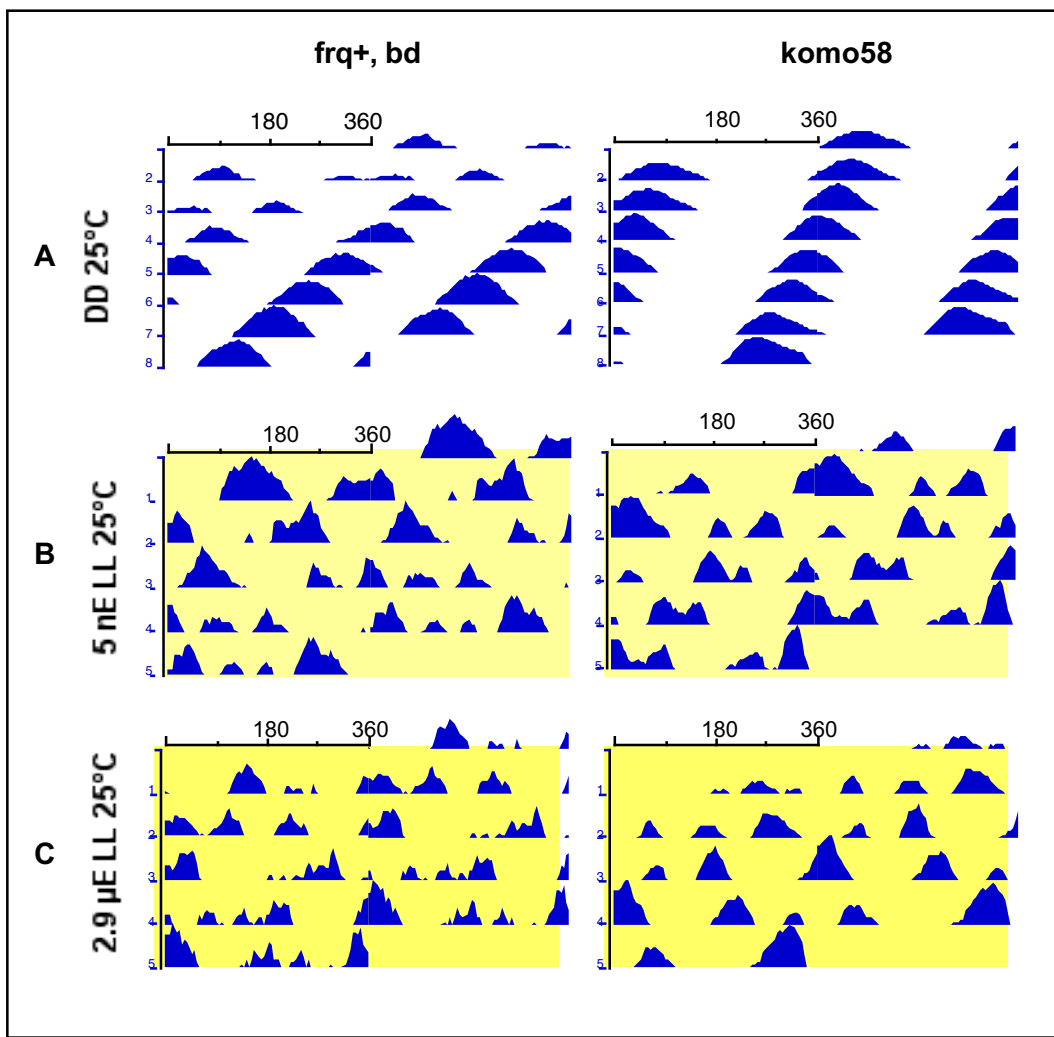
Fig.: 3.16 Banding patterns in DD and in constant light (LL) for the wild type bd (left) and the mutant *komo58* (right). Each double plot represents the conidiation pattern of one race tube per strain. The plots are scaled to a time range of 24h. **A** depicts the free running periods of *bd* (20.5 h) and *komo58* (21.5 h) at 25°C in constant darkness (DD). **B** and **C** depict the conidiation pattern of *bd* and *komo58* (right panels) under constant illumination of 5 nE and 2.9 μE "white light". There was no reasonable entrainement (p<0.05).

3.4.1.3 Molecular Analysis of *Komo58*

Southern hybridisations with DIG-labeled copies of the BAST resistance gene showed a single insertion in the parental strain *komo58* (see figure 3.17 A). In addition to this, a parallel Southern Blot confirmed the existence of single insertions in the offspring of CR40. These isolates showed the mutant phenotype as well a resistance against the drug (see figure 3.17 A and B). These findings were consistent with the genetic segregation pattern (see section 3.4.1.1). The 2 : 2 segregation of phenotypes, i.e. the BASTA resistance, and the advancement of conidiation onset, proved a single insertion mutagenesis in *komo58*.
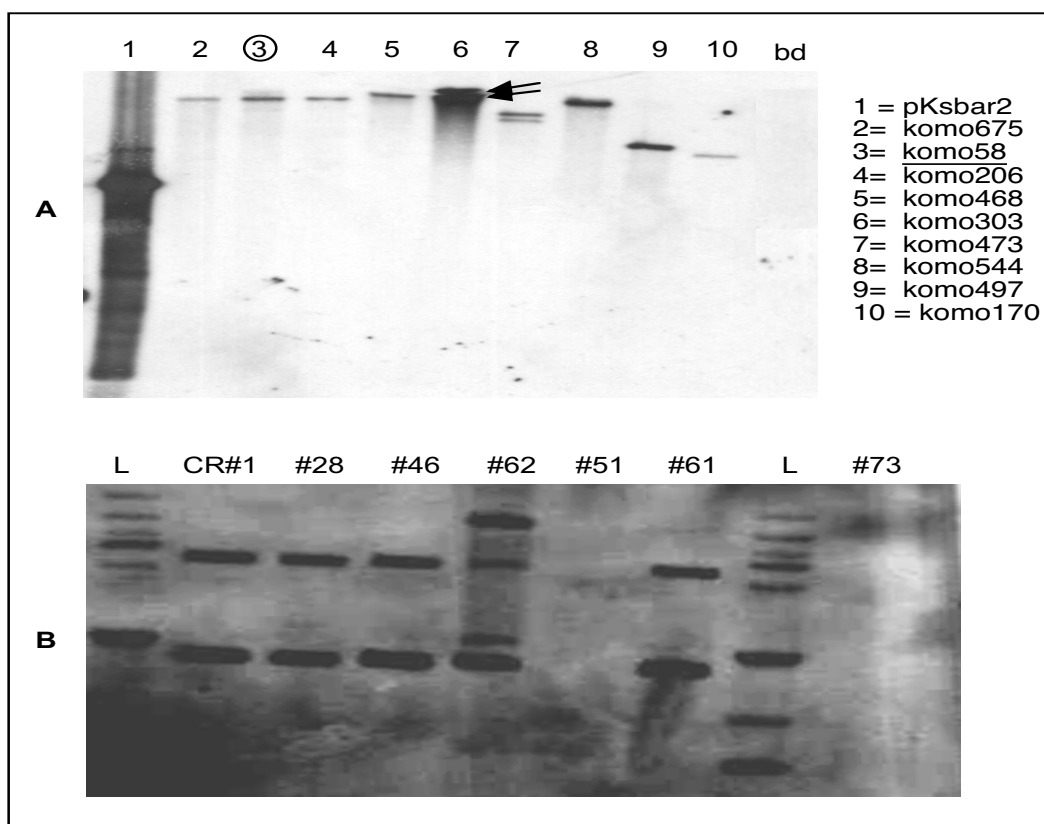
Fig.: 3.17 Southern blots with DIG-labeled copies of baR.

A DNA of different mutants was digested with EcoRI. In lane 3 only one band is visible. **B** The isolates' DNA was digested with HindIII, which cuts into the baR gene.

By now, the obvious chronotype and the single insertion had been proven and were therefore suitable for a further characterisation. A novel method of plasmid rescue was therefore developed and applied (see Methods 2.3.8).

Once a fragment with a pure cutting site (see figure 3.18) was determined by restriction mapping, its size was calculated for the next step: the individual size fractionation of genomic DNA as well as the combined methods of inverse PCR and nested PCR were applied (see Methods 2.3.8.2 and 2.3.8.3).

The fragment of predicted size was amplified successfully and sent for sequencing.

Fig.: 3.18 Results of the genome mapping

A Diversified restriction mapping with DNA of *komo58*. The pure HindIII cutting site can be seen in the right panel in lanes 1 to 3.

B The PCR fragment of predicted size was found for the parental strain as well as for isolates, which displayed the *komo58* phenotype.
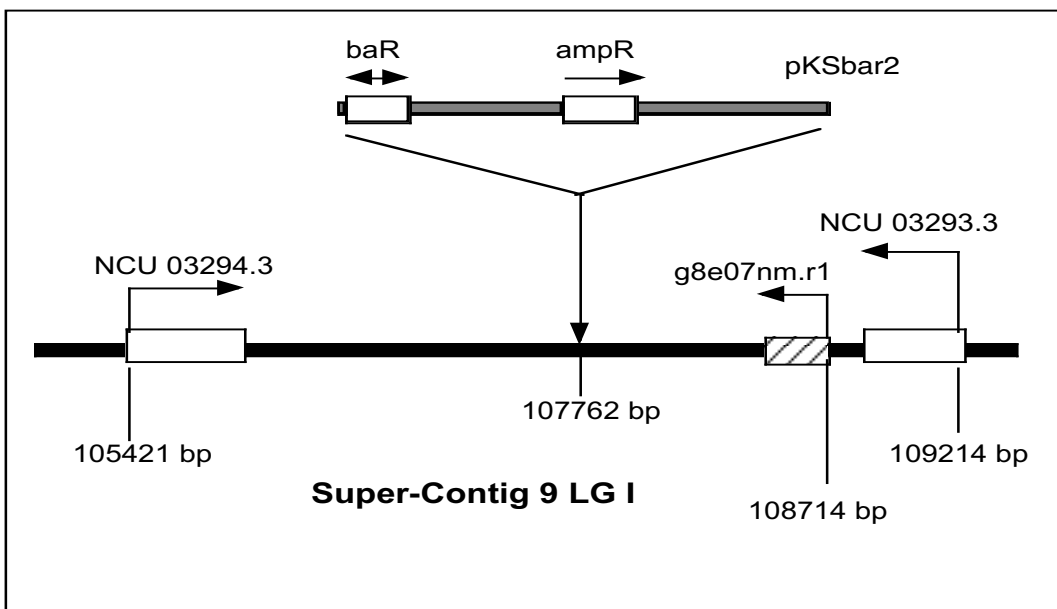
Figure 3.19 Overview of the insertion site of *Komo58* on chromosome I (LGI)
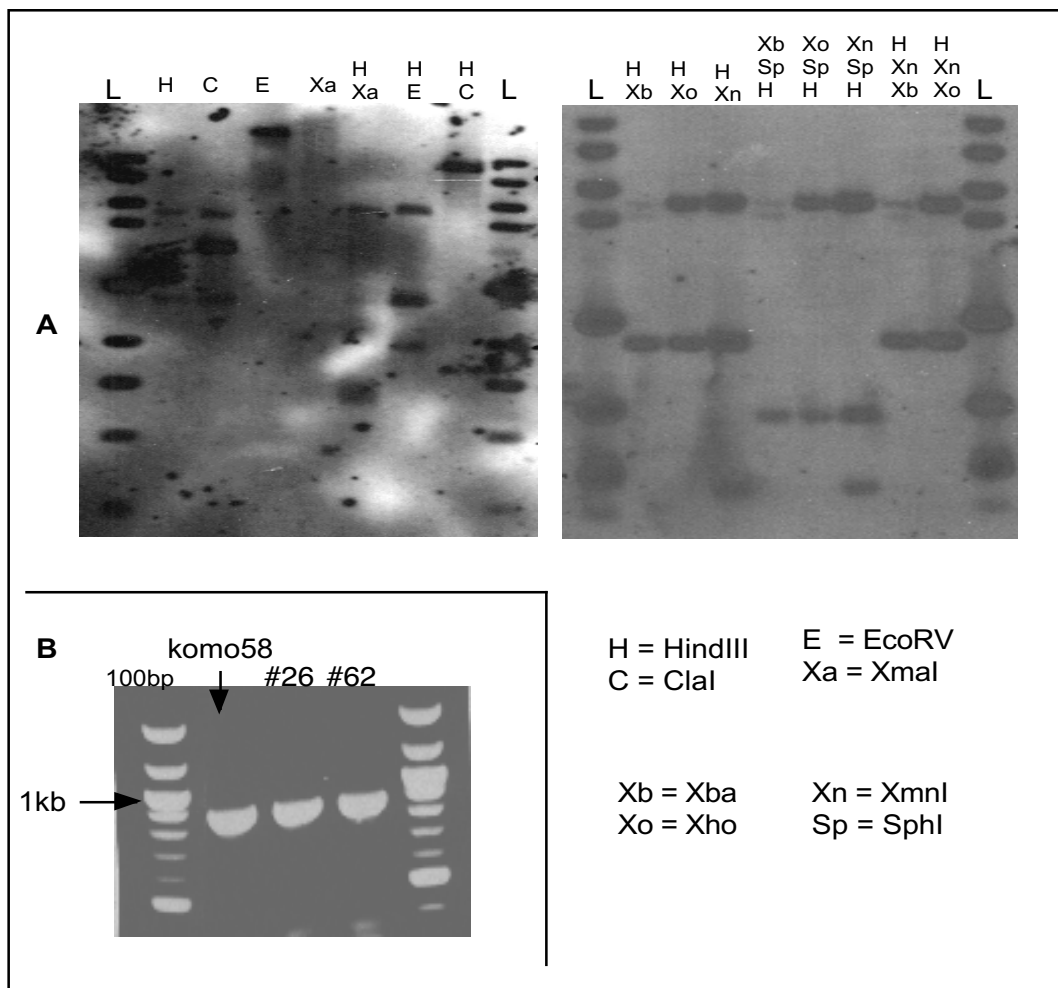
The sequencing results were compared with the newest available *Neurospora crassa* genome database by the alignment algorithm of the Broad Institute, USA. Its insertion site has been identified between two hypothetical proteins (NCU 03294.3 and NCU 03293.3), which are part of Super-Contig 9 of Chromosome I. In addition to these annotated genes, a cDNA "morning" library (g8e07nm.r1, see the reference of the Broad Institute) was found 1000 bp upstream of the insertion site. However, an intensive analysis of its sequence could not determine a reasonable open reading frame (FGenesh; NCBI ORF-Finder). Moreover, no significant homologies for products of the two putative genes could be found (see figure 3.19).

In order to bypass possible misinterpretation of the similarities analysis of sequences, the insertion was further characterised by amplifying the insertion site from the genomic mutant DNA (*CR40#61*, freshly prepared DNA). Primers were designed using the genomic DNA sequence predicted to flank the insertion, based on the sequence recovered in the previous step. First of all, possible deletions or translocations of the drug resistance marker and of other regions of plasmid had to be explored. Next, the results of the previous restriction mapping could be verified.

The fragment generated in the PCR reaction was larger (around 500 bp) than would have been predicted (see figure 3.20 A).

Analysis showed that there are partial duplications in the inserted plasmid. Parts of the ampicillin resistance gene were copied to its neighbourhood, while no deletions of nucleotides occurred in the genomic DNA.

Therefore, an alignment analysis for base-mismatches of the PCR sequence was performed with the known genome and plasmid database. It revealed that 117 Guanosine-Adenosine mismatches were counted on the range of 6500 bps and 90% of these mismatches were allocated in the plasmid itself (see figure 3.20 B).

The BASTA cassette itself showed base pair mismatches, but very few.

Moreover, the results of the previous restriction mapping, which was part of the rescuing assay, could be confirmed by a "virtual" mapping of the PCR sequence (see section about the verification of mutation). The method could be reproduced with this method.

Nevertheless, to determine whether the insertion influences the expression of the flanking genes, a quantitative PCR was performed, concentrating on one particular coding region. The annotated "morning" library was ideally suited for the following investigations. Putative circadian expression patterns could be revealed, if the amount of RNA showed divergent cycling levels.

As a matter of the corresponding night and day levels of this specific RNA persisted on an equal base for *komo58* as well as for the control strains, i.e. *frq1* and *bd* (frq+). Furthermore the amount of RNA under constant light was only two to three times higher in the control samples than in the mutant ones (see figure 3.21). In addition, the overall amount of g8e07nm.r1 RNA was lower for *komo58* (1-1.5 relative units) than for *bd* (2.5-3 relative units).
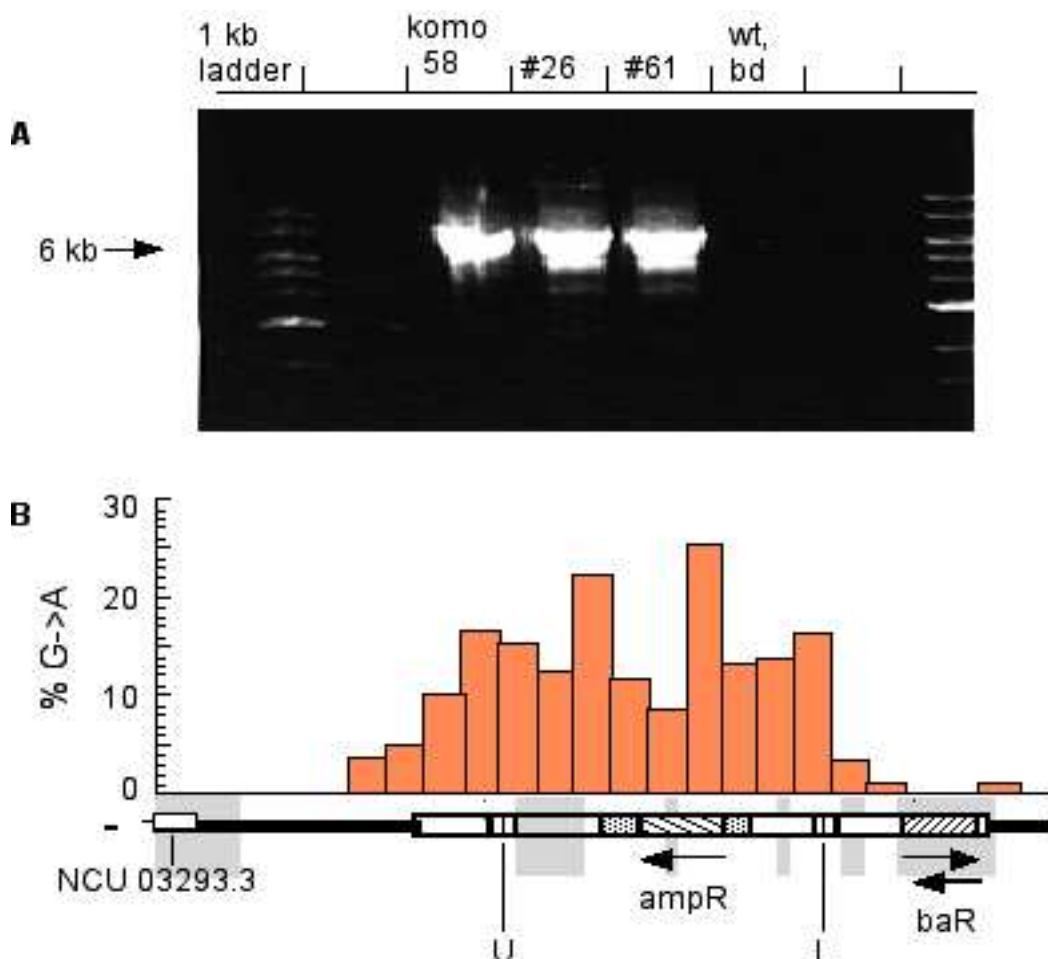
Fig.: 3.20 Verification of the rescue and sequencing results.

Panel **A** displays the results of the verification step of the successfully rescued plasmid. Take into account the similar sizes of fragments (6.5 kb) for those three samples. **B** describes the G-A mismatches as a histogram, where column-widths represent the ranges of 300 nucleotides, while the column-heights indicate the relative percentage of mismatches to the known amount of G nucleotides in the corresponding class. The histogram was scaled exactly to the fragment's figure (see A) for a direct comparison of mismatches with the DNA regions. Grey areas underneath the plasmid's figure indicate G:C rich regions (>50% of mean). The filled boxes next to the ampicillin cassette represent the region of partial duplications, while the L and U marked zones are equivalencies to the genuine promoter regions of pKSbar2. These two regions show homologies with parts of hypothetical *Neurospora* genes on LGII.
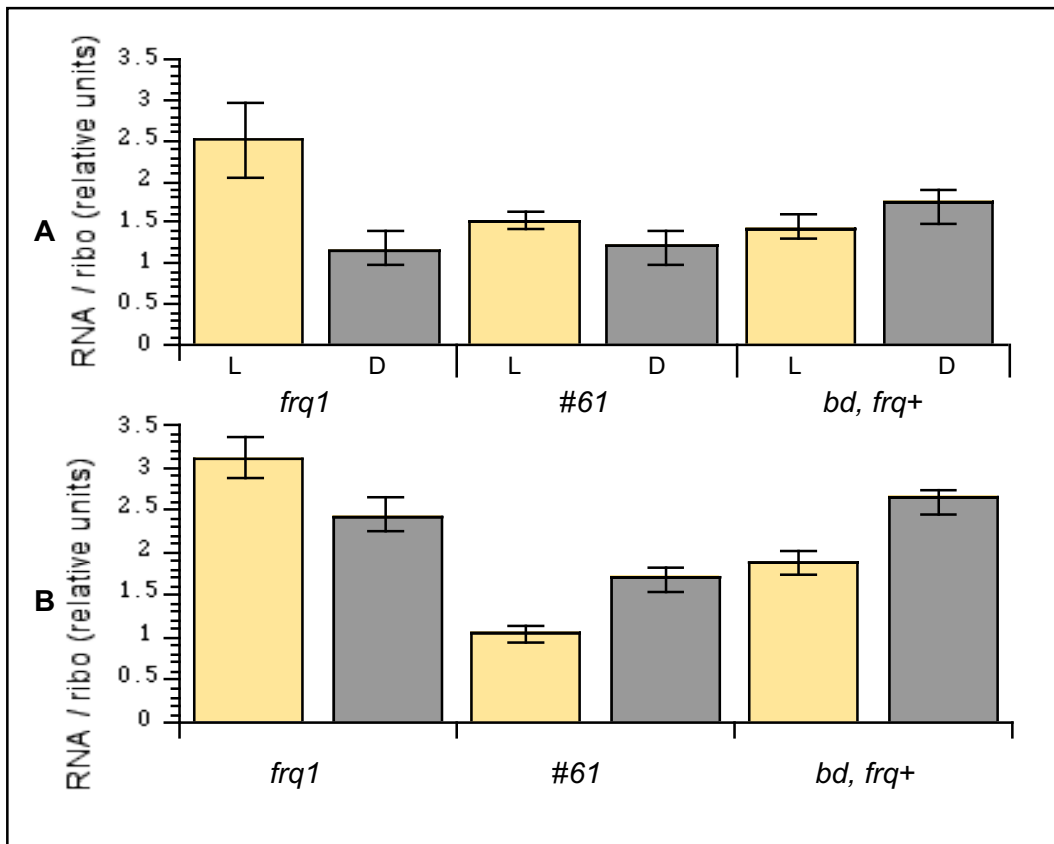
Fig.: 3.21 Expression analysis of frq and g8e07nm.r1 RNA

A The levels of frq RNA showed similar expression levels for all three strains after 49 h of growth under constant light (10 μE, 25°C) and constant darkness (25°C) respectively. A higher amount of RNA in *frq1* at L is accompanied by a wider standard deviation.

B RNA levels derived form the "morning" library were lower in the *komo58* isolate *#61*.

3.4.2 Mutant *Komo303*

The mutant *komo303* showed only reliable but aberrant phase of entrainment in the 16 h TC, and initially no stable entrainment in symmetric 24 h LD cycles with an unstable free running period (τ =14 h to 29 h) in DD. Molecular analysis showed a double insertion of the plasmid in *komo303*, while genetic studies indicated no clear linkage of altered phenotype and resistance.

In addition, *komo303* conidiated less in race tubes and flasks, while its conidia were rather powdery. Both mycelia and conidia had a pale apricot colour, compared to *bd* (frq+) (apricot-orange), *frq10* (deeply orange) and *frq1* (apricot).

3.4.2.1 Genetic Results for *Komo303*

After homokaryon purification of *komo303* a sexual cross (*CR33*) *frq1* was prepared*.* Compared to *bd*, the *frq1* shows a short free running period (τ= 16 h to 17 h) with an advanced phase in LD and in TC cycles (see Introduction).

80 spores of *CR33* were picked, while 55 isolates (69%) grew after heat activation. 46% (n=25) of these isolates showed a BASTA resistance (baR+) and Southern Blot analysis proved two insertions for these baR+ isolates, while no insertions were found in the barR- isolates (segregation baR+ : baR- of 1:1).

21 baR+ isolates were tested for their circadian properties to investigate associations of the mutant's phenotype with the *frq1* ones. The experimental set-up included symmetric 16 h TC and 24 h LD cycles with controls (parental *komo303*, *bd* and *frq1*). The circadian phenotyping revealed three main groups of baR+ isolates of *CR33*:

One group of isolates entrained in TC as well as in LD cycles (n=7). Here, only two isolates (29%) displayed phase angles like the *frq1* mutant, but 71% showed a delayed conidiation onset ($\Delta\Phi$ at 300°) in the LD cycle. The second collection (n=9) entrained in temperature cycles only, while six isolates showed $\Delta\Phi$ comparable to the parental *komo303,* and two isolates resembled the *frq1´*s.

The third group of isolates (n=5) was not entrainable in TC or in LD cycles. In addition, two subgroups of the first and second collection showed an intermediate chronotype that resembled the circadian behaviour of *komo303* and of *frq1.* Figure 3.22 depicts the overall segregation of phenotypes of baR+ isolates into 2:2:2:2:1 (*komo303*-like:r1:r2:r3:*frq1*-like).

Whether *komo303* had a recessive or semi-dominant type of mutation was investigated by a heterokaryon test for complementation (see Methods). Nuclei of *bd* (τ =21 h) and baR+ isolate *CR33#14* (τ = 14 h to28 h) were mixed in different ratios and inoculated on race tubes to analyse the free running period (τ). The results imply a recessive mutation in *komo303*: even a small amount of *bd* nuclei was sufficient to sustain a free running period of τ= 21 h (see figure 3.23).
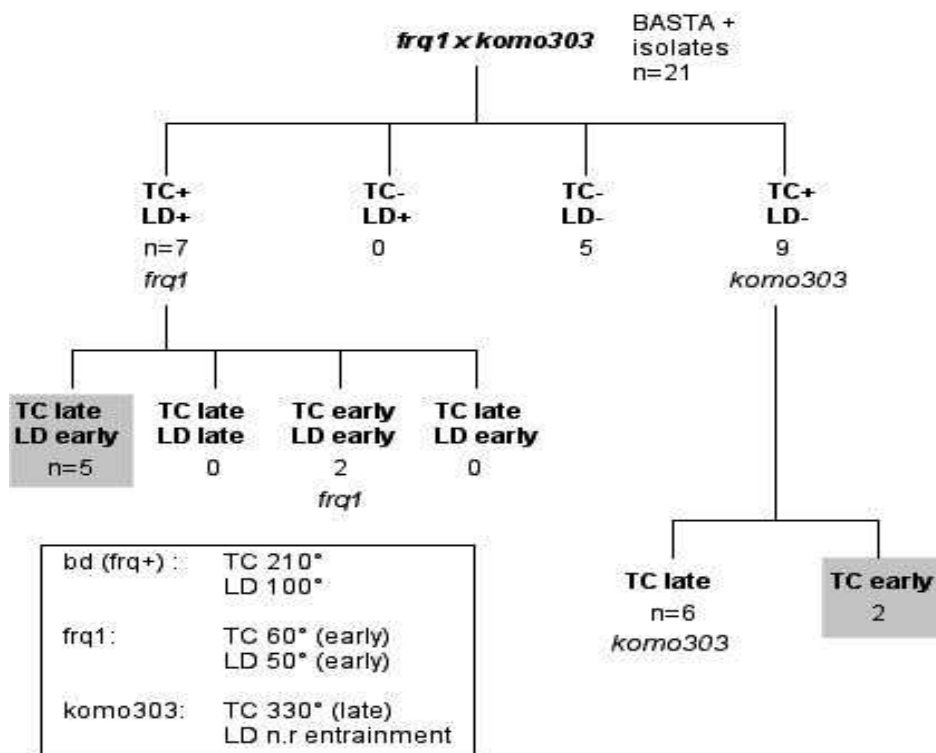
Fig.: 3.22 Taxonomy of phenotypic classification of *CR33*. BASTA resistant isolates (BASTA+) were classified into entrainment behaviour for different Zeitgebers (TC, LD). Minus signs indicate no reliable (n.r) entrainment and plus signs represent stable entrainment. The expressions "late" and " early" describe the phase of conidiation onset compared to *bd* (frq+). The group TC- LD- could be described as a new phenotype. The grey-shaded items represent an intermediate phenotype for entrainment behaviour (see text for details). The left lower box summarise the $\Delta\Phi$ values.
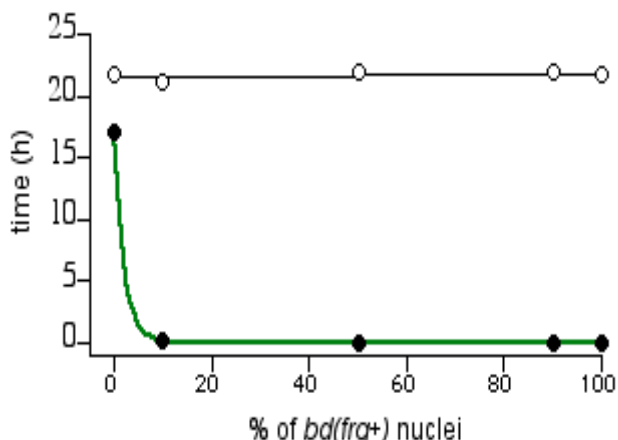
Fig.: 3.23 Complementation test for CR33#14 and *bd* (frq+). Open circles represent the mean τ per ratio, and the filled ones show the corresponding variances. A mixture with only 10% *b d* nuclei reduced the variance of τ (green slope: least square fit with r=0.99, p≤0.01).

3.4.2.2   Physiological Results for *Komo303*

After macroconidial purification, *komo303* was tested for circadian behaviour in asymmetric temperature cycles of T= 24 h with 20° C of cold and 30° C of warm phases, with varying lengths of the cold phase (from 1 h to 23 h). The baR+ isolates of *CR33* and the parental *komo303* strain showed a conidiation onset in anti-phase to *frq1* and *bd* (frq+) strains in symmetric TC cycles as well as in cycles with a very short phase of cold (12% of T), but entrained with an advanced ΔΦ (-80°) in cycles with longer cold portions only. Furthermore, *komo303* displayed low amplitude conidiation peaks after the main peak in TC cycles with longer warm portions of 21 h (3C21W).
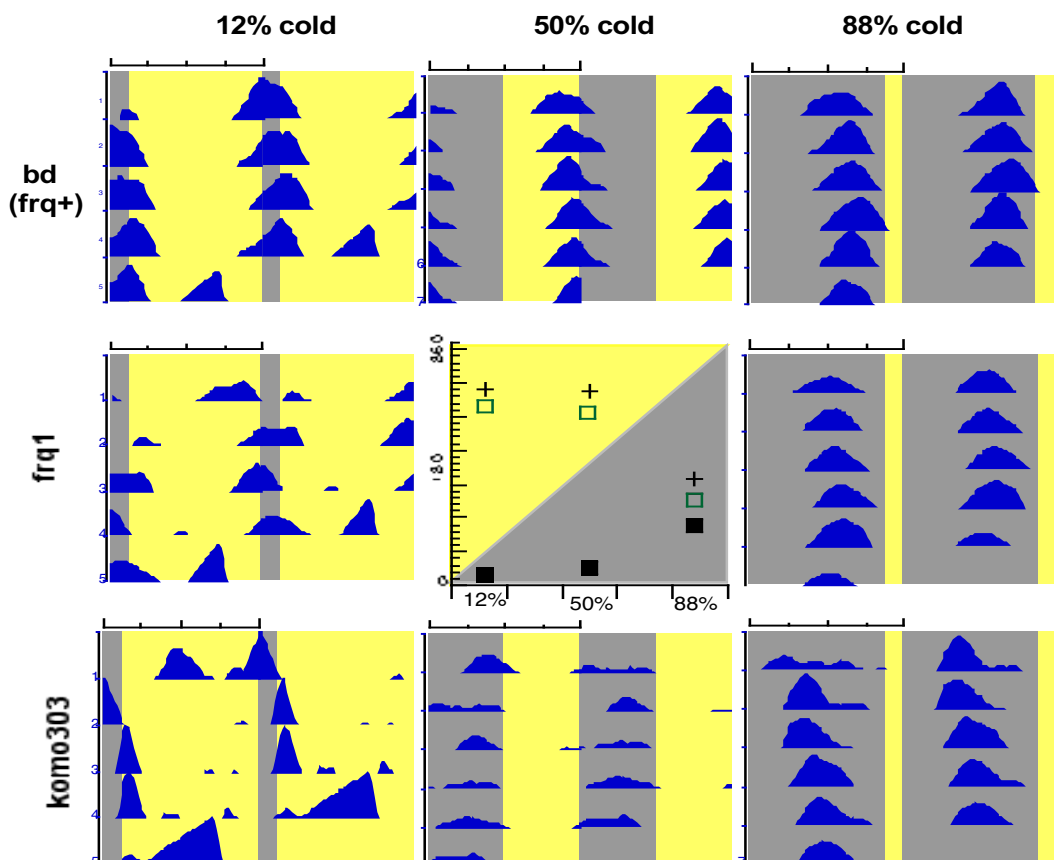
Fig.: 3.24 Double plots for temperature cycles with different lengths of cold (grey area) with T= 24 h. The central panel gives an overview of the onsets of conidiation (ΔΦ) in *komo303* (filled square), *frq1* (empty squares) and *bd* (crosses). Each sign represents the mean of three race tubes.

In opposition to this, little difference was found for TC cycles with a prevalent cold portion. Thus, *komo303* and *bd* started their main conidiation in the middle of the cold portion, but its bandwidth (conidiation activity α) was half as long as the *bd*´s α in cycles with longer warm portions (see figure 3.24).

Komo303 was not entrained sustainably in the symmetric LD cycle with T= 24 h as depicted in figure 3.11 (see page 71). Therefore its synchronisation behaviour was investigated systematically in LD cycles (light-intensity = 3 μE, T= 24 h) with varying duration of the light phase (4 h to 23 h of darkness); *frq1* and *bd* (frq+) were included as controls. The *bd* and *frq1* strains started its conidiation exclusively in the dark phase, but *komo303* displayed no sustained conidiation pattern in all these LD cycles (see figure 3.25).

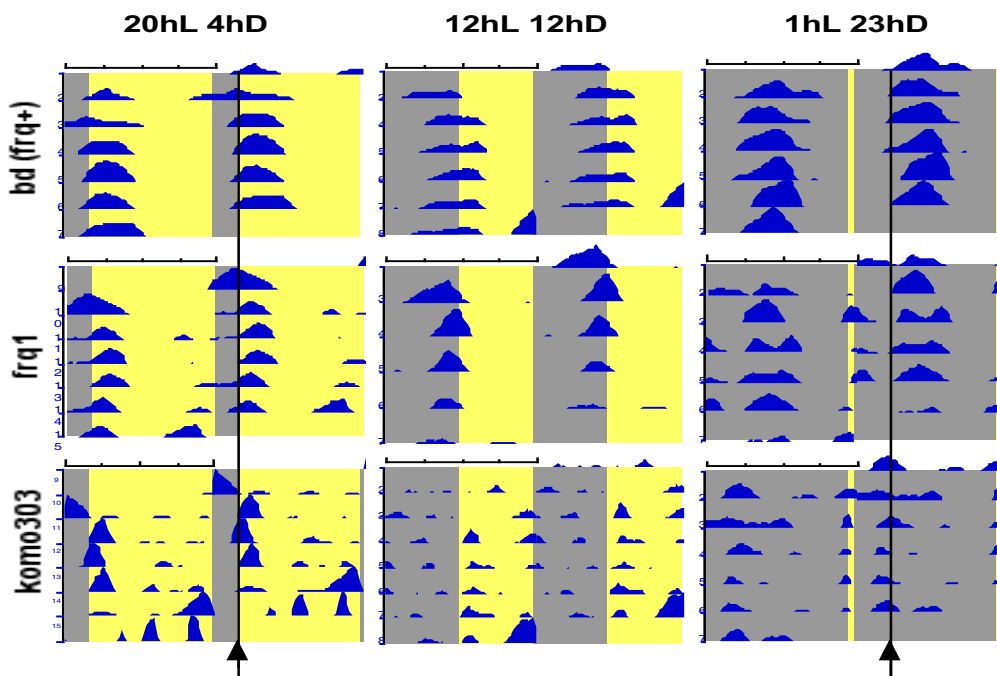**Figure 3.25 Double plots for LD cycles with different lengths of dark** (grey area) with T= 24 h. The vertical lines with arrows denote the onsets of conidiation ($\Delta\Phi$) in *bd*, *frq1*. Each double plot represents the mean of three race tubes. L stands for light and D for darkness, while the numbers indicate the length of phase in hours on the upper side of figure.

The last part of this chapter summarises conidiation onset ($\Delta\Phi$) and conidiation peaks of *komo303* previously studied in these asymmetrical temperature and light dark cycles of varying length (see figure 3.26). $\Delta\Phi$ and conidiation peaks were assessed as described in Lakin-Thomas (2005), in order to enhance significant rhythm patterns and filter less periodic ones. In short: the density traces of all replicate race tubes were split into 24 h segments, averaged to daily profiles for each race tube and treated as an individual daily sample (see Methods section for further details).

The *bd* strain showed one distinct "activity" peak per day in all LD cycles and started its conidiation in the dark phase exclusively, while *komo303* in contrast displayed multiple peaks with varying amplitudes in all LD cycles (see figure 3.26 E to G). The *frq1* strain established similar $\Delta\Phi$ of conidiation, but showed two peaks in cycles with longer dark portions (figure 3.26 H).

However, *komo303* showed entrainement to TC cycles while the oscillation shifted progressively later when T was increased (see figure 3.26 B and D, filled circles). These distinctions were smaller than in *bd*, described by the slopes of the linear regression functions for all phase points, which were flatter in *komo303* (3.75) than in *bd* (7.21). In addition to this, *komo303* displayed a shorter period of conidiation activity alpha compared to the control strain (α= 80° and 165°) in temperature cycles (T=24 h) with a prevalence of warm portions. Furthermore, the peaks of conidiation densities increased as well as decreased very rapidly, fluctuating in low amplitudes afterwards (see figure 3.26 A). The steepness was related to the dark to light transition, while a decrease of the amplitude was bound to the light to dark transition instead as shown in figure 3.26 (E-G) (arrows).

As a consequence, the overall amplitude of these fluctuations increased with the length of dark in T=24 h cycles and then showed similarities to the "primary" peak (figure 3.26 G).

The strain *frq1* showed a similar conidiation trace as *komo303* in LD cycles with longer dark portions (figure 3.26 H).

All density traces were fitted to a two-component cosine function, scaled to the corresponding T length (or its integer (see table 3.8).

The conidiation patterns of *komo303* gave low regression values for both the LD cycles with T= 24 h and the TC cycle with a very long warm phase (3C21W).

Statistical analysis of the mutant's fluctuations of conidiation densities (see Methods) by the fundamental and first harmonic yielded only very low regression values (<0.3), even when varying the period.
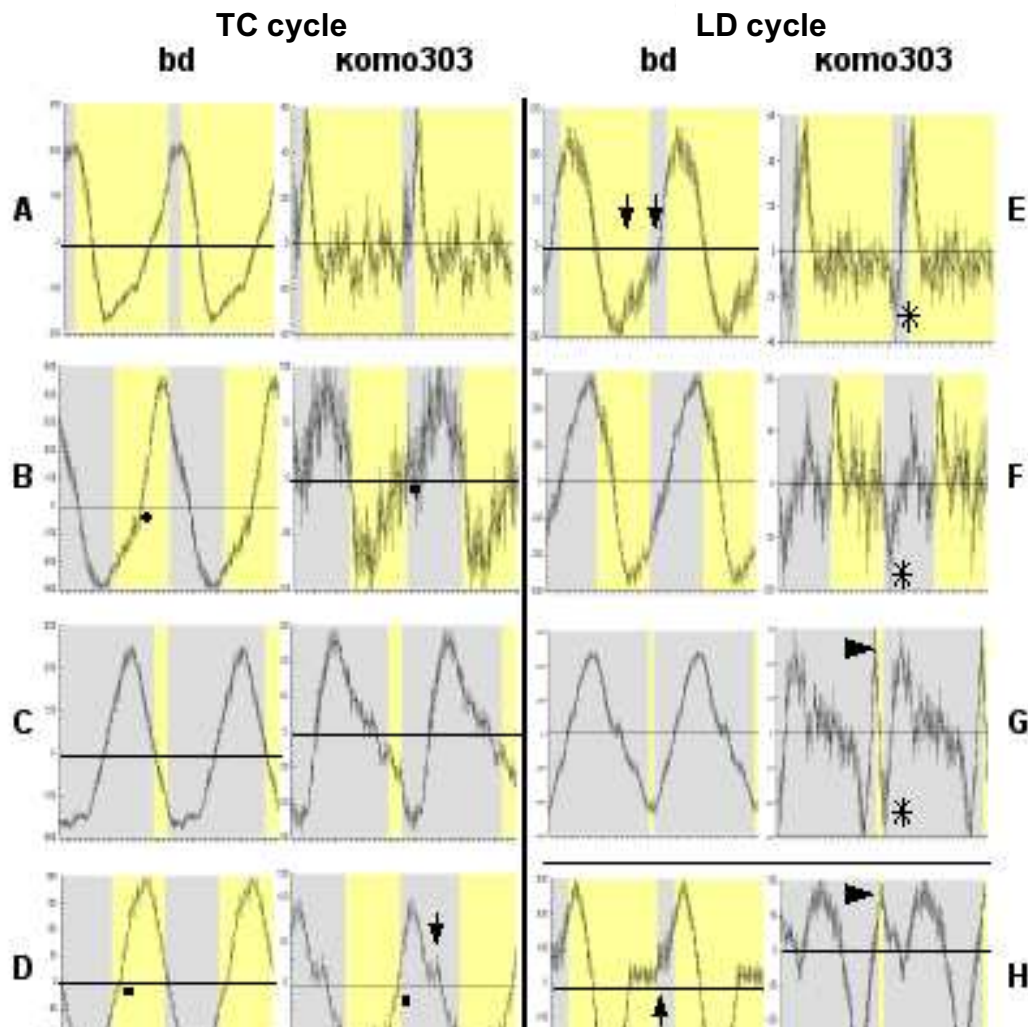
Fig.: 3.28 Collection of average days for different Zeitgebers

For all days the mean of averaged density traces (± SEM) in all replicate tubes are double plotted against hours after the beginning of the cold (left panel) or dark phase (right panel, grey areas). Arrows indicate examples of possible masking responses (see details in text).

Panels **A** to **C** represent temperature cycles of T=24 h, while **D** stands for temperature cycle T=16 h. **H** represents the density traces for *frq1* in LD. Filled circles represent the onsets of conidiation (**B** and **D**). Asterisks indicate the rapid decrease in conidiation (**E-F**). Graphs are composed according to results of figures 3.26 and figure 3.27. LD (light-dark cycles, 3 µE, 25°C), TC (temperature cycles 20°C and 30°C in constant darkness);

Zeitgeber	T cycle	% of cycle cold or dark	bd (frq)	frq1	komo303
				regression coefficient r	
TC	16h	50	0.99	0.95	0.97
	24h	12	0.97	0.81	0.55
		50	0.97	0.94	0.92
		88	0.99	0.96	0.88
LD	24h	16	0.97	0.98	0.57
		5 0	0.98	0.96	0.45
		95	0.97	0.95	0.59

Table 3.8 Results of statistical analysis of data shown in fig. 3.26. The regression coefficients r are calculated by using the means ± SEM as used in figure 3.26 (with p< 0.001). Composite cosine fits are the common waveforms in chronobiology (see Discussion). These harmonics were mathematically "fixed" to the corresponding T cycle length. See methods for the details of calculations.

3.4.2.3   Molecular Results

The previous findings showed an altered and unstable circadian property for *komo303*, while the key components of the molecular clock FRQ, WC1 and VVD had to be investigated (see the introduction section for assigned functions of these elements). A comparison of the protein profiles in *komo303* and the corresponding control strains (*wc1*, *frq1* and *frq10*) with known mutated clock was assigned to describe disturbances in the circadian clock system.

The first step was an experiment in which the strains *bd*, *wc1*, *frq10* and *komo303* grew for 48 h in constant darkness (25° C).

Komo303 and the corresponding null frq-knockout strain *frq10,* showed no or only very low amounts of FRQ as depicted in figure 3.27.

Therefore, the *frq* locus of *komo303* was analysed for insertions of the BASTA resistance cassette with Southern Blot and restriction mapping, revealing double

plasmid insertions in the open reading frame with production of a probably truncated FRQ protein (see figure 3.27, first row).

In addition to this, no WC1 protein was detectable in *komo303* and its baR- isolate *CR33#5* or in the corresponding knock-out strain wc*1*, and the baR- isolates *CR33*#13, *CR33*#14 and *CR33*#28 showed low amounts of this protein only (see figure 3.27, second row).

In mutant *komo303* and in its isolates VVD was detected (see figure 3.27, last row), although induction of mycelial carotinoids revealed normal levels of the orange pigment for *komo303* (see figure 3.28).
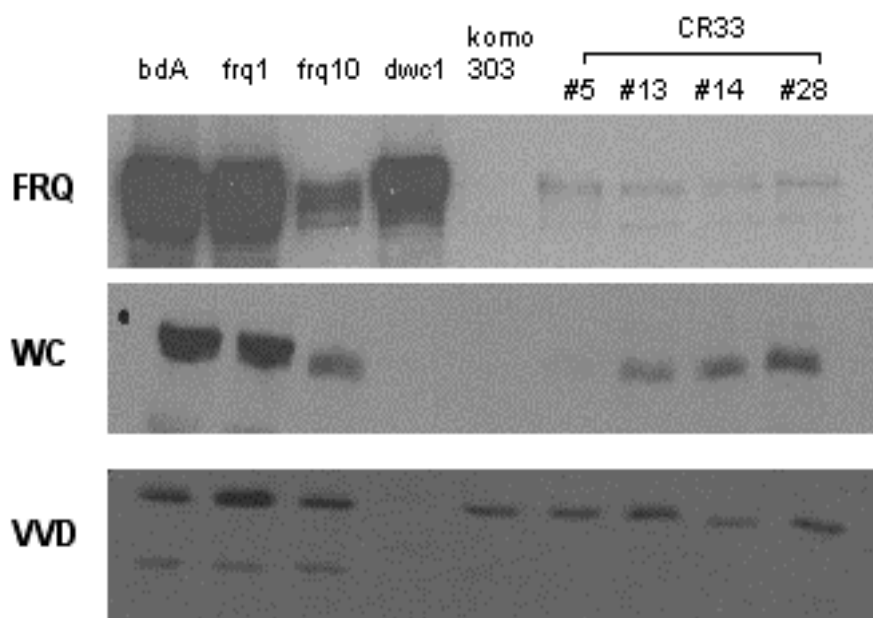
Fig.: 3.27 Accumulated protein profiles of *Komo303* are presented after incubation for 48 h.

X-ray films with exposure times of 5 to 10 seconds are presented here. The differences in protein amounts are clearly observable and therefore not quantified electronically.
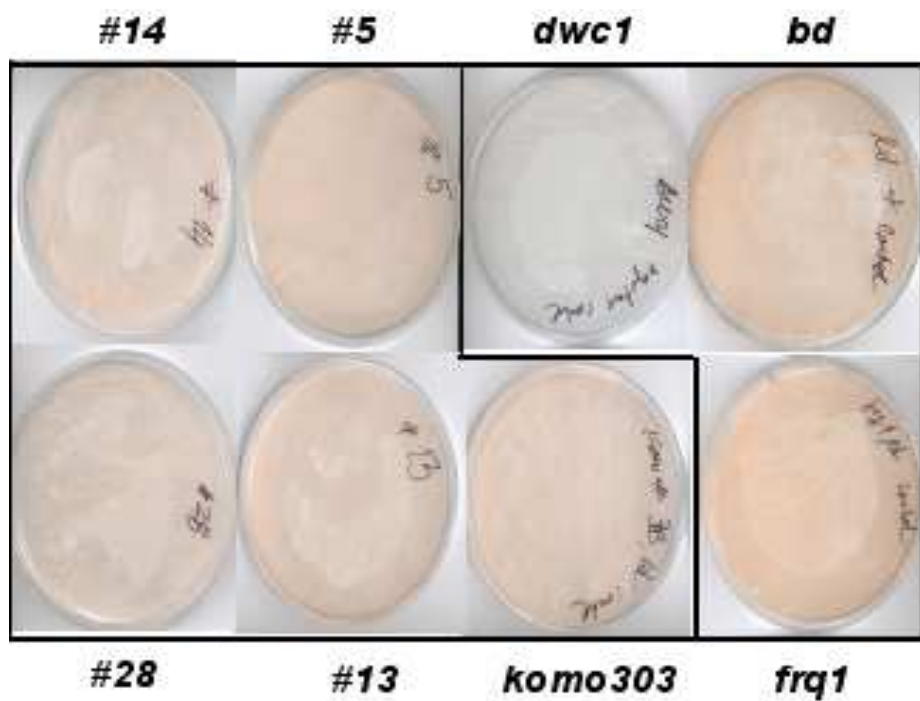
Fig.: 3.28 Induction Experiment of Carotinoids

Mycelial pads grew in DD 25° C until a light exposure of 10 μE light intensity for fives hours was performed.

Komo303 and its isolates produced slightly fewer carotinoids than *frq1* and *bd* in mycelia.

4 Conclusion and Discussion

4.1 Mutant Production and Novel Method of Plasmid Rescue

This study has clearly demonstrated the abundance and inexpensive production of mutants with insertional mutagenesis. The transformation of a resistance gene (BASTA) into conidia via electroporation offers the possibility for rapid identification of the tagged DNA. In contrast, mutagenesis with UV light or with chemical substances makes it difficult to detect the mutagenised DNA region. In this instance, precarious methods had to be applied in order to rescue the mutated gene (see Feldman et al., 1974). Therefore, a novel strategy for the identification of genes in *Neurospora crassa* has been developed. This method combines several protocols to identify the insertion site in mutants by a combination of mapping, partial cloning and PCR (see Methods section).

This novel assay can be easily adapted to various insertional constructs, e.g. alternative selection markers or constructs, which could facilitate over-expression. In addition, this method was established to avoid certain pitfalls, including the possible loss or destruction of the ampicillin resistance gene of the inserted plasmid (Orbach et al. 1988). Otherwise a simple restriction of the mutant's DNA, a self-ligation, a transformation into *Escherichia coli* and a consecutive selection for ampicillin resistant colonies would have been sufficient (Perkins et al. 1997, see Introduction). The general approach of the new method of plasmid rescue was confirmed also by the identification of the insertion region in *komo497* (not part of this study, unpublished data).

## 4.2 Novel Mutant Screen on Short Temperature Cycles in *Neurospora*

The initial experiment of this study described an optimal phenotype for screening mutants in temperature cycles. A symmetric temperature cycle of 16 h supports reliable synchronisation for the demanding screening protocol (see figure 4.1). This cycle length represents the lower limit of the range of entrainment, in which the clock system of *Neurospora crassa* would be exposed to a challenge (Aschoff et al. 1979). In contrast, earlier studies used traditional Zeitgeber cycles, i.e.

simulations of a day length, or conditions under constant darkness, to detect new clock mutants in *Neurospora crassa (*Feldman et al. 1973).

The novel mutant screen detected 37 mutant strains with an altered chronotype, e.g. advanced onset of conidiation. A comparison of results from the novel screening method with data from traditional conditions (LD, DD) revealed that 95% of the "verified" mutants would not have been detected as clock mutants in either DD or LD cycles (T= 24 h) for the same threshold values (see section 3.3.2 and 3.3.3). Only 19% of mutants showed a slower or faster endogenous period in DD, respectively. 60% of mutants entrained with normal phases in the light-dark cycles (see figure 4.2).

In reviewing these findings a reasonable conclusion could be stated: the high yield of mutant phenotypes was accomplished with the extreme Zeitgeber conditions of the novel screen, which probably had a higher sensitivity for "swapped" chronotypes than constant darkness (DD) and 24 h LD cycles.
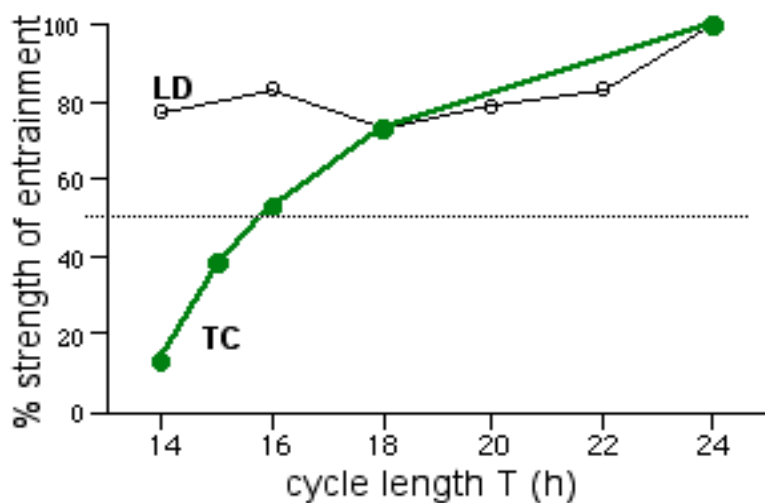
Fig.: 4.1 Entrainment ranges for wild type strain *bd* (rearranged from figure 3.1) in symmetric light-dark cycles (LD, 3 μE, open circles) and in symmetric temperature cycles (TC, 22 °C of cold phase and 27 °C of warm phase; filled circles).
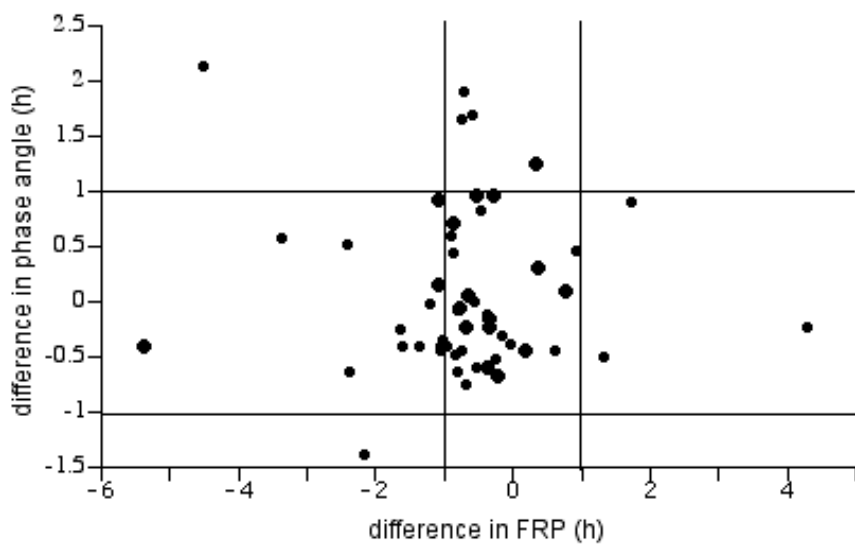
Fig.: 4.2 Comparison of Entrainment Properties in *komo* mutants. Each dot represents one mutant isolate. The standardised differences in conidiation onsets of 24h light cycles (y-axis) and τ in DD (x-axis) are plotted against each other (redrawn from figure 3.10). The wild type strain was set at zero. Horizontal and vertical lines indicate hypothetical threshold values of 1 h standardised time (1.3 h real time). Here only two strains exposed a deviating τ and a significantly altered phase angle.

4.3 Circadian Properties of Screened Mutants

This study revealed a wide range of circadian phenotypes for the *komo* mutants (see section 3.3.3). Several mutants displayed dependencies on the phase angle from their free running period, in which a shorter free running period (compared to the wild type) was associated with an advanced phase in Zeitgeber cycles (e.g. *komo497*). These findings are consistent with previous studies of organisms other than *Neurospora*, where the organisms followed a "phase period law" also known as "Aschoff´s rule" (Pittendrigh et al. 1976). Some *komo* mutants did not "obey" this rule and showed a "deviant" chronotype (see figure 4.1 and figure 3.10). These mutants had a wild-type-like (*bd*) free running period but entrained with

96

advanced phases like *komo58*. Another mutant displayed no stable free running periods and could not synchronise reliably on symmetric LD cycles. Instead it showed advanced phases on temperature cycles as *komo303*. At least one mutant, i.e. *komo262,* had a longer free running period as well as an advanced conidiation onset in short temperature cycles. Its phase of entrainment moved later in light cycles instead.

The variability of all these phenotypes underlines the complexity of circadian clocks. These results may indicate that phase and period is not controlled by one clock mechanism, (i.e. oscillator) only. Genetic studies in mice showed that neither phases of entrainment nor endogenous period are inherited according to simple Mendelian rules (Oster et al. 2003, Merrow et al. 2005) demonstrating the meagre knowledge of regulation and interaction of clock genes.

In short, this conclusion may suggest the existence of a complex clock composed of a network of interconnected oscillators (Roenneberg and Merrow 2001 and 2002; Lakin-Thomas 2005) rather than of one oscillator (see Introduction for background). The existence of only one transcription translation feedback loop could hardly explain all these different phenotypes (Pregueiro and Dunlap, 2005).

4.4 Komo58

The mutant *komo58* did not fit into "Aschoff´s rule" in experiments on traditional Zeitgeber cycles (see above). It displayed an advanced phase of conidiation onset in extremely asymmetric light-dark cycles. *Komo58* entrained less stably and with an advanced onset of conidiation in symmetric light cycles (T= 24 h) under low intensities of white light (see figure 3.15 B).

An expression analysis of a cDNA "morning" library flanking the insertion site could not reveal a significantly altered RNA-expression in *komo58* (see figure 3.21). The result of this experiment established that the mutant phenotype was not due to an altered expression of this particular cDNA region. But genetic results clearly showed an association between the mutant's phenotype and the presence of the insert, because all isolates with drug sensitivity, i.e. single insertion, displayed the mutant entrainment behaviour of *komo58* (see 3.4.1.1)

There was no analysis of the expression of the two flaking genes (see 3.4.1.3) or of the intergenic region inspected for gene regulation elements, i.e. binding sites

for transcription factors. These regulatory elements do not necessarily influence genes in the neighbourhood, but they could act far upstream or downstream of their location.

There is, however, another issue that needs to be discussed. The sequencing results of the recovered insertion region of one of the isolates revealed discrepancies in the property of nucleotides. A BLAST analysis of the sequencing results with the *Neurospora* genome database discovered several nucleotide exchanges (see 3.4.1.3). 90% of these mismatches were distributed unevenly in the plasmid, while only very few nucleotide exchanges were found in the drug cassette itself. The absence of severe mutations in the BASTA cassette is consistent with the observed drug resistant phenotype of *komo58* and its baR+ progeny. The amount of base alterations could not be explained by the event of wrong incorporations of nucleotides during the PCR amplification or by base-call errors of the sequencing reaction itself (Keohavong and Thilly, 1989).

Here, restriction maps showed divergent patterns for the parental strain and the corresponding progeny of a sexual cross. It was not known whether a nucleotide exchange or rearrangements of DNA had been the reason for an altered restriction pattern (Orbach et al. 1988, Perkins et al. 1993).

In reviewing the molecular results of *komo58* a preliminary conclusion could be drawn: in *Neurospora crassa* there is a curious mutational process called *repeat-induced point mutation*, or *RIP* for short (described by Singer, Marcotte and Sellker 1995) (see Introduction).

The process of RIP and the associated cytosine methylation may explain the results of restriction mapping in *komo58*, because 30% of the G->A transitions are closely related to not-unique regions of the plasmid pKSbar2. *Komo58* and *komo497* isolates yielded only one copy of the plasmid instead (summarised in section 3.4.1.3). But investigating regions with higher incidents of nucleotide exchanges revealed two domains (each 200 bp long) with homologies to two *Neurospora crassa* genes on Chromosome I (data not shown).

These findings suggest further investigations in order to clarify whether a RIP process or other mechanisms are involved, and whether they could be the source of these nucleotide exchanges (see section 1.4.2.).

4.5 Komo303

The baR+ progeny of CR33 (*frq1* x *komo303*) showed different segregation for drug sensitivity and for entrainement behaviour.

The segregation into 1:1 (baR+ : baR-) for drug sensitivity was verified by Southern analysis and by selection experiments on BASTA. These findings indicate a strong linkage between two insertion sites when independent assortment is assumed. Otherwise recombinant progeny, i.e. those with one single insertion, would be observed more frequently (see Perkins ,1953).

No distinct segregation pattern could be found for entrainement phenotypes on temperature cycles or on light-dark cycles. The baR+ isolates segregated into 3:1 for their ability to entrain on temperature cycles, while only 25% of the same isolates entrained on light-dark. In addition, it was possible to distinguish three groups of progeny, two of which were found to partially resemble the phenotype of the parents (*frq1* and *komo303*). Furthermore, it is possible to create subdivisions for those groups, as one subgroup showed entrainment behaviour similar to *frq1* strains on light cycles but entrained on temperature cycles like *komo303*, while the other group showed no entrainment on light cycles (*komo303*) but displayed the *frq1* phenotype on temperature cycles (see figure 3.22).

In short, the overall segregation of phenotypes into 2:2:2:2:1 (*komo303*-like:r1:r2:r3:*frq1*-like) can not be explained by simple Mendelian rules.

One conclusion is that there is no strong linkage between the inheritance of light entrainment and temperature entrainment abilities. It is not known whether the amount of picked spores was insufficient for representative formal genetics or whether some sort of complex traits genetics caused these crossing results (Salathia, Edwards and Millar 2002; Merrow and Roenneberg 2005).

Komo303 showed a phase of conidiation that was opposite to that of the wild type in symmetrical temperature cycles. A similar entrainment phenotype has been described in earlier studies for the *frq10* mutant (Roenneberg and Merrow 1999), where the majority of conidial activity occurred during cold phases. *Komo303* entrained in symmetrical temperature cycles because it established a phase relationship (Ψ) in dependence on the cycle length (T), although less bound than *bd* (see Results section 3.4.2.2). A driven system would show no changes in Ψ with changing Zeitgeber length (see Introduction and Aschoff et al. 1978).

In LD cycles *komo303* showed driveness but no entrainment. This conclusion is based on the analysis of density traces that were calculated from light-dark experiments with different portions of light for the parental *komo303*.

First of all, the mutant's density traces of conidiation could not be described efficiently by a two-component cosine function, which is highly efficient in describing circadian activity as described previously by Roenneberg and Merrow (2001, 2005). A comparison of the mutant's regression values with corresponding values of the wild-type strain *bd* supports that strongly.

Second, an examination of the density traces for all extreme cycles, with different cold or dark portions, revealed that "spiny" peaks, i.e. activity bands of short width, occurred exclusively during the phase changes of the Zeitgeber cycles, which are the transition from light to dark and the warm to cold.

As stated before, this sort of activity peak did not systematically change its phase angle Φ relative to the Zeitgeber transitions of the different phase portions, and therefore rather represented a "driven" clock.

Similar observations had been described in earlier studies, in which equivalent peaks occurred solely during the warm stimulus of an asymmetric cycle (see figure 4.3). This phenomenon was also explained as "driveness" of conidiation in an *frq10* strain (Roenneberg and Merrow 2005).

Furthermore, the mutant showed a large variability of period lengths, which ranged from 14 h to 29 h in constant darkness (25° C). A mixing test on race tubes demonstrated that a "stabilisation" of the period length, i.e. a decrease of the variances in period, occurred in *komo303* samples with an addition of 10% of wild type -nuclei (see figure 3.23). A kind of instability of period was described earlier in *frq10* mutants (Aronson et al., 1994) and, in addition, Feldman and Hoyle (1973) concluded from experiments similar to those in this study that the corresponding *frq9*-allele represents a recessive mutation.

In reviewing all these experimental results a preliminary statement could be made; on the one hand *komo303* resembles the null *frequency* mutant *frq9*, and on the other hand the *wc1* mutant.

First of all, this judgement is based on the analysis of entrainment phenotypes; this analysis showed that *komo303* and the wild type strain *bd* have an opposing entrainment behaviour in temperature cycles and that *komo303* is "driven" rather than entrained on light-dark cycles. Furthermore, the mutation *komo303* seems to

be recessive and causes an unstable free running period in conditions of constant darkness. All these phenotypes have been demonstrated for *frq9* and *frq10* strains in previous studies. The molecular investigations have demonstrated for *komo303* that the plasmid insertion is localised in the *frq*-locus near the original *frq9* site (Merrow et al. 1994), and Western blot experiments have revealed the absence of any functional FRQ protein (see section 3.4.2.3).

Second, *komo303* and the corresponding *wc1* strain show a defective expression of the WC1 protein, i.e. no detectable WC1 protein (see figure 3.27).

Although *komo303* showed congruity in phenotypes to known clock mutants, the following results cast doubt on the assumption that *komo303* is equal to the *frq9* strain:

No WC protein was detected in *komo303*, although *frq9* or *frq10* strains are supposed to be capable of expressing this protein.

Komo303 also displayed near normal levels of mycelial carotenoids and normal levels of VVD in the light induction test, although *wc* mutants are blind for light induced mycelial carotenoids and show low levels of VVD (see figure3.27) (Delgi-Innocenti and Russo, 1984; Crosthwaite et al., 1997).

Upon considering the mutant phenotype and the above molecular results, one may conclude that *komo303* represents a novel *frq*.

These findings suggest that WC-protein and FRQ-protein may not be necessary for entrainment on temperature cycles; the clock system would be weakened, but not suspended by this constraining of "entrainability".

Lakin-Thompson (2005) came to a similar conclusion when investigating the entrainment behaviour of *frq*- and *wc*-knockout strains and other studies proposed the existence of a FRQ independent oscillator (FLO), although no distinctive components had been found (Merrow, Brunner and Roenneberg 1999; Correa et al. 2003) (see Introduction).

As a consequence*, komo303´s* ability to entrain on temperature cycles obviously contradicts the arbitrary assumption that the FWC-oscillator (FRQ + WCC) is the major clock oscillator in *Neurospora* and is thus essential for any kind of entrainment (*in contrast to* Pregueiro et al. 2005).

However, *komo303´s* behaviour and existence do not provide final evidence for an FRQ-less oscillator, although these findings may lead to this intuitive conclusion.

Circadian time series of clock proteins in *komo303* should be profiled to eventually determine whether truncated FRQ protein and WC1 protein was expressed.

Recent studies suggest that *wc* gene expression and the function of the WC complexes are guided by complex mechanisms not yet fully understood (Lee et al. 2003; Kaldi, Gonzales and Brunner 2006). Moreover, FRQ levels are regulated both by the WC complexes and by different mechanisms at the level of transcription-translation (Diernfellner et. al 2005). Other similar interconnected regulation mechanisms may also be relevant to the expression of *wc* and *frq* in *komo303*. The inquiry into the important interactions between those gene products, i.e. RNA and protein, is important, as it would help to clarify the mutant's phenotype.

This study has successfully characterised a novel *frq* mutant by identifying the insertion into *frequency*.
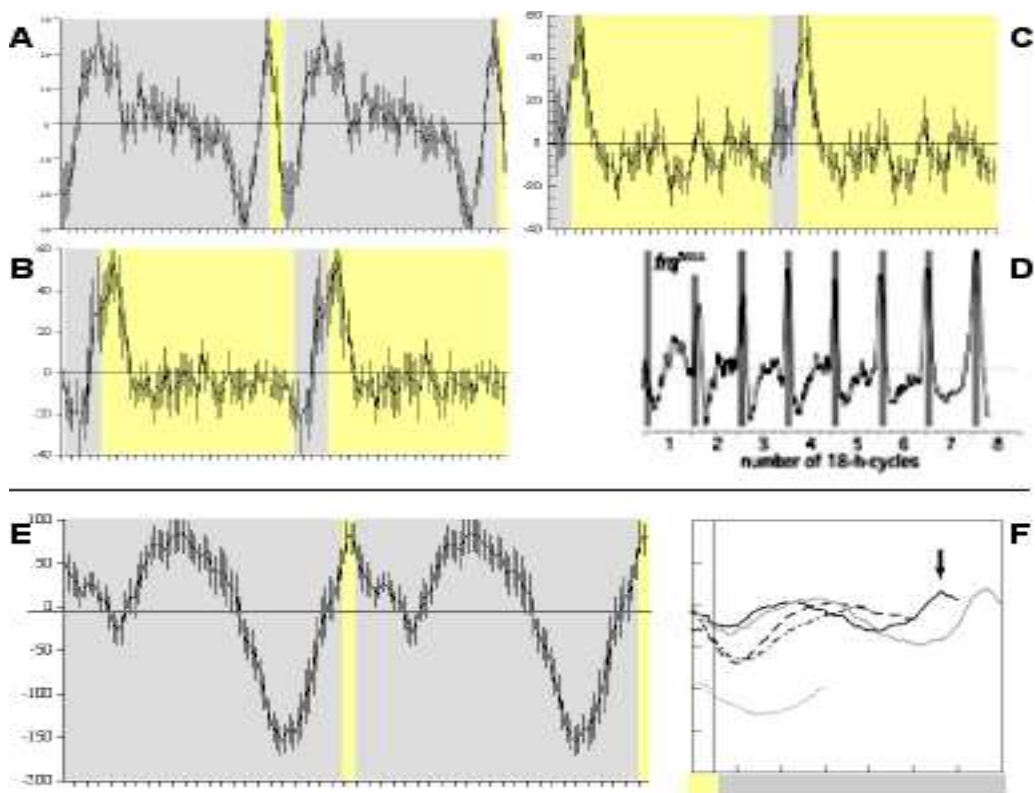
Fig.: 4.3 Resemblance of averaged density traces for *komo303*, *frq10* and *frq1* strains in extremely asymmetric LD and TC cycles. Panels **A-C** and **E** are redrawn from figure 3.27 (see Results and Methods for details). Pictures **D** and **F** are taken from Roenneberg/Merrow (2005) and Lakin-Thompson (2005). **D** shows the conidiation traces for 18 h temperature cycles applied with airflow (2 h of warm air) where the main conidiation peaks are related to the warm portion (dark shading). **A** and **B** show extreme light cycles and **C** depicts the corresponding light cycle. Here, the main peaks are coupled to the L to D or to the W to C transition of Zeitgeber.

F represents the averaged density traces for a temperature cycle of T=24 h (dark line) with 2 h of warm portion. Herein, a second peak (arrow) is found for the *frq10* strain. A similar phenomenon was describes for *frq1* on an equivalent light cycle in this study. It is difficult to state whether its first peak represents a second endogenous activity that begins before the next phase of light. This might be expected on one hand for a T cycle (here 24 h) longer than the intrinsic period of the *frq1* strain (τ=16 h). The length of the dark phase (20 h) may enhance the first effect, mimicking a much longer Zeitgeber cycle (2 x 20 h), best described as "frequency multiplication" (see section 1.2.3).

5 Summary

Circadian clocks are endogenous cellular mechanisms that control daily rhythms of physiology and behaviour. The adjustment of the circadian clock to the 24 h period of a day is commonly accomplished by several environmental cues, e.g. temperature, light and nutrition. For one light input pathway the mechanism that synchronises or entrains *Neurospora*'s clock is supposed to be known. Nevertheless, there are plenty more environmental cues that have an obvious impact on the circadian clock, e.g. temperature.

The environmental cue "temperature" was underrepresented in studies about *Neurospora*'s circadian clock, while several clock studies focused on stationary conditions rather than changing ones. As a result, the functionality and adaptation of circadian clocks were underestimated, and thus new clock components could be overlooked due to screening on constant darkness.

It was therefore important to develop a novel strategy in screening mutants that challenged the circadian clock of *Neurospora crassa* entirely on temperature alternations. A temperature cycle of low amplitude (22° C cold and 27° C warm) and of short period (8 h cold and 8 h warm) applied as Zeitgeber stimulus.

A mutant library was created with insertional mutagenesis via electroporation in order to transform a BASTA resistance gene into conidial nuclei. As a consequence, a novel method of rescuing the mutations was established, which combined the process of mapping, partial cloning and PCR and was called *Size Selected Fragment Plasmid Rescue* or *SSFPR* in short.

During the screening of several hundred mutants among the novel protocol, a known clock gene, *frequency*, was identified and characterised. The identification of several mutants with altered clock phenotypes has on one hand confirmed the general approach of this study and on the other proved that the greater sensitivity for the temperature screen can bee used to detect mutant phenotypes.

Zusammenfassung

Die innere Tagesuhr basiert auf einem angeborenen Zellmechanismus welcher den täglichen Stoffwechsel und somit das Verhalten von viel Organismen beeinflußt. Täglich wird diese innere Uhr an den 24 Stunden Tag der Umwelt angepaßt und somit synchronisiert. Zu den wichtigsten Umweltsignalen (Zeitgeber) gehören Licht, Temperatur und Nahrungsangebot.

In der Askomyzete *Neurospora crassa* ist der Perzeptionsmechanismus für Licht bereits ausgiebig untersucht. Dennoch ist die Spannweite an anderen wichtigen Umweltsignalen wie zum Beispiel der Temperatur nur unzureichend erforscht. Diese Untersuchungen werden bei *Neurospora crassa* mehrheitlich unter konstanten Umweltbedingungen durchgeführt. Bisher erfolgten keine Experiemnte unter verändernden Umweltbedingungen, so dass nur unzureichend Aussagen über eine Anpassungsfähigkeit getroffen werden können, und somit keine Rückschlüsse auf die Dynamik der inneren Uhr des Organismus zu schließen sind. Konsekutiv sind also neue Erkentnisse über potentielle „Uhren-Gene" und deren Wechselwirkung mit deren anderen bisher nur begrenzt möglich.

Aus diesem Grund wurde eine neue Strategie bei der Suche nach neuen Uhren-Genen entwickelt zur Identifikation neuer chronobiologischer Mutanten entwikelt.

Die potenziellen Uhren Mutanten wurden mit Hilfe Elektroporation geschaffen, wobei das Plasmid pKSbar2 mit dem BASTA-Resitenzgen in asexulle Pilzsporen eingeschleußt. Nachfolgend diese - für *Neurospora crass* neuartige Mutagenesis – die Entwicklung einer neuartigen Technik zur Charakterisierung und Knockout-Isolation der Mutationen. Somit wurde eigens eine neuartige Methoden der Genomkartierung entwikelt, in der die partielle Vektorklonierung und Methoden der „nested" Polymerase-Kettenreaktion vereinigt und effizient genutzt wurden.

Mehr als 700 Mutanten wurden untersucht, und davon 37 Mutantenstämme mit neuartigem ciarcadianen Rhythmus identifiziert. Diese neuetablierte Technik erlaubte die Charakterisierung einer nicht beschriebenen Mutation im bekannten Uhrengen, *frequency*. Dieser Mutantenstamm hatte sich hinsichtlich der molekularen und physiologischen Eigenschaften von anderen bereits beschriebenen *frq* Mutanten deutlich abgehoben.

Diese neue Vorgehensweise führte zu einer Neubeschreibung einer *frequency*-Mutante.

6 References

Aronson B.D., Johnson K.A., Dunlap J.C., Circadian clock locus frequency: Protein encoded by a single open reading frame defines period length and temperature compensation, *Proc. Natl. Acad. Sci. USA*, 1994, 91: p. 7683-7687

Aschoff J., Pohl H., Phase relations between a circadian rhythm and its zeitgeber within the range of entrainment. *Naturwiss*. 1978. 65: p. 80-84

Beadle G.W. and Tatum E.L., Genetic control of biochemical reactions in *Neurospora., Proc. Natl. Acad. Sci*. USA, 1942, 27: p. 499-506

Correa A., Multiple oscillators regulate circadian gene expression in *Neurospora.*, *Proc. Natl. Accad. Sci*. USA, 2003, 100: p. 13597-13602

Cranenburgh RM. An equation for calculating the volumetric ratios required in a ligation reaction. *Appl Microbiol Biotechnol*. 2004 Aug;65(2):200-2.

Crosthwaite S.K., Dunlap J.C., Loros J.J., Neurospors wc-1 and wc-2: Transcription, photoresponses, and the origin of circadian rhythmicity. *Science*, 1997, 276: p. 763-769.

Danna KJ. Determination of fragment order through partial digests and multiple enzyme digests. *Methods Enzymol*. 1980; 65(1):449-67.

DeCoursey P.J., Krula J.R., Behaviour of SCN-lesioned chipmunks in natural habit: a pilot study., *J Biol Rhythms*, 1998, 13: p. 229-244

Degli-Innocenti F. and Russo V.E., Isolation of new white collar mutants of Neurospora crassa and studies on their behaviour in the blue light induced formation of protoperithecia., *J-Bacteriol*., 1984, 159(2): p. 757-761

Diernfellner A.C.R., Schafmeier T., Merrow M., and Brunner M., Molecular mechanism of temperature sensing by the circadian clock of *Neurospora crassa. Genes & Dev*., 2005, 19: p. 1968-1973;

Dragovic Z., Tan Y., Görl M., Roenneberg T., Merrow M., Light reception and circadiam behaviour in "blind" and "clockless" mutants of *Neurospora crassa*, *EMBO,* 2002, 12;14: p. 3643 – 3651

Duffy J.F., Rimmer D.W., Czeisler C.A.,, Association of intrinsic circadian period with morningness-eveningness, usual wake time, and circadian phase., *Behav Neurosci*, 2001, 115: p. 895-899

Eskin A ., Identification and physiology of circadian pacemaker. Fed Proc, 1979 38: p. 2570-2572

Feldman J.F., Hoyle M.N., A direct comparison between circadian and noncircadian rhythms in *Neurospora crassa*. *Plant Physiol.*,1974. 53: p. 928-930

Feldman J.F., Hoyle M.N., Isolation of circadian clock mutants of *Neurospora crassa*. *Genetics, 1973.* 75: p. 605-613

Ferraro J.S., Sulzman F.M., Dorsett J.A., Alteration in growth rate associated with normal persisting circadian rhythm in Neurospora crassa during spaceflight., *Aviat Space Environ Med*, 1995, 66(11): p. 1079-1085

Granshaw T., Tsukamato M. and Brody S., Circadian rhythms in Neurospora crassa: farnesol and geraniol allow expression of Rhythmicity in the otherwise arrhythmic strain frq1, wc1 and wc2., *J. Biol. Rhythms*, 2003, 18: p. 287-296

Heintzen C., Loros L.L. and Dunlap J.C., Tha PAS protein VIVID defines a clock-associated feedback-loop that represses light input, modulates gating and regulates clock resetting., *Cell*, 2001, 104: p. 435-464

Keohavong P. and Thilly W.G., Fidelity of DNA polymerase in DNA amplification. *Proc. Natl. Acad. Sci.* USA, 1989, 86: p. 9253-9257

Kramer C., Loros J.J., DunlapJ.C. and Crosthwaite S.K., Role of antisense RNA in regulating circadian clock function in Neurospora crassa., *Nature*, 2003, 421: p. 948-952

Lakin-Thomas PL., Circadian clock genes frequency and white collar-1 are not essential for entrainment to temperature cycles in *Neurospora crassa*. *Proc Natl Acad Sci* U S A. 2006 Mar 21;103(12):4469-74.

Lee K., Loros J.J. and Dunlap J.C. Interconnected feedback-loops in the Neurospora circadian system., *Science*, 2000, 89. p. 107-110

Lee, K., Dunlap, J.C. and Loros, J.J., Roles for WHITE COLLAR-1 in circadian and general photoreception in Neurospora crassa. Genetics, 2003, 168: p. 103-114.

Liu Y., Garceau N., Loros J.J. and Dunlap J.C., thermally regulated translation control mediates an aspect of temperature compensation in the Neurospora circadian clock., *Cell*, 1997, 89: p. 477-486

Liu Y., Loros J., Dunlap J.C., Phosphorylation of the Neurospora clock protein FREQUENCY determiness its degradation rate and strongly influences the period length of the circadian clock., *Proc. Natl. Acad Sci*. USA , 2000, 97: p. 234-239

Liu Y., Merrow M.M.,Loros J.J.,and Dunlap J.C., How temperature changes reset a circadian oscillator., *Science*, 1998, 281: p. 825-829

Lotze M., Treutwein B., Roenneberg T., Daily rhythm of vigilance assessed by temporal resolution of the visual system, *Vision Research*, 2000, 40: p-3467-3473

Margolin B.S., Freitag M., Selker E.U., Improved plasmids for gene targeting at the his-3 locus of Neurospora crassa by electroporation., *Fungal Genet. Newsl*, 1997, 44: p. 34-36

McClung, C.R. (ed.). The higher plant Arabidopsis thaliana as a model system for the molecular analysis of circadian rhythms. Marcel Dekker, NY, 1992.

McCormick MH, McGuire JM, Pittenger GE, Pittenger RC, Stark WM. Vancomycin, a new antibiotic. I. Chemical and biologic properties. *Antibiot Annu*. 1955-1956;3:606-11.

McFadden E.R., Jr., Circadian rhythms. *Am J Med*, 1988, 85: p. 2-5.

McWatters H.G., Bastow R.M., Hall A., Millar A.J., The ELF3 zeitnehmer regulates light signalling to the circadian clock, Nature, 2000, 408: p. 716-720

Merrow M, Boesl C, Ricken J, Messerschmitt M, Goedel M, Roenneberg T. Entrainment of the Neurospora circadian clock. *Chronobiol Int*. 2006; 23 (1-2):71-80.

Merrow M, Boesl C, Roenneberg T. Cellular clocks: circadian rhythms in primary human fibroblasts. *J Biosci*. 2005 Dec;30(5):553-5.

Merrow M, Dragovic Z, Tan Y, Meyer G, Sveric K, Mason M, Ricken J, Roenneberg T., Combining theoretical and experimental approaches to understand the circadian clock. *Chronobiol Int*. 2003 Jul;20(4):559-75.

Merrow M, Mazzotta G, Chen Z, Roenneberg T. The right place at the right time: regulation of daily timing by phosphorylation. *Genes Dev*. 2006 Oct 1;20(19):2629-3.

Merrow M, Roenneberg T. Cellular clocks: coupled circadian and cell division cycles. *Curr Biol*. 2004 Jan 6;14(1):R25-6.

Merrow M, Roenneberg T. Enhanced phenotyping of complex traits with a circadian clock model. *Methods Enzymol*. 2005;393:251-65.

Merrow M, Spoelstra K, Roenneberg T. The circadian cycle: daily rhythms from behaviour to genes. *EMBO Rep*. 2005 Oct;6(10):930-5.

Merrow M., Roenneberg T., Circadian clocks: running on redox. *Cell* , 2001, 106: p. 141-143

Merrow MW, Dunlap JC. Intergeneric complementation of a circadian rhythmicity defect: phylogenetic conservation of structure and function of the clock gene frequency*. EMBO J.* 1994 May 15;13(10):2257-66.

Montgomery D.C. and Runger G.C., Applied statistics and Probability for Engineers, 1999, second edition, *John Wiley and Sons Pub.*

Ochman H., Gerber A.S., Hartl D.L., Genetic applications of an inverse polymerase chain reaction. *Genetics*. 1988 Nov;120(3):621-3.

Orbach M.J., Schneider W.P. and Yanofsky C., Cloning of methylated transforming DNA from *Neurospora crassa* in *Escherichia coli*., *Mol.Cell.Biol.*, 1988, 8: p. 2211-2213

Oster H., Baeriswyl S., Horst G.T., Albrecht U-, Loss of circadian rhythmicity in aging mPer1 mCry1 mutant mice. Genes Dev., 2003, 17: p. 1366-1379

Pandit, A. and Maheshwari, R. - A simple method of obtaining pure microconidia in *Neurospora crassa, Fungal Genet. Newsl*, 1993

Perkins D.D. The detection of linkage in tetrad analysis, *Genetics*, 1953, 38: p. 187-197

Perkins D.D., Kinsey J.A., Asch D.K. and Frederick G.D., Chromosome rearrangements recovered following transformation of *Neurospora crassa*., *Genetica*, 1993, 134: p. 729-736

Pittendrigh C.S. and Caldarola P.C., General Homeostasis of the Frequency of Circadian Oscillations, *Proc. Nat. Acad. Sci. USA* ,1973, 70: 9: p. 2687-2701

Pittendrigh C.S., Bruce V.G. and Kraus P., On the Significance of Transients in Daily Rhythms. Proc. Nat. Acad. Sci., 1958, 44: p. 965-973.

Pittendrigh C.S., Bruce V.G., Daily rhythms as coupled oscillator systems and their relation to thermoperiodism and photoperiodism, American Association for the Advancement of Science, Washington, D. C., 1959

Pittendrigh C.S., Circadian Systems: Entrainment. In: Handbook of Behavioral Neurobiology, *Biological Rhythms*, ed., J. Aschoff, 1981, 4: pp. 95-124, Plenum Press, New York.

Pittendrigh C.S. and Daan S., A functional analysis of circadian pacemaker in nocturnal rodents. IV. Entrainement as clock. *J Comp Physiol.*, 1976, A 106: p. 291-331

Pregueiro, A., Price-Lloyd, N., Bell-Pedersen, D., Heintzen, C., Loros, J. J. & Dunlap, J. C. *Proc. Natl. Acad. Sci.* USA, 2005, 102: p. 2210–2215.

Refinetti R., Non-stationary time series and the robustness of circadian rhythms., *Journal of Theoretical Biology*, 2004, 227: p. 571 –581

Roenneberg T. and Merrow MM., in *Zeitgebers, Entrainment and Masking of the circadian System*, 2001, eds. *Homma K. and Homma S.* (Hokkaido Univ. Press Sapporo, Japan), pp. 113-129

Roenneberg T., Wirz-Justice A. and Merrow M., Life between Clocks: Daily Temporal Patterns of Human Chronotypes, *Journal of biological rhythms*, 2003, 1: p. 80-90

Roenneberg T, Dragovic Z, Merrow M. Demasking biological oscillators: properties and principles of entrainment exemplified by the Neurospora circadian clock. *Proc Natl Acad Sci* U S A. 2005 May 24;102(21):7742-7

Roenneberg T, Kumar CJ, Merrow M. The human circadian clock entrains to sun time. *Curr Biol*. 2007 23;17(2):R44-5.

Roenneberg T, Merrow M. Circadian clocks: translation. *Curr Biol*. 2005 21;15(12):R470-3.

Roenneberg T., Merrow M., Life before the clock - modeling circadian evolution, *L Biol Rhythms*, 2002, 17: p. 495-505

Roenneberg, T. and Morse D., Two circadian clocks in a single cell. *Nature*, 1993, 362: p. 362-364.

Roenneberg T. and Taylor,W. *Methods Enzymol.*, 2000, 305: p.104 –119

Salathia N., Edwards K., and Millar A.J., QTL for timing: a natural diversity of clock genes. *TIGS,* 2002, 18: p.115-118

Sambrook, J., Fritch, E.F. and Maniatis T. Molecular cloning: A laboratory manual. (1989)

Sargent ML, Kaltenborn SH. Effects of Medium Composition and Carbon Dioxide

on Circadian Conidiation in *Neurospora*. *Plant Physiol*. 1972 Jul;50(1):171-175.

Schulze P.M., Beschreibende Statistik, 4. Auflage, 2000, *Oldenbourg Verlag*, München

Seed B, Parker, Davidson N., Representation of DNA sequences in recombinant DNA libraries prepared by restriction enzy. - *Gene*, 1982

Selker E.U., Cambareri E.B., Jensen B.C. and Haack K.R., Rearrangement of duplicated DNA in specialised cells of *Neurospora., Cell,* 1987, 51: 41-752

Shearman L.P., Sriram S., Weaver D.R., Maywood E.S., Chaves I., Zeng B., Kume K., Lee C.C., van der Horst G.T.J., Hastings S.M, *Science*, 2000, 288: p. 1013–1019.

Singer M.J., Marcotte B.A., and Selker E.U., DNA Methylation Associated with Repeat-Induced PointMutation in Neurospora crassa. *Molecular and Cellular Biology*, Oct. 1995, 25: p. 5586–5597

Sokolove, P.G. and Bushell, W.N., The chi square periodogram: Its utility for analysis of circadian rhythms. J*. Theoret. Biol*., 1978, 72, 131-160.

Talora C., Franchi L., Ballario P. and Macino G., Role of a white collar-1-white collar-2 complex in blue light signal transduction., *EMBO*, 1999, 18: p. 4961-4968

Tan Y, Dragovic Z, Roenneberg T, Merrow M. Entrainment dissociates transcription and translation of a circadian clock gene in *Neurospora*. *Curr Biol*. 2004 Mar 9;14(5):433-8.

Tan Y, Merrow M, Roenneberg T. Photoperiodism in Neurospora crassa., *J Biol Rhythms*. 2004, 19(2): p. 135-43.

Vogel, HJ. - A convenient growth medium for *Neurospora* (Medium N*), Microb Genet Bull*, 1956

Westergaard M., and Hirsch H.M., Environmental and genetic control of differentiation in Neurospora. *Proc Symp. Colson Res*., 1954. 7: p.171-183

Yang Y., Cheng P., Zhi G. and Liu Y., Identification of a calcium/calmodulin-dependent protein kinase that phosphorylates the Neurospora circadian clock protein FREQUENCY., J Biol Chem, 2001, 276: p. 41064-41072

Yang Y., He Q., Wrage P., Yarden O. and Liu Y., Distinct roles for PP1 and PP2A in the Neurospora circadian clock., *Genes and Development*, 2004, 18: p. 255-260

Zolan ME, Pukkila PJ. Inheritance of DNA methylation in Coprinus cinereus.
Mol Cell Biol. 1986 Jan;6(1):195-200**.**

7 Appendix

7.1 List of Instruments

Autoclave, type 300, Varioklav

Blotting apparatus, Trans-Blot cell (with plate electrodes), BioRad

Blotting apparatus, custom made; Specification: Helmut Klausner, workshop of
Inst. für Med Psych. Goethestr. 31/U1, 80336 Munich, Germany

Centrifuge, 5415C, Eppendorf

Centrifuge, 5417R, Eppendorf

Centrifuge, Biofuge Primo-R, Heraeus

Cooling unit, FBC 620, Fisher

Cooling unit, RM6, Lauda

Dark-room light bulb, E27 PF 712E, Philips

Developer for X-films, Curix 60&35 compact, AGFA

Dispenser, Multipette-plus, Eppendorf

Dispenser, Seripettor, Brand

Electrophoresis apparati, vertical (gel size 120x140x0.75, 1.00 or 1.50mm) and
horizontal (for DNA and RNA, gel size 5x7.5, 9x7.5, 11x14 and 14x23 cm)
all custom made; Specification: Helmut Klausner, workshop of Inst.für Med
Psychologie. Goethestr. 31/U1, 80336 Munich, Germany

Electrophoresis apparatus, Mini Protean II cell, BioRad

Electrophoresis apparatus, Protean II xi cell, BioRad

Freezer,-20°C, different models for household

Freezer,-80°C, Heraeus

Gene-Pulser, Pulse controller and Capacitance extender, BioRad

Homogenizer&cell-disruptor, Ribolyzer, FP120, Savant, Hybaid

Hybridization oven Bachofer, Germany

Incubator, 50L&100°C, Memmert (Germany)

Incubator, BD 240/E2, Binder

Incubator, KB 240/E2, Binder

Magnetic mixer, Ikamag, Junke&Kunkel-Ikawerk

Monochromator, T.I.L.L Photonics (Germany)

Picoammeter, Autoranging 485, Keithley

pipet, with positive displacement, Biomaster, Eppendorf

Pipets, Pipetman (10,20,100,200,1000µl), Gilson

Pipets, Reference (10,20,100,1000,2500µl), Eppendorf

Power Supply, EC 105, EC

Power Supply, EPS 2A200, Amersham

Power Supply, EPS 301, Amersham

Power Supply, EPS 601, Amersham

Power Supply, Model 1000/500, Biorad

Power supply, SP340, Tectron

Pulse-giving Unit (0.01-9.99 Period & 0.001-9.999 seconds Time)

Pump (with diaphragm), ME2, Vacuubrand

Radioactivity-counter, 900 Mini Monitor, Mini Instrments (England)

Radioactivity-counter,LB122, Berthold

Real Time PCR system, ABI PRISM 7000, Applied Biosystems

Scale, Handy H 110, Sartorius

Scale, L2200S Sartorius

Scale, Mettler, AE 50, Mettler,

Scintillation counter, LS 1801, Beckman

Shaker, KL2, Bachofer

Shaker, LS10, Gerhard

Shutter (photo), WILD MPS 51, Heerburg, Swiss

Spectrophotometer, DU64, Beckman

Spectrophotometer, Ultrospec 3000, Pharmacia

Speed-Vac, Bachofer

Thermal cycler, Primus, MWG Biotech

Thermomixer, 5436, Eppendorf

Thermomixer, comfort, Eppendorf

Timer, mechanical, Junghans

Timers,WB-388 and TR-118, Oregon Scientific;

Ultrasonic bath, Ultrason E, Greiner, Germany

Vortex, k-550-GE, Bender&Hobein AG

Writer (analog), ABB SE 120, Bachofer (Germany)

7.2 List of chemicals

Substance	Company	Order No
Acetic Acid	SIGMA	A-6283
Acetone	ALDRICH	17,997-3
Acrylamide	APPLICHEM	A3705,0500
Agarose LOW EEO	APPLICHEM	A2114,0500
Agarose QA TM	Q-BIOGEN	AGR0050
Albumin Bovine	SIGMA	A-3350
Ammonium acetate	SIGMA	A-1542
Ammonium chloride	SIGMA	A-4514
Ammonium nitrate	SIGMA	A-1308
Ammonium peroxodisulfate (APS)	ROTH	9592.3
Ammonium sulfate	ALDRICH	22.125-2
Ampicillin, sodium salt	SIGMA	A-9518
Arginine hydrochlorid (L+)	USB	US 11500
Bacto Agar	DIFCO	214010
BASTA	Roche	Schulte U.
Biopterin	SIGMA	B-2517
Bis acrylamide	SIGMA	M-7279
Boric acid	APPLICHEM	A2940,1000
Boric acid	APPLICHEM	A3581,0500
Bromphenol blue sodium salt	USB	US12370
Calcium chloride x 2H2O	ROTH	5239.1
Casein Enzymatic Hydrolysate	SIGMA	C-0626
Celite	ROTH	535
Chloroform	SIGMA	C-5312
Chloroform:Isoamylalcohol	SIGMA	C-0549
Citric acid	ALDRICH	24,062-1
Comassie brilliant blue	SIGMA	B-0149

Diethyl pyrocarbonate	USB	14710
DMSO / Dimethylsulfoxide Lsg.	MERCK	109678.01
EDTA 0.5M solution	AMBION	9261
EDTA Ehtylenediaminetetraacetic acid	SIGMA	EDS
Ethanol	ROTH	9065.2
Formaldehyde	SIGMA	F-8775
Formamide	SIGMA	F-7508
Glucose monohydrate	MERCK	1.04074
Glycerol	APPLICHEM	A2926,1000
Heparin	SIGMA	H-9768
Hepes	SIGMA	H-3375
Hexane	ALDRICH	29,325.30
IPTG	APPLICHEM	A-1008,0005
Isoamyalcohol	ROTH	8930.1
Leupeptin	USB	18413
Magnesiumchlorid x 6H2O	MERCK	1.05835.0500
Methanol	ROTH	4627.1
MOPS	APPLICHEM	A1076,0250
Orange-G	MERCK	1.15925.0025
Pepstatin A	USB	US20037
Phenol	APPLICHEM	A1153,0100
Phenol (DNA/RNA)	ROTH	A.156.1
Phenol (RNA)	ROTH	A.980.1
Phenylmethanesulfonyl fluoride (PMSF)	FLUKA	78830
Polyethyleneglycol PEG 4000	ROTH	156.1
Ponceau S	FLUKA	81460
Potassium chloride	SIGMA	P-3911
Sand	SIGMA	S-9887
SDS / Sodium Dodecyl Sulfate	ROTH	2326.2
Sodium acide	SIGMA	S-2002
Sodium chloride	MERCK	1.06404
Sodium chloride	APPLICHEM	A2942,1000
Sodium citrate	ROTH	3580.1
Sodium dihydrogenphosphate	MERCK	6346

Sodium hydroxid	ROTH	6771.1
Sodium nitrate	FLUKA	71755
Sodium nitrit	ALDRICH	20,783-7
Sorbitol	USB	21710
Sorbose	SIGMA	S-2001
Sucrose	FLUKA	84100
Temed	SIGMA	T-8133
Tergitol NP 40	SIGMA	NP-40
Trichloracetic acid	SIGMA	T-4885
Tris	USB	US 75825
Tris	APPLICHEM	A1086,100
Triton X-100	SIGMA	X-100
Tween 20	USB	20605
Urea	SIGMA	U-0631
Urea	USB	US 75826
Vitamin B12	SIGMA	V-2876
X-Gal	APPLICHEM	A1007,0001
Xylencyanole	ROTH	A513.1
Yeast Extract	SIGMA	Y-1625

7.3 List of Biochemicals

Substance	Company	Order No
Anti.Mouse Polyvalent immunoglobulins	SIGMA	A-0412
Deoxyribonucleic acid; (salmon testes)	SIGMA	D-1626
DNA ladder 100 bp	NEB	N3231
DNA ladder 1Kbp	INVITROGEN	15615-016
DNA Ligase T4	NEB	M0202M
DNase1 (RNase free)	ROCH	776785
dNTPmix	AB	N8080260
Lambda BstEII digest (DNA ladder)	NEB	N3014
Lysing enzyme (for N.crassa cell wall)	SIGMA	L-2265
PCR system, Exp. Long Template	ROCHE	1-681-842

Protein Assay (Bradford)	BIORAD	500-0006
Protein Assay (gamma glob. standard)	BIORAD	500-005
Protein Markers (pre-stained ladder)	BIORAD	161-0373
Restriction enzymes	NEB	misc.
Reverse Transcription reagents	AB	N8080234
Reverse Transcriptase	AB	4311235
Ribonuclease A	ROTH	7156.1
RNA polymerase	PROMEGA	P2075
RNA Secure	AMBION	7005
RNAguard Rnase inhubitor	AMERSHAM	27-0815-01
SYBR Green PCR master mix	AB	4309155
Western. blotting sub. ECL	ROCHE	2015196

7.4 Abbreviations

µ	micro (10^{-6})
A	Ampere
aa	amino-acid
al-1	albino-1
Amp	Amplicillin
APS	Amoniumperoxosulfate
bp	base pairs
BSA	Bovine serum albumin
cDNA	Complementary DNA
DD C	Constant darkness
DMSO	Dimethylsulfoxide
DNA	Deoxyribonucleic acid
dNTP	Deoxynucleoside triphosphate
E Einstein,	1 mol photons per second and square meter
E. coli	Escherichia coli
FGSC	Fungal Genetic Stock Centre
FRP	Free running period
frq	frequency gene
FRQ	frequency gene product (FRQ protein)

g	gram
h	hour
HEPES	4-(2-Hydroxyethil)-1-piperazineethanesulfonic acid (buffer)
IgG	Immunoglobulin G
IPTG	Isopropyl-b-D-thiogalactopyranoside
k	kilo (10^3)
L	liter
LB	Luria-Bertani (medium)
LD	Light-Dark
LL	Constant light
M	molar
m	milli (10^{-3})
min	minute
mRNA	Messenger ribonucleic acid
n	nano (10^{-9})
NTP	Nucleoside triphosphate
OD	Optical density
PAGE	Polyacrilamide gel electrophoresis
PCR	Polymerase Chain Reaction
PMSF	Phenyl-methyl-sulfonyl-fluoride
RNA	Ribonucleic acid
rpm	Rotation per minute
RTPCR	Real Time Polymerase Chain Reaction
Taq	Thermus aquaticus
UTP	Uridine-triphosphate
V	Volt
v/v	Volume in volume
w/v	Weight in volume
wc-1	white collar-1gene
WC-1	white collar-1 gene product (WC-1 protein)
wc-2	white collar-2gene
WC-2	white collar-2 gene product (WC-2 protein)
wt	wild type
X-Gal	5-Bromo-4-chloro-3-indolyl-b-D-galactopyranoside

7.5 Recipes

Acrylamide solution

29.2 g	Acrylamide
0.8 g	N, N'-Methylene-bis-acrylamide
Up to 100 ml	Water

Lysis buffer

0.2 M	NaOH
1%	SDS

Ampicilline stock 1000X

1 g	Ampicillin
Up to 10 ml	Water

Filter sterilize and keep at –20°C

Biotine stock 10,000X

10 mg	Biotine
100 ml	Ethanol

Keep at –20°C

Blotting Buffer for semi-dry blot

14.4 g	Glycin
3 g	Tris
200 ml	Methanol
Up to 1 liter	Water

First dissolve salts in aprox. 0.5 liter water then add Methanol

Blotting Buffer for wet-blot

288 g	Glycin
60 g	Tris
2 L	Methanol
Up to 1 L	Water

First dissolve salts in aprox. 5 liter water then add Methanol

Bottom Agar

10ml	Vogel's salts
440ml	Water
7.5g	Agar
91g	Sorbitol

Add 50 ml 10X Figs after autoclaving

Carot-media

20 g	Glucose
1X	Vogel's salts
Up to 1L	Water

CBB staining solution

0.1 % w/v	Coomassie-Blue G250
10 % v/v	Acetic acid
40 % v/v	Methanol

CTAB buffer 2X

10ml 1 M	Tris pH 7.5
2g	CTAB (First dissolve this substance in water!)
28ml	5M NaCl
4ml	0.5 M EDTA pH 8.0
1g	Sodium bisulfite
To 100 ml	Water

Denhards 50X

5g	Ficoll
5g	Polyvinylpyrrolidine
5g	BSA
Up to 500 ml	Water, Rnase free

RNase free chemicals, filtrate and freeze at –20°C. Denhards 50X is very hard to thaw. Make aliquots before freezing.

DNA/RNA loading dye

0.5 ml	Glycerol
40 mg	EDTA
40mg	Bromphenol Blue
40mg	Xylene Cyanol
0.5 ml	Water

DNA agarose gel

0.8-2.0% w/v	Agarose
1X	TAE
0.02-0.05 µg/ml	Ethidium bromide

Work in hood if possible!

Destaining solution (for CBB stained gels)

10 % v/v	Acetic acid
40 % v/v	Methanol

DNase1 buffer 10X

200 mM	TRIS pH 8.3
500 mM	KCl
20 mM	$MgCl_2$

RNase free chemicals!

Electrophoresis buffer (SDS-PAGE) 10 X

144.13 g	Glycin
30.28 g	TRIS
10 g	SDS
To 1 L	Water

Electrocompetent cells, media and buffers

• 1 liter LB media with pH adjusted to 7.5 and sterilised by autoclaving

• 2 liters of autoclaved 1 mM HEPES pH 7.0

• 3 liters of sterile water stored in the cold room

• LB plates with no additional supplements (i.e. ampicillin)

Elution buffer for gel purification of transcript

260 µl	Ammonium acetate
100 µl	10 % SDS
20 µl	0.5 M EDTA pH 8.0
Up to 10 ml	Water

RNase free chemicals have to be used!

FIGS 10X

100 g	L-sorbose
2.5 g	D-fructose
2.5 g	Glucose
To 500 ml	Water

Autoclave!

GET

25 ml	40% Glucose stock
2.5 ml	1M TRIS pH 7.5
2.0 ml	0.5 m EDTA pH 8.0
70.5 ml	Water

Add 3 mg/ml (final) lysozyme before use!

Laemmli buffer 4X (Reductive)

4 mg or 100µl Solid or 100X stock Bromphenol Blue	
800 mg	SDS
5 ml 1M	TRIS pH 6.8
350 µl	2-mercapto ethanol
To 10 ml	Glycerol

Follow the order! After adding 1M TRIS warm solution up (50°C)!

Luria-Bertani medium

5 g	Tryptone
2.5 g	Yeast extract

| 5 g | NaCl |
| 7.5 g | Agar |

For liquid LB omit Agar!

Mg solution

12 g	MgSO4
9.5 g	MgCL2
To 100 ml	Water

MOPS 20X

92.4 g	MOPS
33.3 g	3MSodium Acetate
40 ml	0.5 M EDTA

Up to 1L Water

First adjust pH to 7.0 with 10 M NaOH then add water to 1L

TBE buffer 10X

54.5 g	TRIS
27.8 g	Boric acid
4.47 g	EDTA
Up to 1 L	Water

PBS 10X

80 g	NaCl
2 g	KCl
11.5 g	Na2HPO4x7H2O
2 g	K2HPO4
Up to 1 L	Water

PTC and PMC

40 % w/v	PEG 4000
50 mM	CaCl2
For PTC	50mM TRIS pH 8.0
For PMC	10 mM MOPS pH 6.3

Ponceau-S solution (water based)

0.2 % w/v	Ponceau S
3% w/v	TCA

Hybridization solution

100 ml	50 X Denhards
250 ml	Formamide
25 ml	1M TRIS pH 7.5
29.2 g	NaCl
0.5 g	Sodium pyrophosphate
5 ml	10 mg/ml denatured salmon sperm DNA
90 ml	Water

Protein extraction buffer

1.2 g	HEPES
10 ml	Glycerol
2.7 ml	5M NaCl
1 ml	0.5 M EDTA pH 8.0

To prevent proteolysis PMSF (5mM final concentration), leupeptin (10µg/ml final) and pepstatine-A (10 µg/ml final were added). PMSF is poorly dissolvable in water and usually partially precipitates after adding. This does not influence protein quality.

rG buffer

0.8 ml	5M NaCl
0.5 ml	1M TRIS pH 7.5
0.1 ml	0.5 M EDTA pH 8.0
5 ml	50% v/v Glycerol
200 µM	final DTT
Up to 50 ml	Water

RNA extraction buffer

2 ml	0.5 M EDTA pH 8.0

10 ml	1 M Tris pH 8.0
40 ml	10 % SDS
12 ml	5 M NaCl
36 ml	Water

SOC

2.5 g	Yeast extract
10 g	Tryptone
0.25 g	NaCl

Fill water to 500 ml and autoclave, then add 2.5 ml sterile Mg solution and 5 ml 2M glucose. Make aliquots and keep sterile.

SSC 20X

526 g	NaCl
265 g	Sodium citrate
To 3 L	Water

RNase free solution!

STC

1M	Sorbitol
50 mM	CaCl2
50 mM	Tris pH 8.0

STE

2 ml	5 M NaCl
2 ml	Tris pH 7.5
2 ml	0.5 M EDTA pH 8.0
94 ml	Water

TBS 10X

90 g	NaCl
200 ml	1 M Tris pH 7.5
To 1 L	Water

Top agar

10 ml	50 X Vogel's salts
91 g	Sorbitol
14 g	Agar
450 ml	Water

Add 50 ml 10X FIGS after autoclaving (for mutant selection addition of BASTA)

Trace elements-standard

In 95 ml distilled water, dissolve successively with stirring at room temperature:

5 g	Citric acid x 1 H_2O
5 g	$ZnSO_4$ x 7 H_2O
1 g	$Fe(NH_4)_2(SO_4)_2$ x 6 H_2O
0.25 g	$CuSO_4$, x 5 H_2O
0.05 g	$MnSO_4$, x 1 H_2O
0.05 g	H_3BO_3, anhydrous
0.05 g	Na_2MoO_4 x 2 H_2O

The resulting total volume is about 100 ml. Chloroform (1 ml) is added as a preservative, and the trace element solution is stored at room temperature.

Westergaard's salts (5X), standard

2.5 g	KNO_3
2.5 g	KH_2PO_4
1.25 g	$MgSO_4$
0.25 g	$CaCl_2$
0.25 g	NaCl
0.5 µl/ml	Trace elements

To 500 ml Water

Westergaard's media with 2% sucrose

2 %	Sucrose
5 µg/ml	Biotin

1X Westergaard's salts

For solid Westergaard's media add agar (2%).

Vogel's salts 50X

750 ml	Water
150g	Na3Citrate
250g	KH2PO4 (anhydride)
100g	NH4NO3
10g	MgSO4x7H2O
5g	CaCl2x2H2O
5ml	Biotin stock
5ml	Trace elements stock
To 1L	Water

Additions were made in the following order always with continuous stirring. Each ingredient was completely dissolved before adding next. With 5 ml Chloroform added, solution can be stored at room temperature for few months.

Vogel's minimal media with 2% glucose

20 g	Glucose
5g	Arginine
1X Vogel's salts	
Up to 1L	Water

Vogel's minimal solid media with 2% glucose = *standard race tube medium*

20 g	Glucose
20 g	Agar
5g	Arginine
Up to 1L	Water

8 ERKLÄRUNG

Hiermit erkläre ich, daß die vorliegende Dissertation selbständig verfaßt und nur unter Verwendung der angegebenen Quellen und Hilfsmittel angefertigt wurde. Die Dissertation wurde in dieser oder änlicher Form noch keiner anderen Fakultät oder sonstiger Prüfungsbehörde vorgelegt.

9 Danksagung